arXiv:1109.6315v1 [quant-ph] 28 Sep 2011

Nonperturbative theory of weak pre- and post-selected measurements

Abraham G. Kofman, Sahel Ashhab, Franco Nori

Advance Science Institute, RIKEN, Wako-shi, Saitama 351-0198, Japan

Physics Department, The University of Michigan, Ann Arbor, Michigan 48109-1040, USA

Abstract

This paper starts with a review of the topic of strong and weak pre- and post-selected (PPS) measurements, as well as weak values, and afterwards presents original work. In particular, we develop a nonperturbative theory of weak PPS measurements of an arbitrary system with an arbitrary meter, for arbitrary initial states of the system and the meter. New and simple analytical formulas are obtained for the average and the distribution of the meter pointer variable. These formulas hold to all orders in the weak value. In the case of a mixed preselected state, in addition to the standard weak value, an associated weak value is required to describe weak PPS measurements. In the linear regime, the theory provides the generalized Aharonov-Albert-Vaidman formula. Moreover, we reveal two *new regimes* of weak PPS measurements: the strongly-nonlinear regime and the inverted region (the regime with a very large weak value), where the system-dependent contribution to the pointer deflection *decreases* with *increasing* the measurement strength. The optimal conditions for weak PPS measurements are obtained in the strongly-nonlinear regime, where the magnitude of the average pointer deflection is equal or close to the maximum. This maximum is *independent of the measurement strength*, being typically of the order of the pointer uncertainty. In the optimal regime, the small parameter of the theory is comparable to the overlap of the pre- and post-selected states. We show that the amplification coefficient in the weak PPS measurements is generally a product of two qualitatively different factors. The effects of the free system and meter Hamiltonians are discussed. We also estimate the size of the ensemble required for making a measurement. Exact solutions for a qubit coupled to several types of meters are also obtained. These solutions are used for numerical calculations which agree with the theory. We also discuss time-symmetry properties of PPS measurements and the relation between PPS and standard (not post-selected) measurements of any strength.

Keywords: measurement theory, weak values, foundations of quantum mechanics, precision metrology, quantum information processing

---

Contents

1 Introduction **4**
1.1 Measurement in quantum mechanics 4
1.2 Standard quantum measurements of arbitrary strength 7
1.2.1 Von-Neumann-like measurement scheme 8
1.2.2 Canonically conjugate meter variables 8
1.2.3 Non-ideal and weak standard measurements 9
1.3 Measurements with pre- and post-selection 10
1.3.1 General considerations 10
1.3.2 Strong (ideal) PPS measurements 11
1.3.3 Contextuality of strong PPS measurements 12
1.3.4 Model for PPS measurements of arbitrary strength 13
1.4 Weak PPS measurements 13
1.4.1 Simple approach 13
1.4.2 The pointer distribution 15

1.5 Discussion of weak values . . . 17
    1.5.1 Interpretation of weak values in terms of probabilities . . . 17
    1.5.2 Sufficient conditions for usual weak values . . . 18
    1.5.3 Quantum interference in PPS measurements . . . 19
    1.5.4 Sum rule for weak values . . . 19
1.6 Experimental realizations of weak PPS measurements . . . 20
1.7 Applications of weak PPS measurements . . . 22
1.8 General theory of weak PPS measurements . . . 25

2 Theory of standard measurements of arbitrary strength **27**
2.1 General formulas for standard measurements . . . 27
2.2 Weak standard measurements . . . 27

3 Theory of pre- and post-selected measurements of arbitrary strength **28**
3.1 General formulas for PPS measurements . . . 28
3.2 Expansions in the coupling parameter . . . 29

4 Weak pre- and post-selected measurements: Nonlinear theory **30**
4.1 Validity conditions for weak PPS measurements . . . 30
4.2 Quantifying the strength of a measurement . . . 31
4.3 General nonlinear formula for the average pointer deflection . . . 32
4.4 Regimes of weak PPS measurements . . . 32
    4.4.1 Linear response . . . 32
    4.4.2 Inverted region (the limit of very large weak values) . . . 33
    4.4.3 Intermediate regime . . . 34
4.5 Estimation of the average pointer deflection . . . 34
    4.5.1 Linear response . . . 35
    4.5.2 Strongly-nonlinear regime . . . 35
4.6 Amplification in weak PPS measurements . . . 36
    4.6.1 Proper amplification due to a large weak value . . . 36
    4.6.2 Enhancement due to an increased pointer uncertainty . . . 37
4.7 Measuring weak values and coupling strengths . . . 38
    4.7.1 Measuring the coupling strength γ . . . 38
    4.7.2 Measuring A_w: One unknown parameter . . . 38
    4.7.3 Tomography of weak values . . . 39
    4.7.4 Tomography of weak values: Linear regime . . . 39
    4.7.5 Tomography of weak values: Nonlinear regime . . . 39
4.8 Large average input variable, $|\bar{F}| \gg \Delta F$ . . . 40
4.9 The minimum size of the ensemble and the signal-to-noise ratio . . . 42
    4.9.1 The linear and intermediate regimes . . . 42
    4.9.2 Comparison of weak measurements with and without post-selection . . . 43
    4.9.3 Inverted region . . . 43

5 Mixed preselected state **45**
5.1 The general nonlinear formula . . . 45
5.2 Validity conditions for weak PPS measurements . . . 46
5.3 Different regimes . . . 47
5.4 Measuring the coupling strength and weak values . . . 47
5.5 Large average input variable, $|\bar{F}| \gg \Delta F$ . . . 48
5.6 The ensemble size needed for weak PPS measurements . . . 48

6 Effects of the system and meter Hamiltonians on pre- and post-selected and standard measurements 48
- 6.1 Effects of the Hamiltonians on pre- and post-selected measurements . . . 49
- 6.2 Effects of the Hamiltonians on standard measurements . . . 49
- 6.3 Special cases for the meter Hamiltonian . . . 49

7 Examples of meters 50
- 7.1 Non-standard meters . . . 50
  - 7.1.1 Coinciding input and output variables, $R = F$ . . . 50
  - 7.1.2 Meters with zero pointer uncertainty, $\Delta R = 0$. . . . 51
- 7.2 Continuous-variable meters . . . 51
  - 7.2.1 Canonically conjugate variables . . . 51
  - 7.2.2 Invariance with respect to a meter gauge transformation . . . 53
  - 7.2.3 Measuring physical parameters . . . 54
  - 7.2.4 Effects of the meter Hamiltonian . . . 55
- 7.3 Two-level meter . . . 57
- 7.4 Experiments where the average input variable is nonzero, $\bar{F} \neq 0$ . . . 60

8 Distribution of the pointer values 61
- 8.1 General meter . . . 61
- 8.2 Continuous-variable meter . . . 62
  - 8.2.1 Coinciding meter variables, $R = F$ . . . 62
  - 8.2.2 Canonically conjugate R and F . . . 63

9 Weak values for a qubit 65
- 9.1 General formulas . . . 65
- 9.2 Conditions for maximizing weak values . . . 66
- 9.3 Explicit formulas for a typical case . . . 66

10 PPS measurements of arbitrary strength: Exact solution for a qubit 68
- 10.1 Formulas for a general meter . . . 69
  - 10.1.1 Average pointer value . . . 69
  - 10.1.2 Pointer distribution . . . 69
- 10.2 Specific types of meters . . . 69
  - 10.2.1 Coinciding meter variables, $F = R$ . . . 69
  - 10.2.2 Two-level meter . . . 70
  - 10.2.3 Continuous-variable meter . . . 70

11 Numerical results and discussion 70

12 Discussion of two recent interferometric experiments 74
- 12.1 Unified theory of two interferometric measurement schemes . . . 74
- 12.2 Amplification coefficient for phase measurements . . . 78
- 12.3 A comparison of the phase-amplification technique with projective measurements . . . 78

13 PPS measurements with a general post-selection measurement 79
- 13.1 General formulas . . . 79
- 13.2 Relation between PPS and standard measurements of any strength . . . 80
- 13.3 Weak PPS measurements . . . 81
- 13.4 Time-symmetry properties for PPS measurements of any strength . . . 81
- 13.5 A pure preselected state . . . 82

14 Conclusion 83

Acknoledgements **83**

Appendix A Gauge invariance of PPS measurements **83**
A.1 System transformations 84
A.2 Meter transformations 84

Appendix B Operator identities **84**

Appendix C Estimation of moments of meter variables **86**
C.1 Generalized uncertainty relation 86
C.2 Estimating the moments 87

Appendix D Calculation of moments for canonically conjugate variables **88**

References **89**

1. Introduction

This paper starts with a review, and afterwards presents many original contributions. Indeed, most of this paper is original work, which sometimes is explicitly linked to previous theoretical and experimental work. Many special cases are considered in some detail, because the study done here is systematic and quite general, spanning many specific cases —some of which have been studied before, while most are new. These general results are presented in this journal because it may thereby reach a wider audience.

In this section we review both standard and pre- and post-selected (PPS) measurements, with the emphasis on weak PPS measurements, some of the results of this section being original. In the following sections, we generalize the theory of Sec. 1 and, in particular, develop a nonperturbative theory of weak PPS measurements. Some important symbols used in this paper, with their description and the places where they are defined, are listed in Tables 1 and 2.

1.1. Measurement in quantum mechanics

The issue of measurement is of fundamental significance in quantum mechanics (see, e.g., Refs. [1–7]). Recent developments in fabricating ever smaller nano-devices as well as in quantum information processing (see, e.g., Refs. [8–17]) have made it more important to understand quantum measurement.

The mathematical apparatus of quantum mechanics and its (Copenhagen) interpretation were created about eighty years ago, and since then they were confirmed in a countless number of experiments in various arias of physics. In spite of this, a complete understanding of quantum mechanics has not been achieved yet. From time to time, there occur revelations of phenomena which illuminate from an unexpected side the nonclassical nature of quantum mechanics and thus deepen our understanding of this discipline. Examples include experiments on Bell-inequality violations [18–23], which show the impossibility of local hidden-variable theories, and the emerging fields of quantum computation and quantum communication [8], where tasks which are believed to be impossible or very difficult to solve in the realm of the classical world were shown to be solvable. Weak values of physical quantities [24] are another example of nonclassical phenomena with unexpected results, as discussed below.

In quantum mechanics, each physical quantity A is described by a Hermitian operator $\hat{A}$ in the Hilbert space of a quantum system S. Ideal (or projective or strong) measurements of a system S are described by the projection postulate. Let the operator $\hat{A}$ have discrete, nondegenerate eigenvalues a_i and corresponding eigenvectors $|a_i\rangle$, and let the system S be in the state ρ. Then the projection postulate states that each measurement of A yields the value a_i with probability

$$P_i = \langle a_i|\rho|a_i\rangle \tag{1.1}$$

and that due to this measurement the state of the system becomes $|a_i\rangle$ (the so called wave-function collapse).

When the operator $\hat{A}$ has degenerate eigenvalues, the projection postulate is not essentially different, as follows. A general Hermitian operator $\hat{A}$ with discrete eigenvalues has the spectral decomposition

$$\hat{A} = \sum_i a_i \, \Pi_i, \tag{1.2}$$

Symbol	Description	Defined in:
A	A physical quantity for the system S	Sec. 1.1
$\hat{A}$	The operator for A	Sec. 1.1
A_w	The weak value of A	Eqs. (1.36), (1.58), (13.13)
$A_w^{(1,1)}$	The associated weak value of A	Eqs. (5.4), (13.15)
a	The (proper) amplification coefficient for the linear and strongly-nonlinear regimes	Sec. 4.6.1
a_T	The total amplification coefficient for the linear and strongly-nonlinear regimes	Eq. (4.55)
a'	The (proper) amplification coefficient for the inverted region	Eq. (4.91)
a'_T	The total amplification coefficient for the inverted region	Eq. (4.95)
b	The parameter characterizing the quadratic phase	After Eq. (1.49)
E	The POVM operator corresponding to the post-selection	Sec. 1.3.2
F	The input meter variable	After Eq. (1.8)
$\hat{F}$	The operator for F	After Eq. (1.8)
F_c	The "centered" variable F	After Eq. (4.3)
f	The enhancement factor	Eq. (4.53)
I_{M}	The identity operator for the meter M	After Eq. (3.5)
I_{S}	The identity operator for the system S	After Eq. (1.3)
N_0	The minimum ensemble size	Secs. 2.2, 4.9
$\overline{O}$	The average of the operator O over the initial state of the system or meter	Footnote 3
p	The meter momentum	Sec. 1.2.2
q	The meter coordinate	Sec. 1.2.2
R	The pointer (or output) meter variable	After Eq. (1.11)
$\hat{R}$	The operator for R	Footnote 1
R_c	The "centered" variable R	Before Eq. (3.9)
$\overline{R}_f$	The average pointer value for a standard measurement	Eq. (2.1)
$\overline{R}_s$	The average pointer value for a PPS measurement	Sec. 1.3.4
$\mathcal{R}$	The signal-to-noise ratio for quantum noise	Eq. (4.76)
U	The unitary transformation due to the system-meter coupling	Eq. (1.10)

Table 1: The list of the important symbols used in this paper, their description, and the places where they are defined. Part 1—Latin letters.

where $a_i \neq a_j$ for $i \neq j$ and Π_i is the projection operator on the subspace of eigenstates with the eigenvalue a_i. The set of all Π_i is the projection-valued measure associated with the measurement of A, the projectors Π_i possessing the properties

$$\Pi_i \Pi_j = \Pi_i \, \delta_{ij}, \qquad \sum_j \Pi_j = I_{\mathrm{S}}, \tag{1.3}$$

where δ_{ij} is the Kronecker symbol and I_{S} is the identity operator for the system. A projective measurement of the quantity A yields an eigenvalue a_i with probability

$$P_i = \mathrm{Tr}\,(\Pi_i \, \rho), \tag{1.4}$$

leaving the system in the state

$$\rho_i = \frac{\Pi_i \, \rho \, \Pi_i}{\mathrm{Tr}\,(\Pi_i \, \rho)}. \tag{1.5}$$

Note that for a degenerate a_i, the state ρ_i is generally not known.

A peculiar feature of quantum mechanics is that a measurement changes the state of the measured system [cf. Eq. (1.5)]. As a result, consecutive measurements of a quantum system result in an evolution of the system, which is

Symbol	Description	Defined in:
γ	The strength of the system-meter coupling	Eq. (1.11)
ΔO	The uncertainty of the operator O	Footnote 3
$\Delta R_{\max}$	The shift of the maximum of the pointer distribution due to measurement	Sec. 1.4.2
$\zeta(p)$	The phase of the meter state in the momentum space	Eq. (7.11)
θ	The argument of the weak value	Eq. (4.14)
θ_0	The argument of $\overline{R_c F}$	Eq. (4.14)
μ	The small parameter for weak PPS measurements	Eq. (4.5)
μ_0	The measurement strength	Eq. (4.9)
μ_1	The strength of the unitary transformation due to $\bar{F}$	Eq. (4.10)
$\xi(q)$	The phase of the meter state in the coordinate space	Eq. (7.11)
Π_ϕ	Projector on the state $\lvert\phi\rangle$	Eq. (1.22)
ρ	The preselected (possibly mixed) state of the system	Sec. 1.2.1
ρ_{M}	The initial (possibly mixed) state of the meter	Sec. 1.2.1
σ_{FR}	The covariance for the meter variables F and R	Eq. (4.15)
$\Phi_s(R)$	The pointer distribution after a measurement	Sec. 1.3.4
$\lvert\phi\rangle$	The post-selected state of the system	Sec. 1.3.1
$\lvert\psi\rangle$	The (pure) preselected state of the system	Sec. 1.2.1
$\lvert\psi_{\mathrm{M}}\rangle$	The (pure) initial state of the meter	Sec. 1.2.1

Table 2: The list of the important symbols used in this paper, their description, and the places where they are defined. Part 2—Greek and Latin letters.

basically different from the unitary evolution due to the Hamiltonian. The measurement-induced evolution is a purely quantum phenomenon. This evolution is generally random.

Thus, quantum measurements can play, at least, two fundamentally different roles. One role is proper measurements, i.e., obtaining information on the values of physical observables. The other role is generating an evolution of the quantum system. An example of the second role is the possibility to transform an arbitrary state of a quantum system to any other state with a probability arbitrarily close to one by means of a sufficiently large number of projective measurements [1]. Generally, the evolution of a quantum system is generated both by the Hamiltonian and by measurements. Examples of evolution driven simultaneously by the Hamiltonian and frequent measurements are the quantum Zeno and anti-Zeno effects [25–37].

The situations where measurements play both roles simultaneously are especially interesting. One example is the conditional evolution due to post-selected measurements. In this case the information provided by the measurements is used to choose only a subset of realizations of the measurement-induced random evolution. Postselection has recently grown in importance as a tool in fields such as quantum information, e.g., for linear optics quantum computation [38], where it is used to implement quantum gates. Another example where measurements play both roles is cluster-state computing [39–45], where in a series of measurements the second and subsequent measurements are chosen using the information provided by the previous measurements in order to achieve the required evolution. As an additional example, we mention the problem of preparing an arbitrary state of a quantum system by a restricted set of measurements [46, 47].

In recent decades, there have appeared generalizations of the projection postulate to non-ideal and weak measurements [8, 48, 49]. In particular, when the state of the system after the measurement is not important, the measurement in the most general case is described by a positive operator valued measure (POVM) $\{E_k\}$, where E_k are Hermitian operators with nonnegative eigenvalues satisfying the relation

$$\sum_k E_k = I_{\mathrm{S}}. \tag{1.6}$$

The operator E_k determines probability of kth measurement outcome by

$$P_k = \mathrm{Tr}\,(E_k\,\rho). \tag{1.7}$$

Note that the above generalizations do not change the postulates of quantum mechanics. Namely, the most general measurement is *equivalent to a projective measurement* of a composite system consisting of the system S and an auxiliary system [8, 48, 50].

The measurement-induced change of the state (measurement backaction) is commensurate with the measurement strength [51], so that weak measurements change the state weakly. Recently, significant attention has been given to the subject of multiple and continuous weak measurements, and many interesting topics were touched upon, such as measurement-induced decoherence, interplay of the unitary evolution and measurement backaction, quantum feedback control, etc. [52–65].

Pre- and post-selected (PPS) measurements, which are of primary interest here, were introduced by Aharonov, Bergmann, and Lebowitz (ABL) [66] in an attempt to achieve a better understanding of the role of measurements in quantum mechanics. PPS measurements are performed on ensembles of quantum systems chosen (pre- and post-selected) in the given initial and final states. In particular, PPS measurements and the closely related two-wave-functions formalism were applied for an analysis of time symmetry in the quantum process of measurement [67–69]. In Ref. [66], ABL considered only strong PPS measurements.

As an important extension of the ABL theory [66], Aharonov, Albert, and Vaidman (AAV) [24] introduced the concept of weak PPS measurements. Such measurements of an observable A produce the so called weak value A_w, which has unusual properties. In particular, generally a weak value is a complex number, and its magnitude is unbounded, so that $\mathrm{Re}\,A_w$ can be far outside the range of eigenvalues of the operator $\hat{A}$. Unusual (or strange) weak values, i.e., weak values that are complex or outside the spectrum of $\hat{A}$ were observed in a number of experiments [70–91].

It has been shown that, at least in some cases, unusual weak values cannot be explained classically. In particular, as shown in Ref. [92], a negative weak value of the energy of an oscillator contradicts all classical models; Johansen and Luis [92] also proposed a method for measuring such a value in a coherent state of the radiation field. Furthermore, as shown by Williams and Jordan [93], there is a one-to-one correlation between achieving real unusual weak values A_w for a projection of a spin 1/2 (i.e., A_w such that $|A_w| > 1/2$) and violating the Leggett-Garg inequality for a qubit [94–98], i.e., violating one or both of the assumptions required for classicality: macrorealism and a noninvasive detector. This relation between weak values and the Leggett-Garg inequality violations was verified experimentally in Ref. [88].

The unusual properties of weak values initially gave rise to controversy over their meaning and significance [99, 100]. However, subsequent research has made significant progress in elucidating the interpretation of weak values and indicating a variety of situations where they provide interesting physical insights [67, 76, 79, 81, 82, 90, 101, 102]. Moreover, irrespective of the interpretation of unusual weak values, they have proved clearly useful in such important physical phenomena as signal amplification and superluminal propagation.

Weak values are of significant current interest. They were discussed extensively [92, 101, 103–122] and reviewed in Refs. [67–69]. Weak values were measured in a number of experiments [70–91], primarily in the field of optics, though one of the early experiments was in NMR [71]. There are recent proposals for the observation of weak values using electrons in solids [93, 123, 124] and photons and atoms [121]. The experiments included applications to metrology [70, 80, 83–86, 89], optical communications [74, 75], and Hardy's paradox [81, 82].

In the rest of Sec. 1 we review PPS measurements, whereas in subsequent sections we extend the theory of PPS measurements, the emphasis being on developing a nonperturbative theory of weak PPS measurements.

1.2. Standard quantum measurements of arbitrary strength

Here the term "standard measurement" refers to measurement of a physical quantity A without a post-selection. Standard measurements may be ideal (i.e., projective or strong) or non-ideal, with an arbitrary measurement strength (e.g., standard measurements can be weak). Standard measurements are discussed here with the help of the von-Neumann-like measurement scheme.

1.2.1. Von-Neumann-like measurement scheme

Quantum measurements are usually performed in the laboratory by bringing the system under study into an interaction with the measuring apparatus (the meter) and then measuring the meter. Von Neumann developed a model which describes how the above process produces projective measurements [1]. Many studies of quantum measurements are based on the von Neumann measurement model or its generalizations.

Consider the von-Neumann-like measurement scheme, which is a direct extension of the original von Neumann measurement model [1]. In this scheme, the quantum system S and the measurement apparatus M (meter) are coupled by the interaction described by the Hamiltonian

$$H = g(t)\,\hat{A} \otimes \hat{F}, \tag{1.8}$$

where $g(t)$ is the instantaneous coupling rate, which differs from zero in the interval $(t_\mathrm{i}, t_\mathrm{f})$, $\hat{A}$ is the operator representing the measured quantity A, and $\hat{F}$ is the operator[1] corresponding to the "input" meter variable F.

We assume that initially (at $t = 0 \leq t_\mathrm{i}$) the system and meter are uncorrelated, being in the pure states $|\psi\rangle$ and $|\psi_\mathrm{M}\rangle$, respectively (the case of arbitrary system and meter states, ρ and ρ_M, is discussed in Sec. 2). Then for $t \geq t_\mathrm{f}$ the state of the system and meter becomes correlated,

$$|\psi_f\rangle = U\,|\psi\rangle|\psi_\mathrm{M}\rangle, \tag{1.9}$$

by the unitary transformation

$$U = \exp(-i\gamma\,\hat{A} \otimes \hat{F}), \tag{1.10}$$

where γ is the coupling strength,

$$\gamma = \int_{t_\mathrm{i}}^{t_\mathrm{f}} g(t)\,dt \tag{1.11}$$

(we use measurement units in which $\hbar = 1$). Finally, a measurement of the "output" meter observable R (the "pointer variable") at $t_\mathrm{M} \geq t_\mathrm{f}$ provides information about the system. This process is depicted schematically in Fig. 1. (In Figs. 1 and 3 the standard quantum-circuit notation [8] is used; in particular, double lines carry classical information.) Here we make the common assumption that the free Hamiltonians of the system and meter can be neglected [1, 24]; the effects of the free Hamiltonians of the system and meter are discussed in Secs. 6 and 7.2.4.

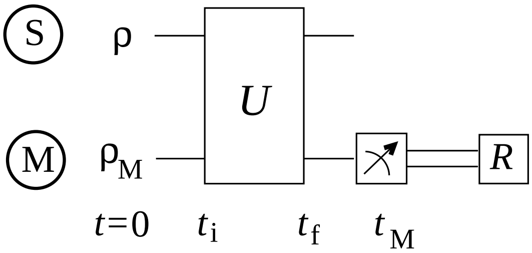

Figure 1: Schematic diagram for standard quantum measurements of arbitrary strength. The system S is correlated with the meter M by the unitary transformation U in Eq. (1.10), and then a projective measurement of the meter pointer variable R is performed. The double line carries classical information. Initially ($t = 0$), the system state is ρ and the system state is ρ_M.

1.2.2. Canonically conjugate meter variables

The problem becomes drastically simplified, when the meter is a continuous-variable system, e.g., a free linearly moving particle, whereas F and R are canonically conjugate variables. We also make the customary assumption that the free Hamiltonian of the meter can be neglected, which implies that the particle mass is very large. As in the original von Neumann model [1], we assume that F is the momentum p and R is the coordinate q,

---

[1] Generally, we denote a Hermitian operator and the corresponding physical quantity by the same symbol, the exception being only the notation for the operators $\hat{A}$, $\hat{F}$ and $\hat{R}$ of the quantities A, F, and R.

$$F = p, \quad R = q. \tag{1.12}$$

To simplify the problem even more, we assume here that $\hat{A}$ has discrete and nondegenerate eigenvalues. Then, expanding $|\psi\rangle$ in the basis of the eigenvectors of $\hat{A}$, $|\psi\rangle = \sum_j \alpha_j |a_j\rangle$, Eq. (1.9) yields

$$\begin{aligned} |\psi_f(q)\rangle &= \exp(-i\gamma\hat{A}\otimes p)\sum_j \alpha_j\,|a_j\rangle\,\psi_{\mathrm{M}}(q) \\ &= \sum_j \alpha_j \exp(-i\gamma a_j p)\,\psi_{\mathrm{M}}(q)\,|a_j\rangle \\ &= \sum_j \alpha_j\,\psi_{\mathrm{M}}(q-\gamma a_j)\,|a_j\rangle, \end{aligned} \tag{1.13}$$

where $|\psi_f(q)\rangle = \langle q|\psi_f\rangle$, and $\psi_{\mathrm{M}}(q) = \langle q|\psi_{\mathrm{M}}\rangle$. A projective measurement of q at $t \geq t_{\mathrm{f}}$ results,[2] to a very good approximation, in a projective measurement of A, when different wavepackets $\psi_{\mathrm{M}}(p-\gamma a_j)$ practically do not overlap in Eq. (1.13). This is realized when the coupling is sufficiently strong,

$$|\gamma|\,(\delta a) \gg \Delta q, \tag{1.14}$$

where δa is the minimal distance between different a_j and Δq is the uncertainty[3] of q at $t = 0$.

1.2.3. Non-ideal and weak standard measurements

When the coupling is not sufficiently strong, a measurement is non-ideal (partial). However, for any γ one can still measure the average (expectation value) of A over the initial state $|\psi\rangle$,

$$\bar{A} = \langle\psi|\hat{A}|\psi\rangle, \tag{1.15}$$

since Eq. (1.13) implies that [24]

$$\bar{q}_f - \bar{q} = \gamma\bar{A}, \tag{1.16}$$

where $\bar{q}$ and $\bar{q}_f$ are the averages of q at $t = 0$ and $t \geq t_{\mathrm{f}}$, respectively.

A standard measurement with a small coupling strength γ is called a weak standard measurement or simply a weak measurement.

Note that a weak measurement of one system provides almost no information, since the average pointer deflection (1.16) is much less than the pointer uncertainty. Therefore, to obtain $\bar{A}$, one must perform measurements on each member of a sufficiently large ensemble of systems prepared (preselected) in the same state and then average the results of the measurements. The measurement error decreases when increasing the size of the ensemble and thus can be made arbitrarily small. The way of extracting the expectation value $\bar{A}$ in weak measurements differs conceptually from that in projective measurements. Indeed, projective measurements provide probabilities P_i of the eigenvalues a_i of an observable A, and $\bar{A}$ is obtained from the standard definition of expectation value by the formula

$$\bar{A} = \sum_i a_i P_i. \tag{1.17}$$

In contrast, in weak measurements $\bar{A}$ is extracted by Eq. (1.16) directly, without measuring each P_i individually.

In the general case, when the input and output meter variables F and R are not canonically conjugate to each other, Eq. (1.16) does not hold for arbitrary γ. However, for a sufficiently small coupling strength, when the linear response holds, the average deflection of the pointer R is generally proportional to $\bar{A}$, i.e., weak standard measurements are still possible (see Sec. 2 for further details).

---

[2] Since q is a continuous variable, projective measurement of q always has a finite error. For our purposes, this error should be much less than $|\gamma|\,(\delta a)$.

[3] The average of an arbitrary variable O, described by the operator $\hat{O}$, in a state ρ_0 is given by $\bar{O} = \mathrm{Tr}(\hat{O}\rho_0)$ (in particular, for a pure state $|\Psi\rangle$, $\bar{O} = \langle\Psi|\hat{O}|\Psi\rangle$), whereas the uncertainty $\Delta O = (\overline{O^2} - \bar{O}^2)^{1/2}$.

1.3. Measurements with pre- and post-selection

1.3.1. General considerations

In classical mechanics, knowing the state of an isolated system at some moment as well as the Hamiltonian of the system, one can completely determine the motion for all times, both in the future and in the past. In quantum mechanics, only a fraction of the observables can be completely determined in a given state of a system, other observables being not determined, which is demonstrated explicitly by the Heisenberg uncertainty principle. This makes the evolution of the system non-deterministic, i.e., probabilistic.

In the usual approach, the (random) behavior of a quantum system is studied assuming the knowledge of the state at some initial time t_0. As an extension of the usual approach, ABL [66] asked the question: How does the description of a quantum system in the interval (t_0, t_S) change, when not only the initial state at time t_0 but also the final state at time t_S are known, so that one has a more complete information on the system than in the usual approach?

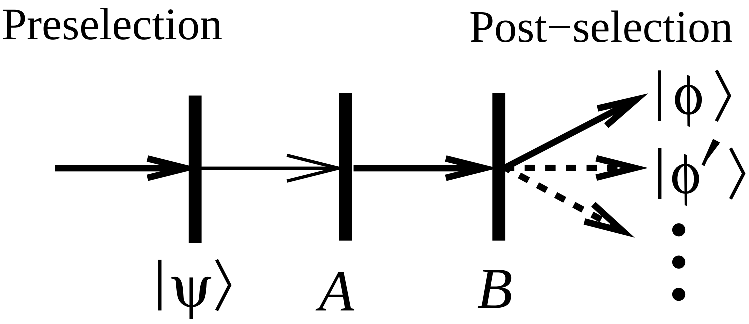

Figure 2: A schematic diagram of pre- and post-selected quantum measurements. It involves the preselection of the initial state $|\psi\rangle$, measurement of a variable A (the thin arrow), and the postselection by means of a projective measurement of a variable B and selecting the systems in a final state $|\phi\rangle$.

To answer this question, ABL [66] devised pre- and post-selected measurements described as follows (see Fig. 2). Consider an ensemble of quantum systems prepared initially (preselected) in the same state $|\psi\rangle$. Each member of the ensemble is subjected to a measurement of the quantity A, which may be strong or weak (the thin arrow before A in Fig. 2). Then, at a later moment, a final projective measurement of a variable B with a discrete, nondegenerate spectrum is performed, which, in view of the projection postulate (Sec. 1.1), leaves the system in one of the orthogonal states $|\phi\rangle, |\phi'\rangle, \ldots$. The ensemble of the system can be broken into subensembles with different final (post-selected) states $|\phi\rangle, |\phi'\rangle, \ldots$; such a subensemble is called a pre- and post-selected ensemble. The statistical distribution of results of the measurement of A are different for each subensemble and different from the statistical distribution over the whole ensemble. Thus, the possible results of the measurement of A depend both on the initial and the final states of the system. A measurement in a pre- and post-selected ensemble is called a PPS measurement. Above we considered one measurement in a pre- and post-selected ensemble, but there may be two or more such measurements of some observables $A, A', \ldots$ [66, 68].

Until now we discussed *pure* PPS ensembles, i.e., ensembles with pure initial and final states. More generally, we will consider also *mixed* PPS ensembles, where the preselection is incomplete, i.e., the initial state ρ is mixed. In addition to the aforementioned preselected and PPS ensembles, there is also a third type of ensemble—post-selected only ensembles [67], i.e., ensembles of systems with a pure final state $|\phi\rangle$ and the completely mixed initial state

$$\rho_{\text{c.m.}} = \frac{I_S}{d}, \tag{1.18}$$

where d is the dimension of the Hilbert space of the system. Post-selected ensembles are the limiting case $\rho \to \rho_{\text{c.m.}}$ of mixed PPS ensembles.

Another important generalization of PPS ensembles is for the case where the post-selection measurement is a projection on a *degenerate* eigenvalue of a variable B. Such a measurement is generally not "complete" in the sense that it does not specify a single post-selection state [67, 125]. Indeed, in this case the post-selection state generally depends on the result of the intermediate measurement of A, according to the projection postulate, Eq. (1.5).

This generalization allows one to connect PPS and preselected ensembles. Namely, when B is a multiple of the unity operator, the measurement of B does not provide new information which could be used for the post-selection, and a PPS ensemble becomes a preselected (only) ensemble. As a result, in this case PPS measurements coincide with standard measurements, as was formally proved in Ref. [67] for the cases of strong and weak measurements with a pure preselected state (see also Sec. 1.3.2) and will be proved in Sec. 13.2 for measurements of arbitrary intensity with an arbitrary preselected state. Furthermore, we note that in the most general case, a PPS ensemble is obtained by performing a general post-selection measurement described by a POVM; then the PPS ensemble includes the systems with a certain measurement outcome.

PPS ensembles have unusual properties. In particular, the observables which have an eigenstate $|\psi\rangle$ or $|\phi\rangle$ have definite values in a pure PPS ensemble [126]. Hence, when $|\phi\rangle \neq |\psi\rangle$, there are, at least, two non-commuting observables with no common eigenstates (e.g., components of spin 1/2), which have definite values in a pure PPS ensemble. This is in sharp contrast with systems preselected only in a state $|\psi\rangle$ (post-selected only in a state $|\phi\rangle$), for which solely the observables with the common eigenstate $|\psi\rangle$ ($|\phi\rangle$) have definite values.

Moreover, not only PPS ensembles but also PPS measurements have unusual properties. These properties generally depend on the measurement strength. One such unusual property, peculiar for strong PPS measurements but not for weak PPS measurements, will be discussed in Sec. 1.3.3.

1.3.2. Strong (ideal) PPS measurements

Let us discuss PPS measurements in more detail. Consider first strong (ideal) PPS measurements.

Let an ensemble of quantum systems be prepared (preselected) in a (pure or mixed) state ρ. According to the projection postulate (Sec. 1.1), a projective measurement of an observable A with discrete eigenvalues provides an eigenvalue a_i with probability P_i (1.4) and leaves the system in the state ρ_i (1.5). In the most general case, the final measurement is characterized by a POVM (see Sec. (1.3.1)), and the PPS ensemble includes systems with a certain measurement outcome which is characterized by a POVM operator E and occurs with probability $\mathrm{Tr}\,(E\rho_i)$ [cf. Eq. (1.7)]. The joint probability to measure the eigenvalue a_i of A and to observe the outcome corresponding to E is the product of the respective probabilities,

$$P_{iE} = P_i\,\mathrm{Tr}\,(E\rho_i) = \mathrm{Tr}\,(E\Pi_i\rho\Pi_i). \tag{1.19}$$

As follows from Eq. (1.19) and Bayes' theorem, the probability that a projective measurement of A yields the value a_i, provided the system is post-selected by means of E, is

$$P_{i|E} = \frac{P_{iE}}{\sum_j P_{jE}} = \frac{\mathrm{Tr}\,(E\Pi_i\rho\Pi_i)}{\sum_j \mathrm{Tr}\,(E\Pi_j\rho\Pi_j)}. \tag{1.20}$$

This equation is an extension of the ABL formula [66, 68] to general E and ρ. It is obvious from the first equality in Eq. (1.20) that the probability distribution $P_{i|\phi}$ is normalized to one,

$$\sum_i P_{i|\phi} = 1. \tag{1.21}$$

When E is the unity operator, strong PPS measurements become strong standard (not post-selected) measurements (see Sec. 1.3.1), and correspondingly Eq. (1.20) reduces to Eq. (1.4).

Henceforth (with the exception of Sec. 13), we will assume that the post-selection measurement is a projection on a nondegenerate, discrete eigenvalue of a variable B. Such a measurement is "complete" in the sense that it completely specifies the post-selection state $|\phi\rangle$. In this case,

$$E = \Pi_\phi \equiv |\phi\rangle\langle\phi|, \tag{1.22}$$

and Eq. (1.20) becomes the probability that a projective measurement of A yields the value a_i, provided the system is post-selected in the state $|\phi\rangle$,

$$P_{i|\phi} = \frac{\langle\phi|\,\Pi_i\,\rho\,\Pi_i\,|\phi\rangle}{\sum_j \langle\phi|\,\Pi_j\,\rho\,\Pi_j\,|\phi\rangle}. \tag{1.23}$$

Consider now special cases. For a pure initial state $\rho = |\psi\rangle\langle\psi|$, Eq. (1.23) becomes [126]

$$P_{i|\phi} = \frac{|\langle\phi|\,\Pi_i\,|\psi\rangle|^2}{\sum_j |\langle\phi|\,\Pi_j\,|\psi\rangle|^2}. \tag{1.24}$$

For a nondegenerate eigenvalue a_i, one has $\Pi_i = |a_i\rangle\langle a_i|$, and Eq. (1.23) becomes

$$P_{i|\phi} = \frac{|\langle\phi|a_i\rangle|^2\,\langle a_i|\rho|a_i\rangle}{\sum_j |\langle\phi|a_j\rangle|^2\,\langle a_i|\rho|a_i\rangle}. \tag{1.25}$$

In the case of a pure preselected state $|\psi\rangle$, Eq. (1.25) yields the result

$$P_{i|\phi} = \frac{|\langle\phi|a_i\rangle\,\langle a_i|\psi\rangle|^2}{\sum_j |\langle\phi|a_j\rangle\,\langle a_j|\psi\rangle|^2}. \tag{1.26}$$

This equation is a special case of the ABL formula [66, 68] for the vanishing system Hamiltonian.

In the case when the pre- and post-selected states are pure, strong PPS measurements are invariant under time reversal [66–68], which is seen from the fact that the ABL formulas (1.24) and (1.26) are symmetric with respect to an exchange of the initial and final states. In Sec. 13.4, we obtain a more general time-symmetry relation, which holds for PPS measurements of arbitrary strength and for arbitrary (possibly mixed) pre- and post-selected states.

In the limit $\rho \to \rho_{\text{c.m.}}$ [see Eq. (1.18)], Eq. (1.23) provides the following probabilities of measurement outcomes for an ensemble post-selected in the state $|\phi\rangle$,

$$P_{i|\phi} = \langle\phi|\Pi_i|\phi\rangle. \tag{1.27}$$

This formula coincides with the result (1.4) with $\rho = |\phi\rangle\langle\phi|$. Thus, the probability distribution of the outcomes of a measurement performed at time $t,\ t_0 < t < t_S$, in a *post-selected* ensemble is identical to that for the system *preselected* in the state $|\phi\rangle$ [67]. A similar property holds also for weak PPS measurements (see paragraph *f.* in Sec. 1.5.2).

1.3.3. Contextuality of strong PPS measurements

A peculiar property of strong PPS measurements is that the probabilities (1.25), (1.26), and (1.24) are context-dependent, i.e., the probability of an outcome of a strong PPS measurement depends not only on the projector associated with that outcome but on the entire projection-valued measure associated with the measurement [126, 127].

This property is illustrated by the three-box problem [126]. Consider a particle which can be located in one of three boxes. The state of the particle when it is in box i is denoted by $|i\rangle$. At time t_0 the particle is prepared in the state

$$|\psi\rangle = \frac{1}{\sqrt{3}}\,(|1\rangle + |2\rangle + |3\rangle), \tag{1.28}$$

and at a later time t_S the particle is found in the state

$$|\phi\rangle = \frac{1}{\sqrt{3}}\,(|1\rangle + |2\rangle - |3\rangle). \tag{1.29}$$

We assume that in the time interval $[t_0, t_S]$ the Hamiltonian is zero. Opening box i at time $t,\ t_0 < t < t_S$, corresponds to measuring the projection operator

$$\Pi_i = |i\rangle\langle i|. \tag{1.30}$$

The corresponding operators entering Eq. (1.24) are Π_i and

$$\tilde{\Pi}_i = \sum_{j\neq i} |j\rangle\langle j|. \tag{1.31}$$

Hence, one obtains from Eq. (1.24) that the probability to find the particle in box 1, without opening the other boxes, is

$$\text{prob}\,(\Pi_1 = 1) = \frac{|\langle\phi|1\rangle\langle 1|\psi\rangle|^2}{|\langle\phi|1\rangle\langle 1|\psi\rangle|^2 + |\langle\phi|2\rangle\langle 2|\psi\rangle + \langle\phi|3\rangle\langle 3|\psi\rangle|^2} = \frac{(1/3)^2}{(1/3)^2 + (1/3 - 1/3)^2} = 1. \tag{1.32}$$

Similarly,

$$\text{prob}\,(\Pi_2 = 1) = 1 \tag{1.33}$$

and prob $(\Pi_3 = 1) = 1/5$. Thus, we obtain a paradoxical result that on opening any of boxes 1 and 2 one is certain to find the particle in the opened box. The results (1.32) and (1.33) were verified experimentally [76].

For comparison, consider opening the three boxes simultaneously, which corresponds to measuring a nondegenerate observable with the eigenstates $|1\rangle$, $|2\rangle$, and $|3\rangle$. Now the probability to find the particle in box i is given by Eq. (1.24), where the projection-valued measure is (Π_1, Π_2, Π_3) [Eq. (1.30)], or, equivalently, by Eq. (1.26), yielding

$$P_{1|\phi} = P_{2|\phi} = P_{3|\phi} = \frac{1}{3}. \tag{1.34}$$

The discrepancy between Eqs. (1.32) and (1.33), on the one hand, and, respectively, the probabilities $P_{1|\phi}$ and $P_{2|\phi}$ in Eq. (1.34), on the other hand, shows explicitly the contextuality of strong PPS measurements.

1.3.4. Model for PPS measurements of arbitrary strength

Non-ideal PPS measurements can be discussed by analogy with non-ideal standard measurements (Sec. 1.2) [24], with the help of a suitably generalized von Neumann model, as follows (see Fig. 3). Let us consider an ensemble of pairs consisting of a system and a meter in the pure states $|\psi\rangle$ and $|\psi_{\rm M}\rangle$, respectively (extensions to the cases of arbitrary states ρ and/or $\rho_{\rm M}$ are given in Secs. 3-5). For each system-meter pair the coupling (1.8) is turned on in the interval $(t_{\rm i}, t_{\rm f})$; then a PPS ensemble is formed by performing a projective measurement of a variable B for each system at $t_{\rm S} > t_{\rm f}$ and selecting for further consideration only the systems which are in the eigenstate $|\phi\rangle$ of B. A PPS measurement is completed after measuring the pointer observable of the meters at $t_{\rm M} > t_{\rm f}$ and performing the statistical analysis of results in the PPS ensemble, with the goal, e,g., to obtain the average pointer value $\overline{R}_s$ or the distribution of the pointer values $\Phi_s(R)$.

Note that the meters can be measured both after ($t_{\rm M} > t_{\rm S}$) and before ($t_{\rm M} < t_{\rm S}$) the post-selection. The only difference is that for $t_{\rm M} > t_{\rm S}$ it is sufficient to measure only the meters corresponding to the PPS ensemble, whereas for $t_{\rm M} < t_{\rm S}$ all meters in the initial ensemble should be measured, but in the statistical analysis after the post-selection (at $t > t_{\rm S}$) only the meters corresponding to the PPS ensemble should be included.

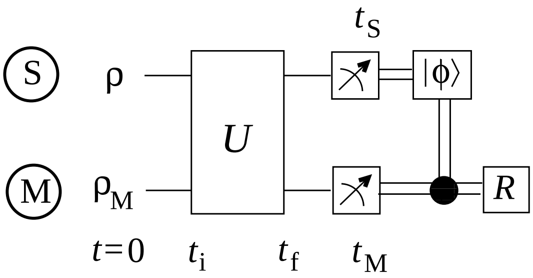

Figure 3: Schematic diagram of a model for pre- and post-selected quantum measurements. This approach differs from the von Neumann scheme in Fig. 1 in that the measurement of R is conditioned ("post-selected") on the measurement of the system S in a state $|\phi\rangle$.

1.4. Weak PPS measurements

1.4.1. Simple approach

Let us now consider weak PPS measurements. Here we describe the simple approach [24, 103, 104], which has been used in most studies studies on weak values; a more general method is discussed in the following sections. As in Secs. 1.2.2-1.2.3, we consider the coupling (1.8) with $F = p$ (the case $F = q$ is discussed in Sec. 1.4.2). When $t_{\rm M} > t_{\rm S}$, then after the post-selection but before the measurement of the meter (for $t_{\rm S} < t < t_{\rm M}$), the (unnormalized) meter state is, in view of Eqs. (1.9) and (1.10),

$$\begin{aligned}\langle\phi|\psi_f(p)\rangle &= \langle\phi|\exp(-i\gamma\hat{A}\otimes p)\,|\psi\rangle\,\psi_{\mathrm{M}}(p)\\ &\approx \langle\phi|1-i\gamma\hat{A}\otimes p\,|\psi\rangle\,\psi_{\mathrm{M}}(p)\\ &= \langle\phi|\psi\rangle(1-i\gamma A_w p)\,\psi_{\mathrm{M}}(p)\\ &\approx \langle\phi|\psi\rangle\exp(-i\gamma A_w p)\,\psi_{\mathrm{M}}(p).\end{aligned} \tag{1.35}$$

Here $|\psi_f(p)\rangle = \langle p|\psi_f\rangle$, $\psi_{\mathrm{M}}(p) = \langle p|\psi_{\mathrm{M}}\rangle$, and A_w is called the weak value of A [24],

$$A_w = \frac{A_{\phi\psi}}{\langle\phi|\psi\rangle}, \tag{1.36}$$

where $A_{\phi\psi} = \langle\phi|\hat{A}|\psi\rangle$. The approximations in Eq. (1.35) hold up to first order in γ; they are discussed below.

To proceed further, it is convenient to assume that $\psi_{\mathrm{M}}(p)$ is a complex Gaussian with a phase linear in p,

$$\psi_{\mathrm{M}}(p) = Z_p \exp\left[-\frac{(p-\bar{p})^2}{4(\Delta p)^2} - i\bar{q}p\right], \tag{1.37}$$

where $Z_p = (\sqrt{2\pi}/\Delta p)^{1/2}$, and $\bar{p}$ and Δp are, respectively, the average and the uncertainty of p at $t = 0$. The Fourier transform of Eq. (1.37) yields a Gaussian wavefunction $\psi_{\mathrm{M}}(q)$ with a phase linear in q,

$$\psi_{\mathrm{M}}(q) = Z_q \exp\left[-\frac{(q-\bar{q})^2}{4(\Delta q)^2} + i\bar{p}q\right], \tag{1.38}$$

where $Z_q = (\sqrt{2\pi}\Delta q)^{-1/2}$ and $\Delta q = (2\Delta p)^{-1}$.

Inserting Eq. (1.37) into Eq. (1.35) yields a Gaussian wavefunction which differs from the initial wavefunction (1.37) only by the average values of q and p, the shifts of $\bar{q}$ and $\bar{p}$ being determined by $\mathrm{Re}\,A_w$ and $\mathrm{Im}\,A_w$, respectively. As a result, a measurement of q provides a Gaussian distribution of q which is shifted relative to the initial distribution by the value

$$\Delta q_{\max} = \gamma\,\mathrm{Re}\,A_w, \tag{1.39}$$

whereas a measurement of p provides a Gaussian distribution shifted relative to the initial distribution by the value

$$\Delta p_{\max} = 2\gamma\,(\Delta p)^2\,\mathrm{Im}\,A_w. \tag{1.40}$$

In Eqs. (1.39) and (1.40) $\Delta q_{\max}$ and $\Delta p_{\max}$ denote the shift of the maximum of the corresponding distribution; these quantities are directly measurable in experiments. Since a weak PPS measurement does not change the Gaussian shape of the wavepackets in the coordinate and momentum spaces, the average values of the coordinate and the momentum are shifted by the values (1.39) and (1.40), respectively,

$$\bar{q}_s - \bar{q} = \gamma\,\mathrm{Re}\,A_w, \tag{1.41}$$

$$\bar{p}_s - \bar{p} = 2\gamma\,(\Delta p)^2\,\mathrm{Im}\,A_w, \tag{1.42}$$

where $\bar{q}_s$ and $\bar{p}_s$ are the post-selected averages of q and p.

Equations (1.41) and (1.42) show that weak PPS measurements in the linear-response (or AAV) regime provide the weak value A_w of the quantity A. Equations (1.41) and (1.42) look very similar to the result (1.16) of weak standard measurements. However, in contrast to standard measurements (Sec. 1.2), now not only q but also p contains information about the system.

The weak value has unusual properties, which drastically distinguish it from the expectation value of a variable (1.15) resulting from a standard measurement. The weak value diverges when the overlap $|\langle\phi|\psi\rangle|$ tends to zero. For instance, the weak value of a component of spin 1/2 can be equal to 100 [24]. Moreover, the weak value can be complex. The weak value will be discussed in more detail below.

The results (1.41) and (1.42) were obtained[4] by AAV [24] for real Gaussian functions $\psi_{\rm M}(p)$ and $\psi_{\rm M}(q)$, i.e., for $\overline{p} = \overline{q} = 0$. As shown above, Eqs. (1.41) and (1.42) also hold for Gaussians with a linear phase. Jozsa [110] considered the case of an arbitrary meter wavefunction and showed that generally there is an additional term, proportional to $\operatorname{Im} A_w$, on the right-hand side (rhs) of Eq. (1.41), whereas Eq. (1.42) remains valid in the general case.

Hosten and Kwiat [80] showed experimentally that the term proportional to $\operatorname{Im} A_w$ may arise in Eq. (1.41) due to the nonzero meter Hamiltonian; they utilized this term to achieve strong amplification in a measurement of a weak optical effect (for details see Sec. 7.2.4). Below we show that in the most general case, i.e., for arbitrary meter variables F and R, the term proportional to $\operatorname{Im} A_w$ arises in the linear-response regime whenever there is (classical) correlation between F and R (see Sec. 4.4 for more details), the presence of a nonzero meter Hamiltonian being only one of several possible ways to generate this correlation (see Sec. 7.2). Furthermore, below we show that a correlation between p and q arises whenever the phase of the wavefunction $\psi_{\rm M}(p)$ or $\psi_{\rm M}(q)$ is nonlinear in p or q, respectively (see Sec. 7.2, cf. also Sec. 1.4.2).

The conditions for the validity of Eqs. (1.41) and (1.42) were obtained in Ref. [103] for the special case $\overline{q} = \overline{p} = 0$. Namely, the first and second approximations in Eq. (1.35) hold, respectively, for

$$|\gamma| \left| \frac{(A^n)_{\phi\psi}}{A_{\phi\psi}} \right|^{1/(n-1)} \Delta p \ll 1 \quad (n = 2, 3, \ldots) \tag{1.43}$$

and

$$|\gamma A_w|\, \Delta p \ll 1. \tag{1.44}$$

Note that the results (1.41) and (1.42), as well as their generalizations mentioned above, hold up to first order in γ, i.e., in the linear-response regime. As a result, the weak value in these results is bounded by the condition (1.44). For any given γ, the condition (1.44) is always violated for a sufficiently small overlap $\langle\phi|\psi\rangle$. In this case, linear-response results are not applicable, even though the condition (1.43) holds, i.e., PPS measurements are weak. It would be of interest to obtain a simple and general theory of weak PPS measurements, which holds beyond the limits of the linear response and is correct to all orders in the weak value. Such a theory is developed and discussed in subsequent sections.

1.4.2. The pointer distribution

In addition to the average value of the pointer variable R, it is of interest to consider the probability distribution of the pointer values, since it is measured directly in experiments. For simplicity, we assume that the initial pointer distribution $\Phi(R)$ has a bell-like shape (e.g., Lorentzian or Gaussian).

Here we consider situations where the pointer distribution $\Phi_s(R)$, resulting from a weak PPS measurement in the linear-response regime, has the following property, which is advantageous for experimental realizations:
(i) $\Phi_s(R)$ is displaced with respect to the initial distribution $\Phi(R) = |\psi_{\rm M}(R)|^2$ *without a change of the shape* of the distribution (at least, for the central part of the distribution; tails of the distribution can be deformed by the measurement even in the linear-response regime, see Sec. 8.2 for details).
Property (i) implies also the following property:
(ii) The shift of the maximum of the distribution $\Delta R_{\rm max}$ equals the average pointer deflection,

$$\Delta R_{\rm max} = \overline{R}_s - \overline{R}. \tag{1.45}$$

Note, however, that property (ii) does not necessarily imply property (i). [The general case, where properties (i) and (ii) may not hold, is discussed in Sec. 8.2.]

In particular, properties (i) and (ii) hold in the following cases.

a. Real weak value. Let A_w be real, whereas $F = p$ and $R = q$. Then from Eq. (1.35) rewritten in the coordinate representation we obtain that

$$\begin{aligned} \langle\phi|\psi_f(q)\rangle &\approx \langle\phi|\psi\rangle \exp(-i\gamma A_w p)\, \psi_{\rm M}(q) \\ &= \langle\phi|\psi\rangle\, \psi_{\rm M}(q - \gamma A_w). \end{aligned} \tag{1.46}$$

---

[4] Actually Eqs. (1.41) and (1.42) differ somewhat from the AAV results [24] in that here the roles of p and q are exchanged in comparison to Ref. [24], as in some optical experiments [70, 80]. The original AAV results are given below by Eqs. (1.56) and (1.57).

Thus, when A_w is real, an arbitrary coordinate distribution is shifted, due to a weak measurement, by the value [80, 110]

$$\bar{q}_s - \bar{q} = \gamma A_w. \tag{1.47}$$

In particular, if the coordinate distribution is bell-like, we have

$$\Delta q_{\max} = \bar{q}_s - \bar{q} = \gamma A_w. \tag{1.48}$$

b. General complex Gaussian. The most general form of a complex Gaussian state is given by

$$\psi_{\mathrm{M}}(p) = Z_p \exp\left[-\frac{(1+ib)(p-\bar{p})^2}{4(\Delta p)^2} - i\bar{q}p\right]. \tag{1.49}$$

Here b is a real parameter characterizing the quadratic phase—the phase of the state (1.49) is a quadratic function of p, with the quadratic term proportional to the parameter b.

In coordinate space, a general Gaussian state has a similar form,

$$\psi_{\mathrm{M}}(q) = Z_q \exp\left[\frac{(ib-1)(q-\bar{q})^2}{4(\Delta q)^2} + i\bar{p}q\right], \tag{1.50}$$

where Δq is determined by the equality

$$\Delta p\, \Delta q = \frac{\sqrt{1+b^2}}{2}. \tag{1.51}$$

This equation has the meaning of the generalized uncertainty relation with the equals sign [cf. Eq. (7.25) below]. In Eq. (1.50), similarly to Eq. (1.49), the phase is a quadratic function of q, with the quadratic term proportional to b.

Now assume that $F = p$. Inserting Eq. (1.49) into Eq. (1.35) and performing some calculations yields a wavefunction of the same form as Eq. (1.49) with the only difference that $\bar{p}$ is shifted by the value (1.40), whereas $\bar{q}$ is shifted by the value

$$\Delta q_{\max} = \bar{q}_s - \bar{q} = \gamma\,(\mathrm{Re}\, A_w + b\, \mathrm{Im}\, A_w). \tag{1.52}$$

In other words, a weak PPS measurement shifts the Gaussian distributions of p and q, $|\psi_{\mathrm{M}}(p)|^2$ and $|\psi_{\mathrm{M}}(q)|^2$, without a change of the form, by the values (1.40) and (1.52), respectively.

The case of a Gaussian state with a zero or linear phase considered in Sec. 1.4.1 [see Eq. (1.39)] is obtained as a special case of the present case for $b = 0$. The term proportional to $\mathrm{Im}\, A_w$ in Eq. (1.52) arises due to a nonlinear (quadratic) phase.

It is often stated [67, 69, 80] that the imaginary part of the weak value does not affect the probability distribution of the meter coordinate, and $\mathrm{Im}\, A_w$ can be observed only in the distribution of the meter momentum. Equation (1.52) shows that this statement is not exact, since $\mathrm{Im}\, A_w$ enters the shift of the coordinate distribution for a general Gaussian wavefunction. The same holds for a general (non-Gaussian) meter state, as discussed in Sec. 8.2.

c. $R = F$ with a Gaussian distribution of F. When the pointer is the momentum or, more generally, $R = F$, where F is a continuous variable, one obtains, similarly to Eq. (1.35), that

$$\langle\phi|\psi_f(F)\rangle \approx \langle\phi|\psi\rangle \exp(-i\gamma A_w F)\, \psi_{\mathrm{M}}(F). \tag{1.53}$$

The square of the modulus of Eq. (1.53) is the unnormalized distribution of F modified by the measurement. When the initial distribution $\Phi(F) = |\psi_{\mathrm{M}}(F)|^2$ is a Gaussian, the distribution of F after the measurement is also a Gaussian, which differs from $\Phi(F)$ only by a shift of the center equal to

$$\Delta F_{\max} = \bar{F}_s - \bar{F} = 2\gamma\,(\Delta F)^2\, \mathrm{Im}\, A_w. \tag{1.54}$$

Equation (1.54) was proved above [see Eq. (1.40)] for the special case, when $F = p$ and $\psi_{\mathrm{M}}(p)$ is a general Gaussian, i.e., the phase of $\psi_{\mathrm{M}}(p)$ is at most quadratic. Here Eq. (1.54) is shown to be valid for an arbitrary phase of $\psi_{\mathrm{M}}(F)$.

In the above formulas for weak PPS measurements we assumed that $F = p$ [except for Eq. (1.54)]. It is easy to show that for $F = q$, the above formulas for $\bar{q}_s$, $\bar{p}_s$, $\Delta q_{\max}$, and $\Delta p_{\max}$ change according to the rule

$$p \leftrightarrow q, \qquad \mathrm{Re}\, A_w \to -\mathrm{Re}\, A_w. \tag{1.55}$$

For example, Eqs. (1.41) and (1.42) become [24]

$$\bar{p}_s - \bar{p} = -\gamma \operatorname{Re} A_w, \tag{1.56}$$

$$\bar{q}_s - \bar{q} = 2\gamma (\Delta q)^2 \operatorname{Im} A_w. \tag{1.57}$$

Note that Eqs. (1.42) and (1.57) are special cases of the second equality (1.54).

1.5. Discussion of weak values

1.5.1. Interpretation of weak values in terms of probabilities

Until now, we have assumed that the preselected state in a weak PPS measurement is pure. It is of interest to extend the theory to a mixed preselected state. In the case of a mixed preselected state ρ, the definition of the weak value becomes [108, 124] (see Sec. 5 for the derivation)

$$A_w = \frac{(A\rho)_{\phi\phi}}{\rho_{\phi\phi}}. \tag{1.58}$$

For a qubit with a mixed preselected state, weak values are always finite (see Sec. 9 for more details). However, for d-level systems with $d \geq 3$, weak values can be unbounded even with a mixed preselected state, when ρ has one or more zero eigenvalues. In this case, the weak value diverges, when the pre- and post-selected states approach orthogonal subspaces [114]. Below the weak value will be further extended to the case of a general post-selection measurement (see Sec. 13).

The results (1.36) and (1.58) for weak values are surprising in the sense that one might expect, by analogy with Eqs. (1.16) and (1.17), that a weak pre- and post-selected measurement yields the average of A obtained in a strong PPS measurement,

$$A_s = \sum_i a_i \, P_{i|\phi}, \tag{1.59}$$

where $P_{i|\phi}$ are given by Eq. (1.25) or (1.26). Equation (1.59) is a usual value of A, i.e., a real number within the range of the eigenvalues of A, and hence it generally significantly differs from the weak value. Even so, as shown below, there are situations where the weak value coincides with Eq. (1.59).

It is possible to obtain an expression for the weak value similar to Eq. (1.59). Indeed, inserting Eq. (1.2) into Eq. (1.58) yields the weak value in a useful form

$$A_w = \sum_i a_i \, (\Pi_i)_w, \tag{1.60}$$

where $(\Pi_i)_w$ is the weak value of Π_i,

$$(\Pi_i)_w = \frac{\langle\phi|\Pi_i \, \rho|\phi\rangle}{\langle\phi|\rho|\phi\rangle}. \tag{1.61}$$

The quantity $(\Pi_i)_w$ can be called the weak probability corresponding to the eigenstate a_i [76]. Summing both sides of Eq. (1.61) over i and using the second equality in Eq. (1.3), we obtain that the weak probabilities are normalized [76],

$$\sum_i (\Pi_i)_w = 1. \tag{1.62}$$

The weak probability distribution $\{(\Pi_i)_w\}$ is generally nonclassical, in the sense that some weak probabilities may be greater than one or negative or even complex; such weak probabilities are unusual weak values of the projectors Π_i. However, whenever all $(\Pi_i)_w$ are positive or equal to zero, the normalization (1.62) ensures that the set $\{(\Pi_i)_w\}$ is a classical probability distribution, and hence A_w is a usual value [119].

Equations (1.60) and (1.62) imply that the weak value A_w is the average of the observable A over a nonclassical probability distribution which can assume negative and complex values. It is often stated [90, 117] that the weak value should be understood as the mean value of the observable A when weakly measured between the pre- and post-selected states. However, we stress that, in view of Eq. (1.60), the "mean value" here is not a usual (classical) mean value, since it is taken over a nonclassical probability distribution. Nonclassical discrete [76, 81, 82] and continuous [79] probability distributions were measured experimentally.

An additional insight into weak values is provided by the fact that the weak probability $(\Pi_i)_w$ in Eq. (1.60) has the meaning of a (nonclassical) conditional probability of the measurement result a_i given that the subsequent measurement result corresponds to the state $|\phi\rangle$ [128]. Indeed, the weak probability (1.61) can be recast in the form of Bayes' theorem

$$(\Pi_i)_w \equiv \tilde{P}_{i|\phi} = \frac{\tilde{P}_{i\phi}}{P_\phi} = \frac{\mathrm{Tr}\,(\Pi_\phi \Pi_i \rho)}{\mathrm{Tr}\,(\Pi_\phi \rho)}, \tag{1.63}$$

where Π_ϕ is given in Eq. (1.22) and

$$\tilde{P}_{i\phi} = \mathrm{Tr}\,(\Pi_\phi \Pi_i \rho), \qquad P_\phi = \sum_i \tilde{P}_{i\phi} = \mathrm{Tr}\,(\Pi_\phi \rho). \tag{1.64}$$

The measurement probability in quantum theory is represented in quantum theory by an average of a projection operator [see Eq. (1.4) or the expression for P_ϕ in Eq. (1.64)]. The quantity $\tilde{P}_{i\phi}$ in Eq. (1.64), being an average of a product of projection operators $\Pi_\phi \Pi_i$, plays the role of the joint probability for weak PPS measurements. Generally, $\tilde{P}_{i\phi}$ is nonclassical, since $\Pi_\phi \Pi_i$ is not Hermitian, when Π_ϕ and Π_i do not commute, and hence $\tilde{P}_{i\phi}$ may be complex.

1.5.2. Sufficient conditions for usual weak values

The most interesting situations occur when the weak value is unusual. It is not easy to provide necessary and sufficient conditions for unusual weak values. However, it is easy to list some situations where weak values are usual. In particular, weak values are usual in the following cases:

a. In the case $|\phi\rangle = |\psi\rangle$, Eq. (1.36) yields

$$A_w = A_{\psi\psi} = \overline{A}. \tag{1.65}$$

Now A_w is equal to the result $\overline{A}$ of a weak standard measurement (see Sec. 1.2.3). The reason for this is seen from the fact that in the present case the post-selection probability equals approximately $|\langle\phi|\psi\rangle|^2 = |\langle\psi|\psi\rangle|^2 = 1$, i.e., the post-selected ensemble almost coincides with the total ensemble. Hence, now there is practically no difference between weak PPS and weak standard measurements.

b. When $|\phi\rangle$ is an eigenstate of ρ with a nonzero eigenvalue λ, then Eq. (1.58) yields

$$A_w = \frac{A_{\phi\phi}\lambda}{\lambda} = A_{\phi\phi}. \tag{1.66}$$

The present situation reduces to case *a.* when ρ is a pure state.

c. When $|\psi\rangle$ or $|\phi\rangle$ is an eigenstate of $\hat{A}$ with eigenvalue a_i, then

$$A_w = a_i. \tag{1.67}$$

d. When, in a *pure* PPS ensemble, a strong measurement yields a particular eigenvalue a_j of a variable A with certainty, then the weak value of A is equal to a_j [67, 126]. Indeed, then $P_{i|\phi} = \delta_{ij}$ in Eq. (1.24), i.e., for $i \neq j$, $\langle\phi|\Pi_i|\psi\rangle = 0$; hence due to Eq. (1.36) $(\Pi_i)_w = 0$ $(i \neq j)$. The latter result implies, in view of Eq. (1.62), that $(\Pi_i)_w = \delta_{ij}$, and hence Eq. (1.60) yields $A_w = a_j$.

e. When $\hat{A}$ commutes with ρ,

$$[\hat{A}, \rho] = 0, \tag{1.68}$$

then A_w is given by Eq. (1.59). Indeed, taking into account that Eq. (1.68) implies $[\Pi_i, \rho] = 0$ and using the properties of the projection-valued measure (1.3), we obtain that the weak probability (1.61) equals the probability $P_{i|\phi}$ in Eq. (1.23) and hence Eq. (1.60) coincides with Eq. (1.59).

f. When the initial state is completely mixed, Eq. (1.18), i.e., the measurement is made on a post-selected only ensemble, then Eq. (1.58) yields

$$A_w = A_{\phi\phi}. \tag{1.69}$$

Note that paragraph *f.* is a special case of paragraph *e.* The result (1.69) is the same as for a weak standard measurement on an ensemble preselected only in the state $|\phi\rangle$. A similar property holds also for strong measurements in post-selected ensembles (see Sec. 1.3.2). The above two results are special cases of the time-symmetry relation, which states that measurements of any strength in an ensemble *post-selected* only in state $|\phi\rangle$ give the same results as in an ensemble *preselected* only in the same state (see the proof in Sec. 13.2).

The usual weak values obtained in the above paragraphs *c.-f.* (but not in *a.-b.*) coincide with A_s in Eq. (1.59). Note that in the above cases *c., e.,* and *f.*, $\Pi_\phi = |\phi\rangle\langle\phi|$ or ρ commutes with $\hat{A}$. As shown in Sec. 13.2, under such conditions, PPS measurements of any strength produce the same results as standard measurements with a suitable preselected state; hence A_w is an average of A [cf. Eq. (13.14)]. This explains why in these cases A_w is a usual value, described by Eq. (1.59) [cf. Eq. (1.17)].

The requirement that all the above sufficient conditions for usual weak values should be violated provides a necessary (but not sufficient) condition for unusual weak values. A thorough discussion of the conditions needed to obtain unusual weak values in a qubit is given in Sec. 9.

1.5.3. Quantum interference in PPS measurements

In order to understand the reason why the weak value generally sharply differs from Eq. (1.59), it is useful to compare the meter states for standard and PPS measurements, just before the measurement of the pointer. Equation (1.13) implies that in standard measurements, there is no interference between the wave packets $\psi_{\mathrm{M}}(q-\gamma a_j)$, since they are multiplied by mutually orthogonal vectors $|a_j\rangle$. In contrast, for PPS measurements we obtain from Eq. (1.13) that for $t_{\mathrm{S}} < t < t_{\mathrm{M}}$ the meter wavefunction is

$$\langle\phi|\psi_f(q)\rangle = \sum_j \alpha_j \langle\phi|a_j\rangle\, \psi_{\mathrm{M}}(q-\gamma a_j), \tag{1.70}$$

i.e., the post-selection creates interference between the wave packets $\psi_{\mathrm{M}}(q-\gamma a_j)$. In the case of a large γ, different wavepackets in Eq. (1.70) do not overlap, and interference is practically absent in a measurement of q; therefore, a strong PPS measurement results in a projective measurement of a_i with probability

$$P_{i|\phi} \sim |\alpha_j \langle\phi|a_j\rangle|^2 = |\langle\phi|a_j\rangle\langle a_j|\psi\rangle|^2, \tag{1.71}$$

in accordance with Eq. (1.26). In the opposite limit of a small γ, i.e., for a weak PPS measurement, different wavepackets significantly overlap, and interference strongly affects the measurement results. Quantum interference is especially strong (and destructive), when the pre- and post-selected states, $|\psi\rangle$ and $|\phi\rangle$, are almost orthogonal. This strong interference effect explains the striking difference between the weak value and Eq. (1.59).

Thus, it is the interference in the meter state that is the reason for unusual weak values. Let us discuss the physical origin of this interference. As mentioned above, after correlating the system and meter, there is no interference in the meter state, as implied by (1.13). The reason for this is that different wave packets $\psi_{\mathrm{M}}(q-\gamma a_j)$ are "tagged" by the mutually orthogonal system states $|a_i\rangle$ and hence can be completely distinguished by measuring the observable A, even though they can significantly overlap each other. In contrast, a measurement of system S with a post-selection transforms the state of the system and meter into a product state, thus eliminating any correlation between the system and meter. Now, unless the meter is measured, an observer even in principle cannot obtain information in which wave packet the meter is located, which results in interference between different wave packets in Eq. (1.70).

1.5.4. Sum rule for weak values

To provide a further insight into how complex and/or very large weak values and amplification result from the post-selection, we mention an interesting property of weak values, which can be called the "sum rule".

The result of a weak standard measurement [cf. Eq. (1.16)] is the expectation value of the linear-response results of weak PPS measurements [cf. Eq. (1.41) or (1.52)] corresponding to all subensembles resulting from the post-selection measurement of the quantity B (cf. Fig. 2). The weights in the above expectation value are provided by the probabilities of different outcomes of the measurement of B, given approximately by $P_i^B = |\langle\phi_i|\psi\rangle|^2$, where $|\phi_i\rangle$ are the eigenvectors of B. The linearity of the response of the pointer for weak measurements ensures that $\bar{A}$ is an expectation value of the weak values corresponding to different subensembles. Indeed, it is easy to obtain the following relation,

$$\bar{A} = \langle\psi|\hat{A}|\psi\rangle = \sum_i \langle\psi|\phi_i\rangle\langle\phi_i|\hat{A}|\psi\rangle = \sum_i |\langle\phi_i|\psi\rangle|^2 \frac{\langle\phi_i|\hat{A}|\psi\rangle}{\langle\phi_i|\psi\rangle}, \tag{1.72}$$

yielding the sum rule [119]

$$\sum_i P_i^B A_{wi} = \overline{A}, \tag{1.73}$$

where

$$P_i^B = |\langle\phi_i|\psi\rangle|^2, \qquad A_{wi} = \frac{\langle\phi_i|\hat{A}|\psi\rangle}{\langle\phi_i|\psi\rangle}. \tag{1.74}$$

Equation (1.73) shows explicitly that, though weak values can be complex and very large, their average over all subensembles is a usual value of A. In the special case $B = A$, the sum rule (1.73) reduces to Eq. (1.17).

The magnitudes of the contributions from different subensembles in the sums in Eq. (1.72) have the same upper bound, $|\langle\psi|\phi_i\rangle\langle\phi_i|A|\psi\rangle| \leq |\phi_i|A|\psi\rangle| \leq ||A||$, where $||A||$ is the norm of $\hat{A}$ given by the maximum of the magnitudes of the eigenvalues of $\hat{A}$ (here $||A||$ is assumed to be finite). In contrast, the weak values given by the fractions in the last sum in Eq. (1.72) diverge when the overlap $|\langle\phi_i|\psi\rangle|$ tends to zero. Correspondingly, the pointer deflection is strongly amplified in this limit. This amplification increases the signal-to-noise ratio (SNR) with respect to technical noise and hence is very useful. However, since this amplification is achieved in a relatively small number of measurements proportional to $|\langle\phi_i|\psi\rangle|^2$, the SNR with respect to *quantum noise* in weak PPS measurements is *of the same order* as in standard measurements [80] (for details see Secs. 4.6.1 and 4.9.2).

It is easy to see that the sum rule (1.73) holds also for a mixed initial state, as one should expect. In this case, in Eq. (1.73) we have $\overline{A} = \mathrm{Tr}\,(\hat{A}\rho)$ and [cf. Eqs. (1.4) and (1.58)]

$$P_i^B = \langle\phi_i|\rho|\phi_i\rangle, \qquad A_{wi} = \frac{\langle\phi_i|\hat{A}\rho|\phi_i\rangle}{\langle\phi_i|\rho|\phi_i\rangle}. \tag{1.75}$$

1.6. Experimental realizations of weak PPS measurements

The general scheme of performing PPS measurements was described in Sec. 1.3.4. Note that the choice of systems suitable for use as a meter is much broader for weak (standard and PPS) measurements than for strong measurements. Indeed, to perform a projective measurement of a variable A with n_A unequal eigenvalues, one requires the meter to be a d_{M}-level system with $d_{\mathrm{M}} \geq n_A$. This is necessary for correlating n_A eigenstates of $\hat{A}$ corresponding to the unequal eigenvalues with n_A orthogonal meter states [cf. Eq. (1.13)], in order to obtain from the measurement the maximum information allowed by the projection postulate. In contrast, weak standard and PPS measurements provide such parameters as $\overline{A}$ and A_w, respectively, which contain much less information than ideal measurements. In consequence, for weak standard and PPS measurements of *any* system one can use any other system as a meter, including a two-level system (a qubit), see Sec. 7.3. Moreover, the choice of meters is broader for weak PPS measurements than for weak standard measurements. For example, meters with $R = F$ are not suitable for weak standard measurements (see below Secs. 2.1 and 3.1) but are suitable for weak PPS measurements [cf. Eqs. (1.42) and (1.54)].

Below we overview various experiments on weak PPS measurements.

In their seminal paper [24], AAV proposed to perform weak PPS measurements using a Stern-Gerlach setup, where the shift of the transverse momentum of the particle, translated into a spatial shift, yields the outcome of the spin-1/2 measurement. The meter now is a particle performing one-dimensional free motion, the input and output variables being

$$F = q, \quad R = p. \tag{1.76}$$

Postselection of the spin state in a certain direction can be performed by another (now strong) Stern-Gerlach coupling which splits the particle beam. The analysis of the required beam provides the result of the weak PPS measurement. The meters associated with the two measurements should be implemented by two independent systems (here two transverse translational degrees of freedom); this is achieved by arranging the shifts due to the two Stern-Gerlach devices to be orthogonal to each other.

An optical analog of the above Stern-Gerlach experiment was proposed in Ref. [103] and realized in the first experimental study of weak values, Ref. [70]. In this experiment, the system of interest is the optical polarization rather than a spin 1/2. The polarization of a light beam is weakly coupled to a transverse degree of freedom of the beam by a birefringent plate, whereas the pre- and post-selection are performed by polarization filters. In this setup, the meter variables are given by Eq. (1.12) rather than Eq. (1.76). Moreover, in Ref. [70] $\hat{A}$ is the projector on a state with a linear polarization, and γ is the birefringence-induced separation. Figure 2(b) in Ref. [70] and Eq. (1.47) imply that Ritchie et al. [70] obtained a real unusual weak value $A_w \approx 20$, which is very far outside the range of the eigenvalues $(0, 1)$.

Knight and Vaidman [105] proposed a slightly different optical realization of the AAV experiment, which uses a birefringent prism instead of a plate; as a result, the meter variables are given now by Eq. (1.76). This experiment was performed in Ref. [73], where results similar to those in Ref. [70] were obtained.

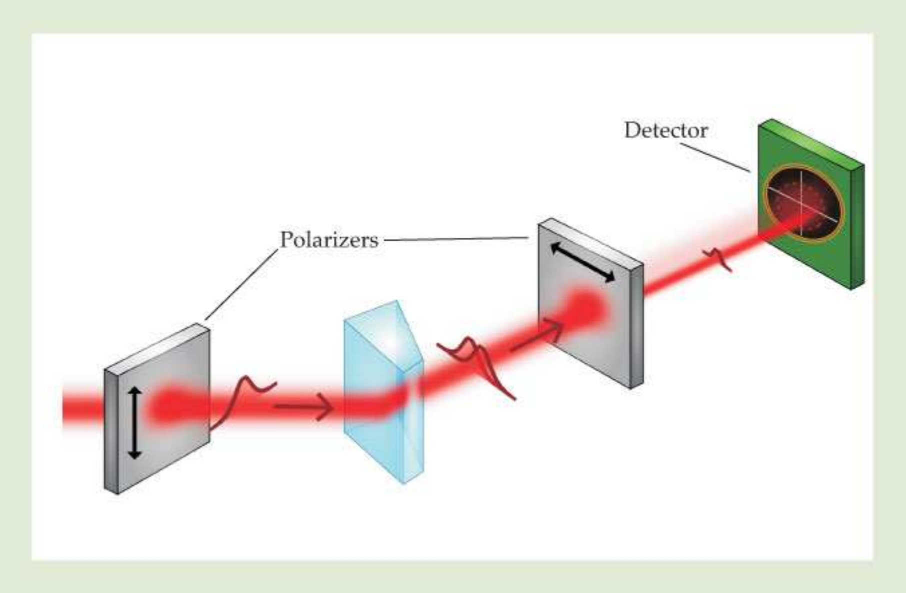

Figure 4: (color online). Schematic diagram of the experiment on measuring weak values in Ref. [80]. The figure is reprinted from Ref. [69].

A typical scheme of a weak PPS measurement is given by Fig. 4, which shows the schematic of the experiment [80]. In this experiment, the system S is the photon polarization, whereas the meter is a transverse degree of freedom of the photon, the meter variables F and R being given by Eq. (1.12). In Fig. 4, the pre- and post-selection are performed by the polarizers, which are almost crossed, whereas the prism in between provides a coupling of the system and the meter due to the spin Hall effect of light. The initial wave packet along the meter coordinate is shown on the left in Fig. 4. After passing through the prism, the wave packet becomes a superposition of two slightly shifted wave packets with mutually orthogonal polarizations [cf. Eq. (1.13)]. The post-selection produces a strong destructive interference of the wave packets [cf. Eq. (1.70)], resulting in a wave packet with a significantly reduced intensity but with a strongly enhanced shift.

In the case studied in Ref. [80], the above simple picture is complicated somewhat by the presence of a nonzero meter Hamiltonian (see the discussion of the Hamiltonian effects in Sec. 7.2.4). Using weak PPS measurements, Hosten and Kwiat [80] succeeded to detect the prism-induced wave-packet shift of 1 angstrom and thus to measure the very weak coupling produced by the spin Hall effect of light [129–131].

Until now, a large body of experimental work on weak PPS measurements has been made [70–91], and a great variety of physical systems, couplings, and experimental setups have been used. Most of the experiments were performed in optics, except for one [71], which was done in NMR. Those optical experiments that use low-intensity light allowing for detection of single photons are evidently non-classical [71, 77, 78, 81, 82, 88, 90, 91], whereas other experiments, which use intense optical beams [70, 72–76, 79, 80, 83–87, 89], admit both classical and quantum interpretations.

A linear classical optical experiment can be always interpreted quantum-mechanically, in terms of single photons. Indeed, photons in laser beams are prepared in a coherent state and behave independently in linear optical systems; hence the intensity measurements one performs are guaranteed to be the same for coherent states as for single-photon states [132]. Note that the theory in Ref. [133] is purely classical. In Sec. 12 we provide a quantum interpretation of the experiment in Ref. [133]; this interpretation is based on the nonlinear theory of weak PPS measurements, which is developed below.

Irrespective of the interpretation adopted, the "weak-value approach" for designing experiments is not conventional in classical physics and thus can lead to new results for classical systems. For example, the enhanced shift of the light-beam distribution in the coordinate or momentum space by passage through a (post-selection) filter is essentially a new classical interference effect [73, 105]. Furthermore, recent weak PPS measurements were applied in new classical optical interferometric techniques for beam-deflection [85], phase [133], and frequency [86] measurements.

The systems for which weak values were measured involved spin 1/2 [71], photon polarization [70, 72–75, 77, 78, 80, 87, 88], photon which-path states in a Sagnac [83–86] and a three-rail Mach-Zehnder [76] interferometers, a transverse translational degree of freedom of the photon [79, 90, 91], and which-path states of two photons in a pair of Mach-Zehnder interferometers [81, 82].

The meters used in the experiments included, in particular, (a) systems with continuous variables F and R: a transverse [70, 73, 76, 79, 80, 83–87] and the longitudinal [75] translational degrees of freedom of the photon, (b) a qubit: spin 1/2 [71], photon polarization [77, 88, 90, 91], and which-path states in a Mach-Zehnder interferometer [72], and (c) two qubits: the positions of two photons on the two sides of a beam splitter [78] (in the Hong-Ou-Mandel interferometer [134]) and the polarizations of the two photons [81, 82].

The coupling between the system and meter was created, in particular, by a tilted birefringent plate [70, 87], a birefringent prism [73], retarders (a Soleil-Babinet compensator [72], a birefringent optical fiber [75], and a birefringent plate [78, 90]), a tilted glass plate [76, 79], a tilted mirror [83–85], a glass prism [86], the spin Hall effect of light [80], a nondeterministic photon-entangling circuit [77, 88], a polarization rotator [81, 82, 91], and an Ising-type spin coupling [71].

In the above experiments, the system and meter were prepared in pure states, except for Ref. [87], where effects of a mixed meter state were studied.

As discussed above, in the present paper we adopt a conventional approach to weak PPS measurements, based on an extension of the von Neumann model (see Fig. 3). For completeness, we mention that there exist also somewhat different approaches to weak values, which do not involve explicitly the von Neumann model and employ instead such theoretical tools as POVM and measurement operators [61, 93, 106], negative probabilities [92, 135], and contextual values of observables [102]. In particular, weak values for continuous measurements in quantum optics [106] and solid state [93] were considered, and an experiment on cavity quantum electrodynamics [136] was interpreted [106] in terms of weak values. A more detailed discussion of these approaches is out of the scope of the present paper.

1.7. Applications of weak PPS measurements

Weak PPS measurements possess a number of unique features, which make possible a host of important applications. Such measurements can play, at least, two different roles.

First, weak PPS measurements can be employed with the aim to obtain the weak value of an observable. The fact that a weak PPS measurement disturbs the system only slightly in the interval between the pre- and post-selection allows one to obtain information about the undisturbed behavior of the system in that interval. Therefore, weak values have been used to shed new light on a great variety of quantum phenomena, especially those related to fundamentals of quantum mechanics.

Second, weak PPS measurements can produce strong amplification of the pointer deflection [24], owing to the fact that the weak value can become arbitrarily large when the overlap of the initial an final states $\langle\phi|\psi\rangle$ is sufficiently small, cf. Eq. (1.41). Correspondingly, in its second role, a weak PPS measurement acts as a peculiar amplification scheme, rather than a "proper" measurement of an observable. This amplification is one of the most important features of weak PPS measurements, since it can be exploited for different uses, e.g., to produce superluminal light propagation and slow light [67, 74, 75, 78, 104, 128]. Moreover, the amplification can yield experimental sensitivity beyond the detector resolution and thus can be used for measuring weak physical effects responsible for the coupling between the system and the meter, as well as for precision measurements of other parameters characterizing the system and the meter.

Furthermore, the weak value can be a complex number, which has important consequences for weak PPS measurements. It is interesting that a complex weak value is always unusual, irrespective of its magnitude, whereas a real weak value becomes unusual only when it is outside the spectrum of the observable. The terms proportional to

$\mathrm{Im}\,A_w$ entering Eqs. (1.42) and (1.52) have no analogues in standard measurements. As a result, in particular, the class of meters which can be used for weak PPS measurements is broader than the class of meters appropriate for weak standard measurements. For instance, meters with commuting F and R (and, in particular, with $F = R$) cannot be used for standard measurements, but they can be used for weak PPS measurements [cf. Eqs. (1.42) and (1.54)]; this point is discussed in more details in subsequent sections. Moreover, the terms involving $\mathrm{Im}\,A_w$ are proportional to a factor characterizing the classical correlation between F and R. This correlation provides an independent source of enhancement in addition to the amplification due to A_w mentioned above [80], as discussed in detail in subsequent sections.

Experiments on weak PPS measurements have involved various interesting applications, all of them being related to unusual weak values. In particular, such measurements were used to elucidate quantum retrodiction (i.e., "prediction" about the past) paradoxes with pre- and post-selection, such as the three-box problem [126] and Hardy's paradox [137]. Such problems show vividly that in quantum mechanics it is difficult to answer the question what is the value of a physical quantity in the middle of a time evolution, especially for a PPS ensemble. Weak PPS measurements are very well suited to answer such questions by two reasons. First, strong measurements utterly change the time evolution, and hence their results are loosely related to the evolution in question, whereas weak measurements almost do not affect the evolution. Second, in contrast to the results of strong PPS measurements, weak values do not depend on the measurement context, just as the standard (preselected) measurements. Indeed, due to the fact that A_w is linear in A, the contributions to A_w from different projectors in Eq. (1.60) are independent of each other.

Consider, for instance, the three-box problem [126]. One can ask the question, in which box the particle is located in between the pre- and post-selection. Strong PPS measurements, being contextual, do not provide an unambiguous answer to this question [cf. Eqs. (1.32)-(1.34)]. In contrast, in weak PPS measurements, which are not context dependent, the "weak probability" $(\Pi_i)_w$ (with $\Pi_i = |i\rangle\langle i|$) is determined uniquely for each state $|i\rangle$. In particular, consider the above case, when the pre- and post-selected states are Eqs. (1.28) and (1.29), respectively. In view of paragraph *d.* in Sec. 1.5.2 and Eqs. (1.32) and (1.33), we obtain that

$$(\Pi_1)_w = (\Pi_2)_w = 1. \tag{1.77}$$

Moreover, Eq. (1.77) together with the normalization condition (1.62), which becomes now $(\Pi_1)_w + (\Pi_2)_w + (\Pi_3)_w = 1$, yield that

$$(\Pi_3)_w = -1. \tag{1.78}$$

Thus, the outcomes (1.77) of weak PPS measurements are consistent with the paradoxical results (1.32) and (1.33), rather than with Eq. (1.34). The outcome (1.78) for box 3 is no less paradoxical, since it is a negative weak probability and hence an unusual weak value. The results (1.77) and (1.78) were verified experimentally in Ref. [76].

Hardy's paradox is a contradiction between classical reasoning and the outcome of measurements on an electron and a positron in a pair of overlapping Mach-Zehnder interferometers (MZI) [137]. It is a variation on the concept of interaction-free measurements [139]. The scheme of Hardy's gedanken experiment and a description of Hardy's paradox are given in Fig. 5. In the case of interest, when the detectors D^+ and D^- are triggered simultaneously, the joint probabilities of different paths taken by the two particles in the interferometers can be obtained with the help of weak PPS measurements [140]. Namely, let P_{ijw} denote the weak probability that the positron and electron go through the arms i and j, respectively. Here $i, j = \mathrm{O}, \mathrm{N}$, where O (N) corresponds to the overlapping (non-overlapping) arm of the respective MZI. Then the theory predicts that [140]

$$P_{\mathrm{OO}w} = 0, \quad P_{\mathrm{ON}w} = P_{\mathrm{NO}w} = 1, \quad P_{\mathrm{NN}w} = -1. \tag{1.79}$$

Here the values of the three latter probabilities are paradoxical. As in the three-box problem, two of these probabilities equal one, whereas the third probability is negative. Equation (1.79) was verified in experiments on photons performed in Refs. [81, 82].

An important feature of the experiments [81, 82] on Hardy's paradox is that there the authors performed joint weak measurements, i.e., obtained weak values of two-particle variables, which are products of one-particle variables. These measurements were performed by two different methods: by calculating the correlations between the pointer variables for the two photons [81] and by using an entangled state of the two qubits (the photon polarizations) comprising the meter [82]. There is also a proposal of performing a joint weak PPS measurement of two qubits with a one-qubit meter,

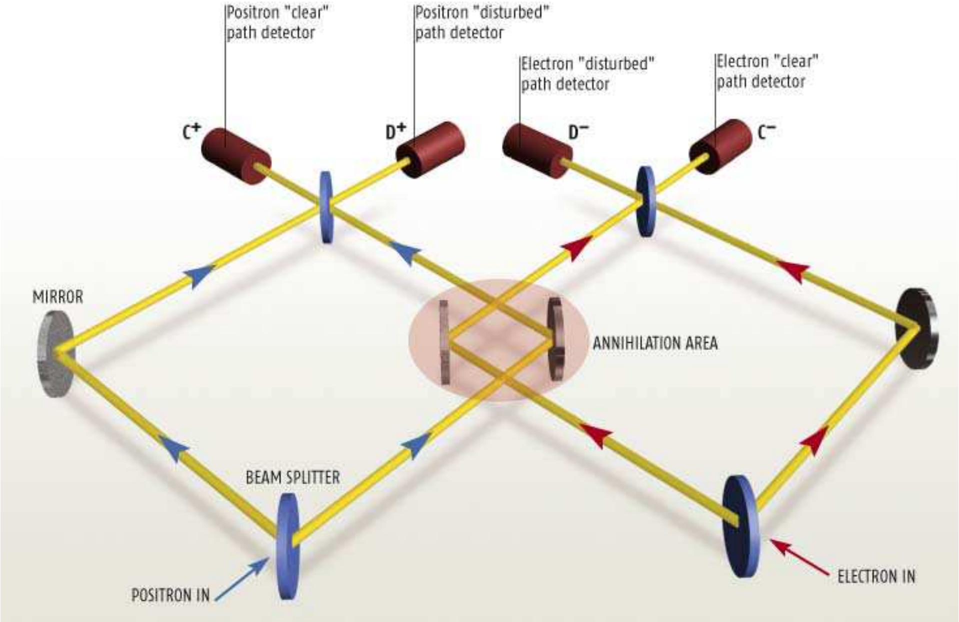
Positron "clear" path detector
Positron "disturbed" path detector
Electron "disturbed" path detector
Electron "clear" path detector
C+
D+
D−
C−
MIRROR
ANNIHILATION AREA
BEAM SPLITTER
POSITRON IN
ELECTRON IN

Figure 5: (color online). Schematic diagram of Hardy's gedanken experiment. The setup consists of a pair of overlapping Mach-Zehnder interferometers (MZI). In each MZI, there is an arm, overlapping with the other MZI, and a non-overlapping arm. In the absence of the other particle, the electron (positron) entering the MZI, as shown in the figure, can only emerge towards the detector C^- (C^+). When both particles enter the setup simultaneously, the presence of one of them in an overlapping arm disturbs the motion of the other particle—the same effect as in interaction-free measurements; as a result, the latter particle may trigger the corresponding detector D^+ or D^-. Assuming the existence of "realistic trajectories" leads to Hardy's paradox, as follows. Quantum mechanics predicts a nonzero probability of simultaneous triggering D^+ and D^-. One should infer that in this case both electron and positron have gone through the overlapping arms. However, this is impossible due to the fact that, when traveling along the overlapping arms, electron and positron should meet in the annihilation area and destroy each other. The figure is reprinted from Ref. [138].

using trapped ions [114]. Weak PPS measurements of multiparticle observables can have important applications in the future, e.g., for the probing and characterization of one-way quantum computing, which involves pre- and post-selected multiparticle states, such as cluster states [39–44].

Furthermore, the weak-value approach was employed to elucidate the complementarity between wave and particle behavior in Young's double-slit experiment [79]. The measured weak value of the momentum-transfer distribution took both positive and negative values and by virtue of this was shown to be compatible with two conflicting claims concerning the complementarity [141, 142]. Recently, weak PPS measurements were applied to obtain information on the wavefunction of a quantum particle [90, 91]. In particular, the proposal in Ref. [101] was realized in Ref. [90], where weak PPS measurements were used to obtain average trajectories of single photons in a double-slit interferometer. In Ref. [91], the transverse spatial wavefunction of a single photon was directly measured with the help of weak PPS measurements. Lundeen et al. [91] also showed how their technique can be extended for directly measuring the quantum state of an arbitrary quantum system.

The shift of the pointer distribution due to weak PPS measurements (see Secs. 1.4.1, 1.4.2, and 8.2) in the cases when the weak value is unusual can result in both superluminal propagation and slow light, as was demonstrated experimentally in Refs. [74, 75, 78]; see also discussions in [67, 104, 128]. Applications of weak values to optical communications were discussed in Refs. [74, 75, 107]. Moreover, weak values are closely related [128] to the method of measuring the tunneling time, which involves the so called "Larmor time" (a recent review on the tunneling time and superluminality see in Ref. [143]).

As mentioned in Sec. 1.5.3, one of the most important applications of weak PPS measurements is strong amplification of the measurement result in comparison to standard measurements. In particular, this amplification allows one to measure very small values of the coupling strength γ and thus to obtain information on weak effects responsible for the system-meter coupling, as, e.g., small differences in the indices of refraction [70, 72, 73, 75, 78, 87], the spin Hall effect of light [80], a mirror tilt [83–85, 89], and an Ising-type spin coupling [71]. In Ref. [86] an amplification factor of 80 was achieved in optical frequency measurements, which can be used in high-resolution relative frequency metrology and for laser locking.

In the early studies, complex weak values attracted much less attention than real weak values. In particular, until recently, weak PPS measurements were performed only with real weak values. However, in recent years the situation began to change. Jozsa [110] revealed theoretically a term proportional to $\operatorname{Im} A_w$ in the coordinate deflection. Moreover, recently a number of experiments using imaginary weak values were performed [80, 83–86, 89]. In such experiments, the amplification is enhanced in comparison to experiments with real weak values. Namely, in experiments with imaginary weak values, the total amplification coefficient is a product of the (proper) amplification coefficient due to a large weak value and the enhancement factor due to correlation between the meter variables F and R (see the discussion in Secs. 4.6 and 7.2). The total amplification does not increase the signal-to-noise ratio due to the quantum noise, but can strongly reduce the effects of technical errors [80] (see Sec. 4.9).

Using imaginary weak values, very precise measurements were made. For example, Hosten and Kwiat [80] detected a light-beam displacement of 1 angstrom, on amplifying it by a factor of 10^4, whereas Dixon et al. [83] measured a mirror-actuator travel of ~ 10 fm and the mirror angular deflection of 400 frad. Turner et al. [89] adjusted the scheme of Ref. [83] for the use in torsion balance experiments in gravity research; they demonstrated picoradian accuracy of deflection measurements. Brunner and Simon [117] showed that in measuring small longitudinal phase shifts, the use of imaginary weak values has the potential to outperform standard interferometry by several orders of magnitude, whereas standard interferometry greatly outperforms weak PPS measurements involving real weak values.

Unfortunately, for a given value of the coupling strength γ, the amplification cannot be made arbitrarily strong, since the linear-response results, such as Eqs. (1.41), (1.42), and (1.52), fail when $|\gamma A_w|$ becomes sufficiently large [cf. the condition (1.44)]. It would be of interest to develop a theory of weak PPS measurements which holds to all orders in γA_w, since such a theory would allow one to perform measurements under optimal conditions, where the magnitude of the pointer deflection is of the order of the maximum. Such a theory is developed in subsequent sections.

1.8. General theory of weak PPS measurements

In Sec. 3 and henceforth we develop a general theory of weak measurements with pre- and post-selection, which extends the existing theory in several respects. In particular,

(i) we derive results valid for *any* value of γA_w,
(ii) we obtain formulas for *arbitrary* meter variables F and R,
(iii) we consider arbitrary, pure and mixed, initial states of the system and the meter,
(iv) we discuss both the average and the distribution of the pointer variable R.

Our main results include the following:

1. We derive a simple and general formula for the average value of the meter pointer deflection, which holds for all orders in the weak value and for arbitrary system and meter.
2. We reveal that there are three qualitatively different regimes of weak PPS measurements: in addition to the AAV linear-response regime, there exist also the inverted region (the limit of very large weak values) and the intermediate, strongly-nonlinear regime.
3. The optical experiment described classically in Ref. [133] is interpreted quantum-mechanically as a weak PPS measurement in the inverted region.
4. The optimal conditions for weak PPS measurements are obtained in the strongly-nonlinear regime, since then the pointer deflection is maximized, and correspondingly the ensemble size is minimal.
5. The maximal pointer deflection is *independent of the coupling strength* γ, being typically of the order of the initial uncertainty of the pointer R.
6. We propose procedures for measuring the coupling strength γ and the weak value A_w in the nonlinear regime.

Average pointer deflection	Preselected state	Formula	Validity condition
The general nonlinear formula	Pure Mixed	(4.11) or (4.12) (5.2) or (5.3)	(4.5) (5.15)
The linear-response (AAV) regime	Arbitrary	(4.13)	(4.22)
The strongly-nonlinear regime	Pure Mixed	(4.11) or (4.12) (5.2) or (5.3)	(4.27) (5.21)
The inverse region	Pure Mixed	(4.24) (5.20)	(4.23) and (4.5) (5.18) and (5.15)
The resonance for $\|\bar{F}\| \gg \Delta F$	Pure Mixed	(4.64) (5.23)	(4.62) and (4.63) (4.62) and (4.63)

Table 3: Some of the main results of the present theory for the average pointer deflection in weak PPS measurements.

7. The amplification due to weak PPS measurements is generally a product of the proper amplification, which increases the quantum signal-to-noise ratio (SNR) in post-selected systems, and the enhancement which does not change the quantum SNR.
8. The measurement enhancement arises due to the correlation between the meter variables F and R; moreover, we find that generally q and p are correlated whenever the phase of the meter state in the p or q representation is nonlinear in the corresponding variable.
9. In the case of a mixed preselected state, in addition to A_w, an associated weak value $A_w^{(1,1)}$ is required to describe weak PPS measurements.
10. Beyond the linear response, weak PPS measurements significantly depend on the average value $\bar{F}$ of the meter variable F. In particular, the optimal regime is significantly different for $|\bar{F}| \lesssim \Delta F$ and $|\bar{F}| \gg \Delta F$, the amplification being proportional to $\bar{F}$ for $\bar{F} \gg \Delta F$.
11. All meters that are efficient for weak standard measurements are also efficient for weak PPS measurements; however, the converse is not true.
12. For continuous-variable meters, we obtain the shift of the maximum of the pointer distribution for a broad class of initial states of the meter, and not only for a real Gaussian state, as was done previously.

Approaches to weak PPS measurements beyond the linear response, resembling some aspects of the present nonperturbative theory, were developed for the special case of a continuous-variable meter in Refs. [116, 121, 122].

Some of the main results of the present theory for the average pointer deflection are listed in Table 3.

The remainder of this article is organized as follows. In Sec. 2 we provide a general theory of standard (i.e., not post-selected) measurements of arbitrary strength and discuss in detail weak standard measurements. In Sec. 3 we provide a general theory of PPS measurements of arbitrary strength. In Sec. 4 we develop a nonperturbative theory of weak pre- and post-selected measurements for the case of a pure preselected state. In Sec. 5 the results of Sec. 4 are extended to the case of a mixed preselected state. In Sec. 6 effects of the free system and meter Hamiltonians are discussed. In Sec. 7 we specialize our general formulas for several types of meters, including continuous-variable and two-level systems; we also discuss possible experiments which could verify the present results. In Sec. 8 we discuss the distribution of the pointer values for various types of meters. In Sec. 9 we consider in detail weak values for a qubit. In Sec. 10 we obtain exact solutions for PPS measurements of arbitrary strength for a qubit coupled to several types of meters, whereas in Sec. 11 we provide numerical calculations and discussions. In Sec. 12 we show that the recent experiments [83, 133] are described by two limits of the same formula, obtained in this paper. In Sec. 13 we consider an extension of the theory to the case of a general post-selection measurement described by a POVM; we also obtain conditions under which PPS measurements of any strength are equivalent to standard measurements and discuss time-symmetry properties of PPS measurements. Concluding remarks are given in Sec. 14. The four Appendices supplement the main text and provide some details of the calculations.

2. Theory of standard measurements of arbitrary strength

Here we provide a general theory of standard measurements of arbitrary strength. Moreover, weak standard measurements are considered in detail.

2.1. General formulas for standard measurements

Before we consider PPS measurements, let us discuss weak measurements without post-selection. Here we extend the results of Sec. 1.2 to the case of any canonically non-conjugate pair of the meter variables F and R and of any, generally mixed, initial states of the system and meter. As mentioned above, such measurements are performed using the standard (von-Neumann-like) scheme of quantum measurements, see Fig. 1. We assume that the coupling of the system and the meter is given by the Hamiltonian (1.8), whereas we neglect the free Hamiltonians of the system and meter. We also assume a general product initial condition: at $t = 0$ the state of the system and meter is $\rho \otimes \rho_{\mathrm{M}}$, where the system and meter states ρ and ρ_{M}, respectively, can be pure or mixed. The average value of a meter observable R (the "pointer") at any time $t \geq t_{\mathrm{f}}$ is given by

$$\bar{R}_f = \mathrm{Tr}\,[(I_{\mathrm{S}} \otimes \hat{R})U(\rho \otimes \rho_{\mathrm{M}})U^{\dagger}], \tag{2.1}$$

where $\hat{R}$ is the operator representing the observable R, U is given by Eq. (1.10), and I_{S} is the identity operator for the system.

It can be seen from Eq. (2.1) that, irrespective of the measurement strength γ, $\bar{R}_f$ in Eq. (2.1) equals the initial value $\bar{R} = \mathrm{Tr}\,(\hat{R}\rho_{\mathrm{M}})$, i.e., a measurement on the system cannot be performed, whenever

$$[\hat{F}, \hat{R}] = 0 \;\text{ or }\; [\hat{F}, \rho_{\mathrm{M}}] = 0. \tag{2.2}$$

Equation (2.1) can be expanded in powers of γ, using the familiar expansion

$$U^{\dagger}CU = C + i\gamma[D, C] + \frac{i^2\gamma^2}{2!}[D, [D, C]] + \ldots \tag{2.3}$$

with $D = \hat{A} \otimes \hat{F}$ and $C = I_{\mathrm{S}} \otimes \hat{R}$. As a result, we obtain that the average pointer deflection is given by

$$\bar{R}_f - \bar{R} = i\gamma\bar{A}\,\overline{[F, R]} + \frac{i^2\gamma^2\,\overline{A^2}}{2!}\,\overline{[F, [F, R]]} + \ldots, \tag{2.4}$$

where $\bar{A} = \mathrm{Tr}\,(\hat{A}\rho)$, $\bar{R} = \mathrm{Tr}\,(\hat{R}\rho_{\mathrm{M}})$, $\overline{[R, F]} = \mathrm{Tr}\,([\hat{R}, \hat{F}]\rho_{\mathrm{M}})$, etc.

2.2. Weak standard measurements

For weak coupling, i.e., a small γ, we can retain in Eq. (2.4) only the terms up to the first order in γ, yielding

$$\bar{R}_f - \bar{R} = \gamma\bar{A}\,\mathrm{Im}\,\overline{[R, F]}. \tag{2.5}$$

Equation (2.5) is an extension of the AAV result (1.16) for weak standard measurements to an arbitrary pair of meter variables R and F and arbitrary states of the system and meter. For canonically conjugate meter variables, $[\hat{R}, \hat{F}]$ is a constant, and the higher-order terms neglected in Eq. (2.5) vanish, as follows from Eq. (2.4), i.e., Eq. (2.5) is exact. An example of this case is provided by Eq. (1.16). However, generally the higher-order terms do not vanish, and Eq. (2.5) holds only for sufficiently weak measurements.

Let us estimate the pointer deflection (2.5). According to the Heisenberg-Robertson uncertainty relation [144],

$$\Delta F\,\Delta R \geq |\,\overline{[R, F]}\,|/2, \tag{2.6}$$

where ΔR and ΔF are the uncertainties[3] of R and F in the state ρ_{M}, so that Eq. (2.5) implies that

$$|\bar{R}_f - \bar{R}| \leq 2\,|\gamma\bar{A}|\,\Delta F\,\Delta R. \tag{2.7}$$

Meters can be called *essentially quantum* when both sides of the Heisenberg-Robertson uncertainty relation (2.6) are of the same order,

$$|\overline{[R,F]}| \sim \Delta F\, \Delta R. \tag{2.8}$$

Such meters are efficient for weak standard measurements, since they provide a pointer deflection, the magnitude of which is of the order of the maximum for given ΔR and ΔF, i.e.,

$$|\bar{R}_f - \bar{R}| \sim |\gamma \bar{A}|\, \Delta F\, \Delta R. \tag{2.9}$$

Moreover, we estimate the minimum size N_0 of the ensemble required for weak measurements without post-selection. To this purpose, we require that the squared shift of the maximum of the distribution of the sum of N_0 pointer values be of the order of the variance of this distribution, $[N_0(\bar{R}_f - \bar{R})]^2 \sim N_0 \Delta R^2$, i.e., in view of Eqs. (2.5) and (2.6),

$$N_0 \sim \left(\frac{\Delta R}{\gamma \bar{A}\, |\overline{[R,F]}|}\right)^2 \gtrsim (\gamma \bar{A} \Delta F)^{-2}. \tag{2.10}$$

For given ΔR and ΔF, the ensemble size is minimal for essentially quantum meters, Eq. (2.8), when

$$N_0 \sim (\gamma \bar{A} \Delta F)^{-2}. \tag{2.11}$$

3. Theory of pre- and post-selected measurements of arbitrary strength

In this section we provide a general theory of PPS measurements, which holds for an arbitrary measurement strength. We consider PPS ensembles with a pure post-selected state. An extension of this theory to the case of a general post-selection measurement is given in Sec. 13.

3.1. *General formulas for PPS measurements*

As discussed in Sec. 1.3.4, the pre- and post-selected (conditional) average $\bar{R}_s$ is obtained in experiments by performing a measurement of R for each member of an ensemble of systems prepared (preselected) in the same state ρ and then averaging only the results for the systems obtained (post-selected) in the state $|\phi\rangle$ after a projective measurement at $t \geq t_\mathrm{f}$. Figure 3 shows a schematic diagram illustrating pre- and post-selected quantum measurements.

The joint probability that after a measurement the system is in the state $|\phi\rangle$ and the meter is in the state $|R\rangle$ is

$$\mathcal{P}_{\phi R} = \mathrm{Tr}\,[(\Pi_\phi \otimes \Pi_R)\rho_f]. \tag{3.1}$$

Here

$$\Pi_\phi = |\phi\rangle\langle\phi|, \quad \Pi_R = |R\rangle\langle R|, \quad \rho_f = U(\rho \otimes \rho_\mathrm{M})U^\dagger, \tag{3.2}$$

where ρ_M is the initial state of the meter. By Bayes' theorem, the probability to obtain the state $|R\rangle$ provided the system is in the state $|\phi\rangle$ is given by

$$\mathcal{P}_{R|\phi} = \frac{\mathcal{P}_{\phi R}}{\mathcal{P}_\phi} = \frac{\mathrm{Tr}\,[(\Pi_\phi \otimes \Pi_R)\rho_f]}{\langle \Pi_\phi \rangle_f} \equiv \Phi_s(R), \tag{3.3}$$

where $\mathcal{P}_\phi = \langle \Pi_\phi \rangle_f$ is the probability to find the system in the state $|\phi\rangle$ at $t \geq t_\mathrm{f}$,

$$\mathcal{P}_\phi = \sum_R \mathcal{P}_{\phi R} = \mathrm{Tr}\,[(\Pi_\phi \otimes I_\mathrm{M})\rho_f] \equiv \langle \Pi_\phi \rangle_f. \tag{3.4}$$

Here in the second equality we used the completeness relation for the meter,

$$\sum_R \Pi_R = I_\mathrm{M}. \tag{3.5}$$

where I_{M} is the identity operator for the meter. The average value of the pointer variable R at $t \geq t_{\mathrm{f}}$ conditioned (post-selected) on the measurement of the system in the state $|\phi\rangle$ is given by

$$\bar{R}_s = \sum_R R\mathcal{P}_{R|\phi}. \tag{3.6}$$

Finally, inserting Eq. (3.3) into Eq. (3.6) yields that $\bar{R}_s$ is given by the normalized cross-correlation function

$$\bar{R}_s = \frac{\langle \Pi_\phi R\rangle_f}{\langle \Pi_\phi\rangle_f}, \tag{3.7}$$

where the cross-correlation function $\langle \Pi_\phi R\rangle_f$ is an average at $t \geq t_{\mathrm{f}}$,

$$\langle \Pi_\phi R\rangle_f = \mathrm{Tr}\,[(\Pi_\phi \otimes \hat{R})\rho_f]. \tag{3.8}$$

[For definiteness, we assumed above that the variable R has a discrete spectrum; when the spectrum of R is continuous, the sums in Eqs. (3.4)-(3.6) should be replaced by integrals over R.] Here we neglect the free evolution of the system and meter; the effects of the Hamiltonians of both the system and meter are discussed in Sec. 6.

The quantity of direct physical interest is the average pointer deflection $(\bar{R}_s - \bar{R})$ rather than the average pointer value $\bar{R}_s$ itself. On substituting $\hat{R} \to \hat{R}_c = \hat{R} - \bar{R}$, where the operator $\hat{R}_c$ corresponds to the "centered" quantity $R_c = R - \bar{R}$, i.e., the fluctuating part of R, Eq. (3.7) yields an expression for the pointer deflection,

$$\bar{R}_s - \bar{R} = \frac{\langle \Pi_\phi R_c\rangle_f}{\langle \Pi_\phi\rangle_f}. \tag{3.9}$$

Equations (3.7) and (3.9) are the starting point for the present theory of PPS measurements. These equations are very similar, but one of them can be more convenient than the other for a specific application.

PPS measurements have useful invariance properties with respect to gauge transformations of the system and meter, as discussed in Appendix A. A necessary condition for a PPS measurement to yield a nonvanishing pointer deflection is

$$\Delta F \neq 0. \tag{3.10}$$

Indeed, the states ρ_{M} with $\Delta F = 0$ are eigenvectors of $\hat{F}$ or mixtures of eigenvectors of $\hat{F}$ with the same eigenvalue $\bar{F}$. For such cases $\hat{F}\rho_{\mathrm{M}} = \rho_{\mathrm{M}}\hat{F} = \bar{F}\rho_{\mathrm{M}}$, and Eqs. (3.7)-(3.8) yield the zero pointer deflection, $\bar{R}_s - \bar{R} = 0$, i.e., PPS measurements are impossible.

In contrast to standard measurements, PPS measurements are generally possible even when the condition (2.2) holds. Hereafter, meters with $\overline{[R,F]} \neq 0$ are called "standard", since such meters are suitable for standard measurements [cf. Eq. (2.2)]. Correspondingly, we call meters with $\overline{[R,F]} = 0$ "non-standard". Examples of non-standard meters are meters with commuting $\hat{F}$ and $\hat{R}$ or with $\Delta R = 0$. As shown below, for weak PPS measurements, non-standard meters provide almost the same information as standard ones.

It may look paradoxical that meters with commuting $\hat{F}$ and $\hat{R}$ are suitable for PPS measurements. Indeed, in this case $\hat{R}$ commutes with the Hamiltonian (1.8) and hence is a constant of motion. As a result, $\bar{R}_f = \bar{R}$, and *standard* measurements are impossible (cf. the second paragraph in Sec. 2.1). However, the post-selection makes the average pointer value proportional to the correlation function $\langle \Pi_\phi R\rangle_f$ [see Eq. (3.7)], which generally *does change* under evolution with the Hamiltonian (1.8), for any F, unless $|\phi\rangle$ is an eigenstate of $\hat{A}$.

3.2. Expansions in the coupling parameter

At least, for some simple cases, Eqs. (3.9) [or (3.7)] and (3.3) allow one to obtain expressions both for the average pointer value and for the distribution of the pointer values, which hold for an *arbitrary* coupling strength γ. The resulting expressions (see Sec. 10 and Refs. [70–72, 74, 75, 77, 79, 93, 103, 105, 107]) significantly differ for different cases. Moreover, they generally do not involve the weak value A_w explicitly, are rather complicated, and can be analyzed only numerically. In contrast, the linear-response results discussed above in Sec. 1.4 (see also Sec. 4.4.1) are simple and general, and, most importantly, they provide the weak value A_w. However, they hold only for sufficiently small values of $|\gamma A_w|$. Fortunately, as shown below, for weak PPS measurements it is possible to obtain simple and general expressions, which involve A_w explicitly and hold for *arbitrarily large* values of $|\gamma A_w|$. To derive these expressions, we expand the numerator and denominator of Eq. (3.9) in the parameter γ, as follows.

From Eq. (3.8) with R replaced by R_c, we obtain that

$$\langle \Pi_\phi R_c \rangle_f = \mathrm{Tr}\,[U^\dagger C U(\rho \otimes \rho_\mathrm{M})] \tag{3.11}$$

with $C = \Pi_\phi \otimes \hat{R}_c$. Then we use the expansion (2.3), where consecutively embedded commutators are expanded by the formula (see Appendix B)

$$\underbrace{[D, \ldots [D,}_{n} C \underbrace{] \ldots]}_{n} = \sum_{k=0}^{n} (-1)^k \binom{n}{k} D^{n-k} C D^k, \tag{3.12}$$

to obtain the formula

$$\langle \Pi_\phi R_c \rangle_f = \sum_{n=1}^{\infty} \frac{i^n \gamma^n}{n!} \sum_{k=0}^{n} (-1)^k \binom{n}{k} (A^k \rho A^{n-k})_{\phi\phi} \, \overline{F^{n-k} R_c F^k}, \tag{3.13}$$

where the overbar stands for the average over ρ_M, so that $\bar{O} = \mathrm{Tr}\,(\hat{O}\rho_\mathrm{M})$ for a meter operator $\hat{O}$. The quantity $\langle \Pi_\phi \rangle_f$ is calculated similarly to Eq. (3.13) with $C = \Pi_\phi \otimes \hat{R}_c$ replaced by $C = \Pi_\phi \otimes I_\mathrm{M}$, yielding

$$\langle \Pi_\phi \rangle_f = \sum_{n=0}^{\infty} \frac{i^n \gamma^n \overline{F^n}}{n!} \sum_{k=0}^{n} (-1)^k \binom{n}{k} (A^k \rho A^{n-k})_{\phi\phi}. \tag{3.14}$$

For completeness, we show also the expansion of $\langle \Pi_\phi R \rangle_f$ obtained similarly to Eq. (3.13),

$$\langle \Pi_\phi R \rangle_f = \sum_{n=0}^{\infty} \frac{i^n \gamma^n}{n!} \sum_{k=0}^{n} (-1)^k \binom{n}{k} (A^k \rho A^{n-k})_{\phi\phi} \, \overline{F^{n-k} R F^k}. \tag{3.15}$$

An advantage of using Eq. (3.9) instead of Eq. (3.7) is that in the expansion (3.13), in contrast to Eq. (3.15), the term with $n = 0$ vanishes.

In the next section we will consider the important case when the system is preselected in a pure state $|\psi\rangle$, so that $\rho = |\psi\rangle\langle\psi|$, whereas the meter state ρ_M is generally mixed (the case of a mixed preselected state is discussed in Sec. 5). In this case Eqs. (3.13) and (3.14) yield that

$$\langle \Pi_\phi R_c \rangle_f = |\langle\phi|\psi\rangle|^2 \{2\gamma\,\mathrm{Im}(\overline{R_c F} A_w) + \gamma^2 \{\overline{F R_c F} |A_w|^2 - \mathrm{Re}[\overline{R_c F^2} (A^2)_w]\} - \gamma^3 \mathrm{Im}[\overline{F^2 R_c F} A_w (A^2)_w^* + \overline{R_c F^3} (A^3)_w / 3]\} + \ldots, \tag{3.16a}$$

$$\langle \Pi_\phi \rangle_f = |\langle\phi|\psi\rangle|^2 \{1 + 2\gamma \bar{F}\,\mathrm{Im}\,A_w + \gamma^2 \overline{F^2} [|A_w|^2 - \mathrm{Re}\,(A^2)_w] - \gamma^3 \overline{F^3}\,\mathrm{Im}\,[A_w (A^2)_w^* + (A^3)_w/3]\} + \ldots. \tag{3.16b}$$

Here $(A^n)_w = (A^n)_{\phi\psi} / \langle\phi|\psi\rangle$ [cf. Eq. (1.36)] and the dots denote the terms of fourth and higher orders in γ.

4. Weak pre- and post-selected measurements: Nonlinear theory

In this section we develop a nonperturbative theory of weak PPS measurements for the case of a pure preselected state. This theory serves as a basis for discussion of many aspects of weak PPS measurements in the following sections. Extensions of this theory to the cases of a mixed preselected state and a general post-selection measurement are given in Secs. 5 and 13.

4.1. Validity conditions for weak PPS measurements

The crucial point that allows us to treat weak PPS measurements nonperturbatively is the fact that, in the limit $\langle\phi|\psi\rangle \to 0$, only terms of orders higher than one survive in Eqs. (3.16). Therefore for a sufficiently weak system-meter coupling, one can neglect in Eqs. (3.16) terms of third and higher orders; however the second-order terms should be retained since they may dominate the zero- and first-order terms, at least, in the most interesting case $|\langle\phi|\psi\rangle| \ll 1$. As a result, for this situation of weak PPS measurements, we are able to obtain a simple analytical formula valid for arbitrarily large weak values (Sec. 4.3).

Here we derive validity conditions for weak PPS measurements. To this purpose, we estimate the terms in the expansions (3.16). To obtain the validity conditions in a simple form, we will make several simplifying assumptions, which hold, at least, for some typical cases.

We begin with the expansion (3.16b). The magnitudes of nth-order terms in Eq. (3.16b) are of the order of

$$|\gamma^n\,(A^k)_{\phi\psi}\,(A^{n-k})_{\phi\psi}\,\overline{F^n}| \quad (0 \le k \le n), \tag{4.1}$$

k being an integer. In weak PPS measurements $|A_{\phi\psi}|$ is typically sufficiently large. For simplicity, we assume that $|A_{\phi\psi}|$ is so large that

$$|(A^n)_{\phi\psi}| \lesssim |A_{\phi\psi}|^n. \tag{4.2}$$

This holds, e.g., when $|A_{\phi\psi}| \sim ||A||$, where the norm $||A||$ of $\hat{A}$ is the maximum of the magnitudes of the eigenvalues of $\hat{A}$. We also assume that

$$|\,\overline{F_c^n}\,| \;\lesssim\; (\Delta F)^n, \tag{4.3}$$

where $F_c = F - \bar{F}$. Equation (4.3) implies that

$$|\,\overline{F^n}\,| \;\lesssim\; (|\bar{F}| + \Delta F)^n. \tag{4.4}$$

Using Eqs. (4.1), (4.2), and (4.4), we obtain that the terms in Eq. (3.16b) of orders higher than two are negligibly small in comparison with the second-order terms under the weak-coupling condition,

$$\mu \;\equiv\; |\gamma A_{\phi\psi}|\,(|\bar{F}| + \Delta F) \;\ll\; 1. \tag{4.5}$$

Here μ is the small parameter of the present theory.

Consider now the expansion (3.16a). The magnitudes of nth-order terms in Eq. (3.16a) differ from Eq. (4.1) only by the replacement

$$\overline{F^n} \to \overline{F^k R_c F^{n-k}} \quad (0 \le k \le n). \tag{4.6}$$

The estimation of the moments $\overline{F^k R_c F^{n-k}}$ is simple for canonically conjugate F and R, but is rather intricate in the general case. As shown in Appendix C, the terms in Eq. (3.16a) of orders higher than two are negligibly small under the above condition (4.5). The assumptions used to derive this result are given in Appendix C.

The small parameter of the theory μ in Eq. (4.5) has a simple physical meaning: μ is an estimation of the exponent $\gamma\hat{A} \otimes \hat{F}$ of the unitary transformation (1.10). Thus the validity condition of the present theory (4.5) is a requirement for the weakness of the unitary transformation (1.10). The condition (4.5) simplifies in two cases,

$$|\gamma A_{\phi\psi}|\,\Delta F \;\ll\; 1 \qquad (\,|\bar{F}| \lesssim \Delta F\,), \tag{4.7a}$$

$$|\gamma A_{\phi\psi}\bar{F}| \;\ll\; 1 \qquad (\,|\bar{F}| \gtrsim \Delta F\,). \tag{4.7b}$$

4.2. Quantifying the strength of a measurement

In the experiments performed so far, the conditions were chosen in such a way that $\bar{F}$ was zero, either exactly or effectively. Here we allow for $\bar{F} \neq 0$. To understand the effects of a nonzero $\bar{F}$, we recast the Hamiltonian (1.8) in the form

$$H = g(t)\,\hat{A} \otimes \hat{F}_c + g(t)\,\bar{F}\hat{A}. \tag{4.8}$$

Here obviously only the first term on the rhs can correlate the system and the meter, whereas the second term is responsible for a unitary transformation of the system alone. Correspondingly, the unitary transformation (1.10) splits into two factors relating to the two types of the evolution.

The evolution due to $\bar{F}$ occurs simultaneously with the coupling evolution and hence affects the results of PPS measurements, the effect of $\bar{F}$ increasing with $|\bar{F}|$. In particular, weak PPS measurements are in a qualitatively different regime for $|\bar{F}| \gg \Delta F$ than for $|\bar{F}| \lesssim \Delta F$ (see Sec. 4.8). However, as shown below, it may be beneficial for experimentalists that $\bar{F}$ have a nonzero value, such as, e.g., $|\bar{F}| \sim \Delta F$ or even $|\bar{F}| \gg \Delta F$.

The two conditions (4.7) ensure the weakness of the two types of evolution shown above. Thus, the small parameter of the theory μ in Eq. (4.5) is the sum of two small parameters, which have different physical meanings. Namely,

$$\mu_0 = |\gamma A_{\phi\psi}|\,\Delta F \tag{4.9}$$

quantifies the degree of correlation between the system and the meter or, in other words, *the measurement strength*, while

$$\mu_1 = |\gamma A_{\phi\psi}\bar{F}| \tag{4.10}$$

characterizes the strength of the unitary transformation due to $\bar{F}$.

4.3. *General nonlinear formula for the average pointer deflection*

Under the condition (4.5) the terms of orders higher than two can be neglected in Eqs. (3.16). Moreover, the terms involving $(A^2)_w$ can also be neglected in Eqs. (3.16), since, in view of Eq. (4.2), $(A^2)_w \ll |A_w|^2$ in the most interesting case $|\langle\phi|\psi\rangle| \ll 1$, whereas for $|\langle\phi|\psi\rangle| \sim 1$ all second-order terms are negligibly small due to the conditions (4.2) and (4.5). Then we obtain from Eqs. (3.9) and (3.16) that

$$\bar{R}_s - \bar{R} = \frac{2\gamma\,\mathrm{Im}\,(\overline{R_cF}A_w) + \gamma^2\,\overline{FR_cF}\,|A_w|^2}{1 + 2\gamma\bar{F}\,\mathrm{Im}\,A_w + \gamma^2\,\overline{F^2}\,|A_w|^2}, \tag{4.11}$$

the numerator and denominator of Eq. (4.11) being approximately equal to $\langle\Pi_\phi R_c\rangle_f/|\langle\phi|\psi\rangle|^2$ and $\langle\Pi_\phi\rangle_f/|\langle\phi|\psi\rangle|^2$, respectively. The approximation (4.11) may fail when both terms in the numerator are vanishing or anomalously small or if they cancel, exactly or approximately; then the $(A^2)_w$ terms and perhaps higher-order terms [see Eq. (3.16)] should be taken into account. However such cases are of little interest, since then $\bar{R}_s - \bar{R}$ is very small.

It is easy to see that Eq. (4.11) can be recast in another form,

$$\bar{R}_s = \frac{\bar{R} + 2\gamma\,\mathrm{Im}\,(\overline{RF}A_w) + \gamma^2\,\overline{FRF}\,|A_w|^2}{1 + 2\gamma\bar{F}\,\mathrm{Im}\,A_w + \gamma^2\,\overline{F^2}\,|A_w|^2}, \tag{4.12}$$

which can sometimes be useful. The general nonlinear formula (4.11) [or (4.12)] *is one of the main results of the present paper*. The remainder of the paper is devoted to a discussion and to extensions of this formula.

Equation (4.11) holds to *all orders in the weak value*. It is remarkable that, according to Eq. (4.11), weak PPS measurements depend on A only through one parameter A_w (at least, for a pure preselected state). Moreover, weak PPS measurements depend on γ and A_w through the product γA_w. Equation (4.11) shows that the average pointer deflection as a function of $\gamma|A_w|$ can have Lorentzian and dispersive lineshapes as well as linear combinations thereof (see also numerical calculations in Sec. 11).

4.4. *Regimes of weak PPS measurements*

Consider the limiting cases of Eq. (4.11).

4.4.1. *Linear response*

In first-order (linear in γ) approximation, Eq. (4.11) yields the result, which we write in three equivalent forms,

$$\begin{aligned} \bar{R}_s - \bar{R} &= 2\gamma\,\mathrm{Im}\,(\overline{R_cF}A_w) && \text{(4.13a)} \\ &= 2\gamma\,|\overline{R_cF}A_w|\sin(\theta + \theta_0) && \text{(4.13b)} \\ &= \gamma\,\mathrm{Im}\,\overline{[R,F]}\,\mathrm{Re}\,A_w + 2\gamma\,\sigma_{FR}\,\mathrm{Im}\,A_w, && \text{(4.13c)} \end{aligned}$$

where

$$\theta = \arg A_w, \quad \theta_0 = \arg \overline{R_cF}, \tag{4.14}$$

$$\sigma_{FR} = \frac{\overline{\{R_c, F\}}}{2} = \frac{\overline{\{R, F\}}}{2} - \bar{R}\bar{F}, \tag{4.15}$$

and {,} denotes the anticommutator. Equation (4.13c) results from Eq. (4.13a), on writing $\overline{R_cF}$ as a sum of a real and an imaginary terms,

$$\overline{R_cF} = \sigma_{FR} + \frac{\overline{[R,F]}}{2}. \tag{4.16}$$

The quantity σ_{FR} in Eq. (4.15) is the quantum analogue of the covariance between the variables F and R; σ_{FR} is a measure of the correlation between F and R [145]. Under the present assumptions, each of Eqs. (4.13) describes in the most general form the linear response for weak pre- and post-selected measurements. In particular, Eq. (4.13c) contains as special cases the previous results on the weak value [24, 110]. Equation (4.13b) shows that the magnitude of the linear response is maximized when the weak-value phase θ is given by

$$\theta = -\theta_0 + \frac{(2k-1)\pi}{2} \quad (k = 0, \pm 1, \ldots). \tag{4.17}$$

In contrast, linear response vanishes for

$$\theta = -\theta_0 + k\pi \quad (k = 0, \pm 1, \ldots). \tag{4.18}$$

The first term in Eq. (4.13c), involving $\mathrm{Re}\, A_w$, is an analog of Eq. (2.5), differing only by the replacement $\bar{A} \to \mathrm{Re}\, A_w$. This term is purely quantum, since it vanishes for commuting F and R. More generally, it vanishes for non-standard meters: $\overline{[R, F]} = 0$. In contrast, the second term, involving $\mathrm{Im}\, A_w$, has no analog in weak measurements without post-selection; it arises for correlated F and R, and hence it generally does not vanish for commuting variables.

Recall that for standard measurements, the average pointer deflection was estimated above with the help of the Heisenberg-Robertson uncertainty relation (2.6). Similarly, weak PPS measurements are closely related to the *generalized* uncertainty relation given by Eq. (C.5) or

$$\Delta R\, \Delta F \;\geq\; |\,\overline{R_c F}\,| \;\equiv\; \sqrt{\left|\frac{\overline{[R, F]}}{2}\right|^2 + \sigma_{FR}^2}, \tag{4.19}$$

where we used the relation $\overline{R_c F_c} = \overline{R_c F}$. Equation (4.19) is used below for estimation of the average pointer deflection (see Sec. 4.5). Since $|\,\overline{R_c F}\,|$ can be much greater than $|\,\overline{[R, F]}\,|$ [cf. the equality in Eq. (4.19)], a comparison of Eqs. (2.5) and (4.13b) shows that the average pointer deflection in weak PPS measurements can be *strongly enhanced* relative to that in standard measurements. Notice that this enhancement is independent of the amplification due to a large weak value discussed by AAV [24] (for further details see Sec. 4.6).

The necessary condition for the validity of linear response, Eqs. (4.13a)-(4.13c), is that the denominator of Eq. (4.11) is close to one, which holds for

$$|\gamma A_w|\, (\overline{F^2})^{1/2} \ll 1. \tag{4.20}$$

The same condition allows one to neglect the quadratic term in the numerator of Eq. (4.11) if the linear term is not too small. Since

$$\overline{F^2} = \bar{F}^2 + (\Delta F)^2, \tag{4.21}$$

Eq. (4.20) is equivalent to the condition

$$|\gamma A_w|\, (|\bar{F}| + \Delta F) \;\ll\; 1. \tag{4.22}$$

4.4.2. Inverted region (the limit of very large weak values)

In the opposite limit of very large weak values,

$$|\gamma A_w|\, (|\bar{F}| + \Delta F) \;\gg\; 1, \tag{4.23}$$

Eq. (4.11) yields that

$$\bar{R}_s - \bar{R} \;\approx\; \frac{\overline{F R_c F}}{\overline{F^2}} + \frac{2}{\gamma\, \overline{F^2}}\, \mathrm{Im}\, \frac{\overline{R_c F}}{A_w^*} + \frac{2\bar{F}\, \overline{F R_c F}}{\gamma\, (\overline{F^2})^2}\, \mathrm{Im}\, \frac{1}{A_w}. \tag{4.24}$$

The first term on the rhs of Eq. (4.24) is the value of the pointer deflection for $A_w = \infty$, i.e., for orthogonal $|\phi\rangle$ and $|\psi\rangle$. Thus, the case of orthogonal pre- and post-selected states provides *no information* on the system.

In the limit of large weak values, the contribution to the average pointer deflection due to the system-meter coupling is small [see the last two terms in Eq. (4.24)]. The region (4.23) can be called *the inverted region*, since here the meter deflection depends on the weak value inversely, this dependence *decreasing* with the increase of the measurement strength.

Equation (4.24) can be also considered as a first-order expansion of the pointer deflection in the overlap $\langle\phi|\psi\rangle$. Correspondingly, the condition (4.23) can be recast as

$$|\langle\phi|\psi\rangle| \ll |\gamma A_{\phi\psi}|\,(|\bar{F}| + \Delta F). \tag{4.25}$$

The regime (4.23) is well suited for measuring very small values of $\langle\phi|\psi\rangle$ (see also Sec. 4.9.3). The inverted region (4.23) has not been discussed explicitly until now. However, the interferometric method of phase measurements demonstrated experimentally in Ref. [133] can be shown to admit a quantum-mechanical interpretation as a weak PPS measurement in the inverted region (see Sec. 12).

In the inverted region, the dependence on the coupling strength and the system parameters is quite different from that in the linear and the intermediate nonlinear regimes, which hold in the region

$$|\gamma A_w|\,(|\bar{F}| + \Delta F) \lesssim 1. \tag{4.26}$$

Therefore below in many cases the regions (4.23) and (4.26) are discussed separately.

4.4.3. *Intermediate regime*

Consider now the region intermediate between linear response and the inverted region,

$$|\gamma A_w|\,(|\bar{F}| + \Delta F) \sim 1. \tag{4.27}$$

We refer to this region as the strongly-nonlinear (or intermediate) regime. In this region, Eq. (4.11) cannot be simplified since the dependence of the average pointer deflection on γ is significantly nonlinear. The condition (4.27) can be recast in the form

$$\mu \sim |\langle\phi|\psi\rangle|, \tag{4.28}$$

i.e., in the intermediate regime the small parameter of the theory is of the order of the overlap of the pre- and postselected states.

In the important case $|\bar{F}| \lesssim \Delta F$, which is of primary interest in most of the present paper, the condition (4.27) becomes

$$|\gamma A_w|\,\Delta F \sim 1 \tag{4.29}$$

or, equivalently,

$$\mu_0 \sim |\langle\phi|\psi\rangle|. \tag{4.30}$$

Equations (4.28) and (4.5) imply that the strongly-nonlinear regime (4.27) can be obtained for weak PPS measurements only when the initial and final states are almost orthogonal,

$$|\langle\phi|\psi\rangle| \ll 1. \tag{4.31}$$

In the case (4.31), the weak value (1.36) is anomalously large, at least, when $A_{\phi\psi}$ is not too small, as in Eq. (4.2).

Below (Sec. 4.5.2) it is shown that optimal conditions for weak PPS measurements are obtained in the nonlinear intermediate regime. Thus, Eq. (4.27) or (4.28) [or, equivalently, (4.30)] provides the optimality condition, at least, for $|\bar{F}| \lesssim \Delta F$, whereas for $|\bar{F}| \gg \Delta F$, the condition (4.27) [or (4.28)] is necessary but not sufficient for the optimal regime (see Sec. 4.8).

4.5. *Estimation of the average pointer deflection*

Let us now estimate the typical magnitude of the average pointer deflection $\bar{R}_s - \bar{R}$ for the linear and strongly-nonlinear regimes.

4.5.1. Linear response

In the linear-response regime, Eq. (4.13b) implies that a typical value of $|\bar{R}_s - \bar{R}|$ for a given $|\gamma A_w|$ is

$$|\bar{R}_s - \bar{R}| \ \sim\ \gamma\, |A_w\, \overline{R_c F}\,|. \tag{4.32}$$

We consider a typical situation, when both sides of the generalized uncertainty relation Eq. (4.19) are of the same order,

$$|\overline{R_c F}| \ \sim\ \Delta R\, \Delta F. \tag{4.33}$$

Then Eq. (4.32) yields an estimate of the typical value of $|\bar{R}_s - \bar{R}|$,

$$|\bar{R}_s - \bar{R}| \ \sim\ |\gamma A_w|\, \Delta F\, \Delta R. \tag{4.34}$$

Equation (4.34) is also an estimate of the maximum of $|\bar{R}_s - \bar{R}|$ for a given $|\gamma A_w|$. Note that this value is limited by the condition (4.20), and hence it is relatively small.

Equations (4.13b) and (4.34) show that the linear response vanishes or becomes very small when the weak-value phase θ is close to $-\theta_0$ or when ΔR is vanishing or very small. For such cases, weak PPS measurements cannot be performed in the AAV (linear) regime. However, as shown below, weak PPS measurements are possible in the nonlinear regime, even when the linear response is vanishing or very weak.

4.5.2. Strongly-nonlinear regime

Consider now the strongly-nonlinear regime (4.27). In this regime, measurements of A_w and/or γ are optimal, since now the dependence of $(\bar{R}_s - \bar{R})$ on A_w and γ is strongest and, moreover, as we will show now, in the regime (4.27) $|\bar{R}_s - \bar{R}|$ achieves the maximum value $|\bar{R}_s - \bar{R}|_{\max}$ or, at least, values of the order of $|\bar{R}_s - \bar{R}|_{\max}$. Let us estimate $|\bar{R}_s - \bar{R}|_{\max}$.

Here we consider the most important case $|\bar{F}| \lesssim \Delta F$ (the case $|\bar{F}| \gg \Delta F$ is discussed in Sec. 4.8). First, we estimate the maximum value of $|\bar{R}_s - \bar{R}|$ for the strongly-nonlinear regime (4.27) and then show that the resulting estimate holds for all parameters. Under the condition (4.27), which becomes now

$$|\gamma A_w|\, \Delta F \ \sim\ 1, \tag{4.35}$$

the denominator of Eq. (4.11) is of the order of one, so that the maximum value of $|\bar{R}_s - \bar{R}|$ is given by

$$|\bar{R}_s - \bar{R}|_{\max} \ \sim\ \frac{|\,\overline{R_c F}\,|}{\Delta F} + \frac{|\,\overline{F R_c F}\,|}{(\Delta F)^2}. \tag{4.36}$$

Using the estimate (4.33) and taking into account that

$$\overline{F R_c F} \ =\ \overline{F_c R_c F_c} + 2\bar{F}\,\mathrm{Re}\,\overline{R_c F}, \tag{4.37}$$

Eq. (4.36) becomes

$$|\bar{R}_s - \bar{R}|_{\max} \ \sim\ \Delta R + \frac{|\,\overline{F_c R_c F_c}\,|}{(\Delta F)^2}. \tag{4.38}$$

This quantity is of the order of or greater than the magnitude of the result (4.24), which means that Eq. (4.38) provides an estimate of the maximum of the magnitude of the pointer deflection (4.11) over all values of γA_w. Equation (4.38) is independent of $\bar{F}$, since the same result is obtained also for $|\bar{F}| \gg \Delta F$ (see Sec. 4.8).

In the peculiar case when ΔR vanishes or is very small, the first term on the rhs of Eq. (4.38) can be neglected, but the pointer deflection generally does not vanish,

$$|\bar{R}_s - \bar{R}|_{\max} \sim \frac{|\,\overline{F_c R_c F_c}\,|}{(\Delta F)^2} \qquad \left[\Delta R \ll \frac{|\,\overline{F_c R_c F_c}\,|}{(\Delta F)^2}\right]. \tag{4.39}$$

This shows that PPS measurements may be performed even for $\Delta R = 0$.

However, in a typical case, ΔR is sufficiently large to obey

$$\Delta R \gtrsim \frac{|\,\overline{F_c R_c F_c}\,|}{(\Delta F)^2}, \tag{4.40}$$

which implies that the second term on the rhs of Eq. (4.38) can be neglected, yielding

$$|\bar{R}_s - \bar{R}|_{\max} \sim \Delta R. \tag{4.41}$$

Note that Eq. (4.41) holds for *any* ΔR, when $[\hat{F}, \hat{R}]$ is a c-number. This occurs, e.g., in the cases when the variables F and R are commuting or canonically conjugate (e.g., $F = p,\ R = q$) or are linear combinations of such variables. Indeed, then

$$|\,\overline{F_c R_c F_c}\,| = |\,\overline{F_c [R, F]} + \overline{F_c^2 R_c}\,| = |\,\overline{F_c^2 R_c}\,| \lesssim (\Delta F)^2 \Delta R \tag{4.42}$$

[see Eq. (C.6)], yielding Eq. (4.40) and hence Eq. (4.41).

Equation (4.38) provides a simple estimate of the maximum magnitude of the pointer deflection over all possible A_w and all allowed γ. Moreover, since the pointer deflection (4.11) depends on A_w and γ through the product γA_w, the maximum (4.38) results also when only one of the parameters A_w and γ is varied, the other being fixed. Thus, we obtain that the maximum of the pointer-deflection magnitude over all A_w for a given γ is independent of γ and hence *remains finite for* $\gamma \to 0$.

This result may look paradoxical. Note, however, that Eq. (4.38) holds for a *subensemble* of the measured systems, the relative size of which $\langle \Pi_\phi \rangle_f$ decreases with the decrease of γ as γ^2 [cf. Eq. (4.30)],

$$\langle \Pi_\phi \rangle_f \sim |\langle \phi | \psi \rangle|^2 \sim \mu_0^2 \propto \gamma^2. \tag{4.43}$$

Correspondingly, the unconditional average over the whole ensemble would yield the result (2.5), which vanishes with $\gamma \to 0$.

4.6. *Amplification in weak PPS measurements*

Weak PPS measurements can result in very significant amplification of the average pointer deflection in comparison with weak standard measurements. There are two different types of amplification in weak PPS measurements, the (proper) amplification due to a large weak value and the enhancement due to an increase of the initial pointer uncertainty ΔR above the minimal value provided by the Heisenberg uncertainty relation. (Note that there can be also an enhancement of the pointer deflection due to the presence of a non-zero meter Hamiltonian H_{M}; this effect generally holds for both standard and PPS measurements, as discussed in Sec. 7.2.4.)

Until now, amplification was discussed in the literature only for the linear response, however it takes place also in the two other regimes—the strongly-nonlinear regime and the inverted region. Here we discuss amplification for both linear-response and strongly-nonlinear regimes in the case $|F_1| \lesssim \Delta F$, i.e., we consider the region (4.26), which now is given by

$$|\gamma A_w|\, \Delta F \lesssim 1. \tag{4.44}$$

The amplification for the other cases will be considered later: in Sec. 4.8 for the case $|F_1| \gg \Delta F$ and in Sec. 4.9.3 for the inverted region.

4.6.1. *Proper amplification due to a large weak value*

To estimate amplification in weak PPS measurements, we should compare the magnitudes of the average pointer deflection in weak PPS and standard measurements. In this comparison, we assume that γ and F are the same in both types of measurements. Moreover, we require that the magnitudes of $A_{\phi\psi}$ and $\bar{A}$ be equal or, at least, of the same order of magnitude,

$$|A_{\phi\psi}| \sim |\bar{A}|. \tag{4.45}$$

In the region of interest (4.44), we define the coefficient a of the proper amplification by the order of magnitude with the help of the relation

$$a \sim \frac{|\bar{R}_s - \bar{R}|}{\mu_0\, \Delta R}. \tag{4.46}$$

In Eq. (4.46) the quantity

$$\mu_0\,\Delta R \;=\; |\gamma A_{\phi\psi}|\,\Delta F\,\Delta R \tag{4.47}$$

is of the order of a typical value of the pointer deflection for standard measurements [cf. Eqs. (2.7) and (4.45)].

In the linear regime, inserting Eqs. (4.34) and (4.47) into Eq. (4.46) yields [24, 70, 80]

$$a \;\sim\; |\langle\phi|\psi\rangle|^{-1}. \tag{4.48}$$

In the nonlinear regime, we assume the validity of Eq. (4.41) (the peculiar case of a vanishing or very small ΔR is out of the scope of the present paper). Inserting Eq. (4.41) into Eq. (4.46) and taking into account Eq. (4.30) yields the relation

$$a \sim \mu_0^{-1} \;\sim\; |\langle\phi|\psi\rangle|^{-1}, \tag{4.49}$$

which results again in Eq. (4.48). Thus, the result (4.48) holds in the whole region (4.44).

The inequality (4.44) with the account of Eq. (4.48) can be rewritten in the form

$$a\,\mu_0 \lesssim 1, \tag{4.50}$$

where the similarity sign is achieved under the optimal conditions. Thus, though a can be very large, for a given μ_0 the amplification coefficient a has the upper bound equal to μ_0^{-1}, as shown by Eq. (4.50).

Equation (4.46) implies that, for a fixed μ_0, the quantum-limited signal-to-noise ratio (per one measurement) in the post-selected subensemble $|\overline{R}_s - \overline{R}|/\Delta R$ increases in direct proportion with the amplification coefficient a,

$$\frac{|\overline{R}_s - \overline{R}|}{\Delta R} \;\sim\; a\,\mu_0 \;=\; a\,|\gamma A_{\phi\psi}|\,\Delta F. \tag{4.51}$$

In view of Eq. (4.41), the maximum value of this ratio is of the order of one, which is achieved under the optimal conditions, i.e., in the strongly-nonlinear regime. (Note, however, that if one takes into account the *total* ensemble, the amplification cannot increase the quantum signal-to-noise ratio; correspondingly, the latter is the same in weak PPS and standard measurements [80, 85]; see Sec. 4.9.2 for further details.) Thus, Eq. (4.51) implies the remarkable fact that for an *arbitrarily small* coupling strength γ, the amplification a can be made so large that the signal-to-noise ratio in the post-selected subensemble is of order one, making measuring γ possible and relatively easy. The price for this is that the size of the total ensemble increases as a^2 [see below Eq. (4.82)].

The amplification coefficient satisfies an important relation, as follows. It is easy to see that in the region (4.44) $\langle\Pi_\phi\rangle_f \sim |\langle\phi|\psi\rangle|^2$. As a result, expression (4.48) can be recast in the form

$$a \;\sim\; \langle\Pi_\phi\rangle_f^{-1/2}. \tag{4.52}$$

This relation holds in all cases for which the proper amplification is considered here (see also Secs. 4.8 and 4.9.3). It shows that the proper amplification is closely related to the post-selection, increasing with the decrease of the post-selection probability $\langle\Pi_\phi\rangle_f$ and disappearing in the limit $\langle\Pi_\phi\rangle_f \to 1$.

4.6.2. Enhancement due to an increased pointer uncertainty

Equations (4.34) and (4.41) indicate that the average pointer deflection is typically proportional to the pointer uncertainty ΔR. Hence, for typical cases, increasing the uncertainty ΔR enhances the average pointer deflection. Though this cannot improve the quantum limit of the measurement accuracy (4.51), an enhancement of the pointer deflection facilitates the readout of the measurement, increases the readout accuracy, and thus is beneficial.

As mentioned above, the pointer-deflection magnitude is maximized when the left- and right-hand sides of the generalized uncertainty relation (4.19) are of the same order [Eq. (4.33)]. In this case, for given ΔF and $\overline{[R,F]}$, increasing the covariance magnitude $|\sigma_{FR}|$ results in an increase of both ΔR and $|\overline{R}_s - \overline{R}|$, the quantum accuracy (4.51) being constant. In contrast, for standard measurements, the average pointer deflection (2.5) is independent of σ_{FR}, and hence an increase of $|\sigma_{FR}|$ decreases the quantum accuracy (4.51). Thus, for weak PPS measurements, a nonzero σ_{FR} results generally in an enhancement of the average pointer deflection with respect to the case $\sigma_{FR} = 0$ or with respect to the standard measurements by the factor

$$f \;=\; \left|\frac{2\,\overline{R_c F}}{\overline{[R,F]}}\right| \;=\; \left[1 + \left(\frac{2\sigma_{FR}}{|\,\overline{[R,F]}\,|}\right)^2\right]^{1/2}. \tag{4.53}$$

This factor provides the maximal enhancement exactly for the linear response (4.13) and by order of magnitude for the intermediate nonlinear regime. Equation (4.53) implies that *the enhancement is large if and only if there is a strong correlation between R and F*, i.e., the covariance is large,

$$f = \left| \frac{2\sigma_{FR}}{\overline{[R,F]}} \right| \gg 1 \qquad \text{when} \quad |\sigma_{FR}| \gg |\overline{[R,F]}|. \tag{4.54}$$

Note that for non-standard meters ($\overline{[R,F]} = 0$) Eq. (4.53) yields $f = \infty$, which is an expression of the fact that standard measurements are impossible for non-standard meters. Equation (4.13c) implies that in the linear regime, the enhancement is possible only when $\operatorname{Im} A_w \neq 0$ [80]. However, in the nonlinear regime, the enhancement is possible not only for $\operatorname{Im} A_w \neq 0$ but also for a real A_w, when the parameter $\overline{FR_cF}$ is nonzero in Eq. (4.11). For a discussion of specific cases, see Sec. 7.2.

The total amplification coefficient due the two above factors is

$$a_T = af. \tag{4.55}$$

The amplification of the signal described by Eq. (4.55) does not amplify technical noise [80, 85] and hence is an important effect with a promise of numerous applications in ultra-sensitive measurements and precision metrology.

4.7. Measuring weak values and coupling strengths

Equation (4.11) allows one to measure any parameter entering this expression provided the other parameters are known. Here we discuss measuring the weak value A_w and the coupling strength γ. Both linear and nonlinear regimes of the measurement are considered.

Since γ is real and A_w is complex, in principle one or two weak PPS measurements are sufficient for obtaining γ or A_w, respectively. Below we discuss extracting γ and A_w for the above minimal number of measurements. Alternatively, to increase the accuracy of the value of A_w, one may perform more than the minimal number of measurements and then fit the measurement results to Eq. (4.11). Note, however, that an increase in the number of measurements requires an increase in time and resources.

4.7.1. Measuring the coupling strength γ

The parameter γ can be measured in either the linear or nonlinear regime. As discussed above, optimal measurements of γ are obtained in the nonlinear regime (4.27), where $|\overline{R}_s - \overline{R}|$ is of the order of its maximum value.

Note a difference between the measurement procedures in the linear and nonlinear cases: given a measured value of the pointer deflection $(\overline{R}_s - \overline{R})$, in the linear (nonlinear) regime γ results from a solution of a linear (quadratic) equation [cf. Eqs. (4.13) and (4.11)]. The roots of the quadratic equation can be obtained in analytic form; only one of them yields the correct solution. Namely, the correct root γ_0 is determined uniquely by the condition $\gamma_0 \to 0$ for $\overline{R}_s \to \overline{R}$.

Thus, the nonlinear Eq. (4.11) allows one to optimize the measurement of the coupling strength. Another advantage of Eq. (4.11) is that it allows for measurement of γ, even when the first-order result (4.13a) vanishes or is very small; in this case, it is required that $\overline{FR_cF} \neq 0$.

4.7.2. Measuring A_w: One unknown parameter

Consider now the measurement of weak values. A_w is a complex quantity, and generally both the magnitude $|A_w|$ and phase θ of A_w are unknown.

Consider first the simple situation, where θ is known, at least, with an accuracy of up to π; for example, when A_w is known to be real, then θ can equal zero or π, i.e., θ is known with an accuracy of up to π. Generally, A_w and $|A_w|^2$ can be presented in the form,

$$A_w = A_{w0} \exp(i\theta'), \quad |A_w|^2 = A_{w0}^2, \tag{4.56}$$

where A_{w0} is real and θ' equals θ for $A_{w0} > 0$ or $\theta + \pi$ for $A_{w0} < 0$. Suppose that θ' is known. (For example, when A_w is known to be real or imaginary, one can set $\theta' = 0$ or $\pi/2$, respectively, i.e., $A_w = A_{w0}$ or $A_w = iA_{w0}$, respectively.) Then, on inserting Eq. (4.56) into Eq. (4.13a) or (4.11), A_{w0} can be obtained similarly to γ (see Sec. 4.7.1), from a linear or quadratic equation, respectively.

4.7.3. *Tomography of weak values*

Consider now tomography of weak values, i.e, measuring a complex A_w in the absence of any preliminary information on A_w. A complex A_w depends on two real parameters and hence to obtain A_w from Eq. (4.11), it is sufficient to perform two measurements with different values of the coupling strength γ and/or of one or more of the meter parameters. The meter parameters which can be varied include the observables R and F [124] and the meter state ρ_{M} [87]. Hereafter, we regard meters with different parameters as different meters, even if they are realized with identical physical systems.

As mentioned above, the nonlinear regime is optimal for measurements. However, the nonlinear regime can be achieved only for sufficiently large weak values or, in other words, for sufficiently small values of the overlap $\langle\phi|\psi\rangle$ (cf. Sec. 4.4.3). Therefore the linear regime is also important, since this is the only regime of weak PPS measurements achievable for not too large weak values. Another reason why the linear regime is of interest is that the linear regime is somewhat easier to analyze than the nonlinear regime. Below we show how to extract A_w with two measurements for both the linear and nonlinear regimes.

4.7.4. *Tomography of weak values: Linear regime*

Since the linear response (4.13) is proportional to γ, in the linear regime, in contrast to the nonlinear regime, a variation of γ cannot be used for tomography of weak values. Thus, in the two required measurements, the meters should necessarily differ by one or more parameters (e.g., the meters may have different pointer variables), so that the parameter θ_0 in Eq. (4.14) has different values in the two measurements. We require that these values, denoted by θ_0 and θ_0', obey the condition

$$|\theta_0 - \theta_0'| \neq 0, \pi, 2\pi, \ldots. \tag{4.57}$$

The two measurements yield by Eq. (4.13b) the quantities

$$\xi = |A_w| \sin(\theta + \theta_0), \qquad \xi' = |A_w| \sin(\theta + \theta_0'). \tag{4.58}$$

The equalities (4.58) can be recast as a set of two linear equations for $\mathrm{Re}\, A_w = |A_w| \cos\theta$ and $\mathrm{Im}\, A_w = |A_w| \sin\theta$, which has a solution under the condition (4.57). As a result, we obtain

$$A_w = \frac{\xi \exp(-i\theta_0') - \xi' \exp(-i\theta_0)}{\sin(\theta_0 - \theta_0')}. \tag{4.59}$$

For instance, in the experiment [91], the tomography of weak values was realized with $\theta_0 = \pi/2$ and $\theta_0' = 0$. In this case, Eq. (4.58) implies that $\xi = \mathrm{Re} A_w$ and $\xi' = \mathrm{Im} A_w$; correspondingly, Eq. (4.59) yields $A_w = \xi + i\xi'$.

The condition (4.57) requires that, at least, in one of the two measurements $\overline{[R, F]} \neq 0$, while in the other measurement $\sigma_{FR} \neq 0$. If $\sigma_{FR} = 0$ ($\overline{[R, F]} = 0$) in the measurements, only $\mathrm{Re}\, A_w$ ($\mathrm{Im}\, A_w$) can be measured in the linear regime. Finally, when $\overline{[R, F]} = \sigma_{FR} = 0$, the linear response vanishes and hence cannot be used for measurements. The situation is drastically different in the nonlinear regime, as follows.

4.7.5. *Tomography of weak values: Nonlinear regime*

Consider now tomography of weak values in the nonlinear regime (4.35) for the important case $|\bar{F}| \lesssim \Delta F$ (the case $|\bar{F}| \gg \Delta F$ is considered in Sec. 4.8). As in the linear case, the two necessary measurements can be performed with different meters. However, now one has also an alternative possibility: to perform the two measurements with different values of the coupling strength γ, using only *one meter for all measurements*. The condition (4.57) is generally not required now. The coupling strength γ can be varied by changing the duration of the interaction and/or the amplitude of the coupling rate $g(t)$, cf. Eq. (1.11).

Inserting the measurement results on the left-hand side of Eq. (4.11) yields two second-order algebraic equations for $\mathrm{Re}\, A_w$ and $\mathrm{Im}\, A_w$. Indeed, multiplying both sides of Eq. (4.11) by the denominator of the fraction on the rhs, transferring all the terms to the left-hand side and simplifying the expression yields for the above two measurements the respective equations of the form

$$D_{0i} + D_{1i}\, \mathrm{Re}\, A_w + D_{2i}\, \mathrm{Im}\, A_w + D_{3i}\, |A_w|^2 = 0 \qquad (i = 1, 2), \tag{4.60}$$

where the coefficients D_{ki} can be easily expressed through the parameters of the problem.

	Measurement type			Measurability of:		
Case	$\overline{[R,F]}$	σ_{FR}	$\bar{F}$	$\mathrm{Re}\,A_w$	$\mathrm{Im}\,A_w$	$\lvert A_w\rvert$
1	$\neq 0$	$\neq 0$	any	yes	yes	yes
2	$\neq 0$	0	0	yes	$\lvert\mathrm{Im}\,A_w\rvert$	yes
3	$\neq 0$	0	$\neq 0$	yes	yes	yes
4	0	$\neq 0$	any	$\lvert\mathrm{Re}\,A_w\rvert$	yes	yes
5	0	0	$\neq 0$	$\lvert\mathrm{Re}\,A_w\rvert$	yes	yes
6	0	0	0	no	no	yes

Table 4: Measurability of $\mathrm{Re}\,A_w$, $\mathrm{Im}\,A_w$, and $|A_w|$ for different types of measurements. Here we used the following conventions: (a) the word "any" means any $\bar{F}$ satisfying $|\bar{F}| \lesssim \Delta F$, (b) the parameters denoted as nonzero should be nonzero, at least, in one of the two measurements; (c) correspondingly, the parameters denoted as zero vanish in all the measurements; (d) when both $\overline{[R,F]}$ and σ_{FR} vanish, we assume that $\overline{F\,R_c\,F} \neq 0$. Note that $|A_w|$ is generally measurable in all the cases listed here.

Equations (4.60) can be solved analytically, as follows. Multiplying Eqs. (4.60) for $i = 1$ and 2 by D_{32} and $-D_{31}$, respectively, and summing the resulting equations cancels the nonlinear terms and yields a linear relation between $\mathrm{Re}\,A_w$ and $\mathrm{Im}\,A_w$. This relation allows one to express $\mathrm{Re}\,A_w$ through $\mathrm{Im}\,A_w$, thus reducing the problem to obtaining $\mathrm{Im}\,A_w$. Finally, inserting the above expression for $\mathrm{Re}\,A_w$ into one of Eqs. (4.60) yields a quadratic equation for $\mathrm{Im}\,A_w$, the quantity $\mathrm{Im}\,A_w$ being equal to the root of this equation, which tends to zero for $\bar{R}_s \to \bar{R}$.

Table 4 shows the feasibility of measuring the weak value parameters $\mathrm{Re}\,A_w$, $\mathrm{Im}\,A_w$, and $|A_w|$ for different types of measurements. Generally, Eq. (4.11) involves A_w through terms proportional to $\mathrm{Re}\,A_w$, $\mathrm{Im}\,A_w$, and $|A_w|^2$. To determine A_w completely, i.e., to obtain $\mathrm{Re}\,A_w$ and $\mathrm{Im}\,A_w$ with correct signs, each of $\mathrm{Re}\,A_w$ and $\mathrm{Im}\,A_w$ should enter linearly in Eq. (4.11) for, at least, one of the two measurements. In particular, this happens when both $\overline{[R,F]} \neq 0$ and $\sigma_{FR} \neq 0$ do not vanish for, at least, one of the two measurements (Table 4, case 1).

In case 2, a term linear in $\mathrm{Im}\,A_w$ is absent in Eq. (4.11), and hence $\mathrm{Im}\,A_w$ can be determined only up to a sign. In case 3, A_w can be determined completely, since $\mathrm{Im}\,A_w$ enters linearly in the denominator of Eq. (4.11) when $\bar{F} \neq 0$. Actually, the optimal values of $\bar{F}$ are those satisfying $|\bar{F}| \sim \Delta F$, since then in the present nonlinear case (4.35) all the three terms in the denominator of Eq. (4.11) are generally of the same order.

In cases 4 and 5, $\mathrm{Re}\,A_w$ can be obtained only up to a sign, whereas in case 6, only $|A_w|$ can be measured. Note that in cases 5 and 6 the linear response is absent, but still information on A_w can be extracted (such a case takes place, e.g., for $\Delta R = 0$, see Sec. 7.1.2).

In summary, generally A_w can be obtained completely when, at least, one of the two measurements is performed with a standard meter ($\overline{[R,F]} \neq 0$), whereas measurements using only non-standard meters ($\overline{[R,F]} = 0$) typically yield $\mathrm{Im}\,A_w$ and $|\mathrm{Re}\,A_w|$, but not the sign of $\mathrm{Re}\,A_w$.

4.8. *Large average input variable, $|\bar{F}| \gg \Delta F$*

Until now we focused mainly on the typical situation when $|\bar{F}| \lesssim \Delta F$. Usually in experiments on weak PPS measurements, the conditions are chosen to make $\bar{F}$ to vanish, exactly or effectively. However, as shown above, a moderately large value of $\bar{F}$, $|\bar{F}| \sim \Delta F$, may be useful in measuring weak values and coupling strengths.

Here we discuss the case of a large $\bar{F}$, $|\bar{F}| \gg \Delta F$. This case differs significantly from the above situation $|\bar{F}| \lesssim \Delta F$. Now the pointer deflection is generally small, except for the optimal regime which has the form of a narrow resonance, the width of which decreases with increasing $|\bar{F}|$. Let us consider the linear response and the optimal region.

The linear-response regime is independent of $\bar{F}$, and it is described in the above Sec. 4.4.1. The region of its validity is given by Eq. (4.22), which now becomes

$$|\gamma\, A_w\, \bar{F}| \ll 1. \tag{4.61}$$

Since now $\bar{F}$ is large, the maximum value of $|\gamma A_w|$ allowed by Eq. (4.61) is small, and hence the average pointer deflection in the linear-response regime is very small in the present case. The amplification coefficient in the linear response is given by the above Eq. (4.48).

Consider now the optimal regime. When $|\bar{F}| \gg \Delta F$, and $\mathrm{Re}\, A_w$ is small or vanishes,

$$|\mathrm{Re}\, A_w| \ \ll \ |\mathrm{Im}\, A_w|, \tag{4.62}$$

then $\bar{R}_s$ versus γ has a narrow resonance at

$$\gamma \bar{F}\, \mathrm{Im}\, A_w \ \approx \ -1. \tag{4.63}$$

In the vicinity of this resonance, Eq. (4.11) simplifies to

$$\bar{R}_s - \bar{R} \ = \ \frac{\overline{F_c\, R_c\, F_c}/\bar{F} - \epsilon\, \mathrm{Im}\, \overline{[R, F]} - 2\, \sigma_{FR}\, x}{\bar{F}\, [x^2 + \epsilon^2 + (\Delta F/\bar{F})^2]}. \tag{4.64}$$

Here

$$x \ = \ 1 + \gamma \bar{F}\, \mathrm{Im}\, A_w, \tag{4.65}$$

$$\epsilon \ = \ \frac{\mathrm{Re}\, A_w}{\mathrm{Im}\, A_w} \quad \text{or} \quad \epsilon \ = \ \mathrm{sgn}\, (\mathrm{Im}\, A_w)\, \frac{\pi}{2} - \theta, \tag{4.66}$$

where the two expressions for ϵ are equivalent in the approximation when Eq. (4.66) holds. In the derivation of Eq. (4.64) we used Eqs. (4.37) and (4.15); moreover, in the numerator and denominator of Eq. (4.64) we neglected terms of higher orders in x, ϵ, and $\Delta F/\bar{F}$.

Equation (4.64) describes a resonance in $\bar{R}_s$ as a function of the two variables x and ϵ or, in other words, versus any of the parameters $\mathrm{Im}\, A_w$, $\mathrm{Re}\, A_w$, γ, and $\bar{F}$. Depending on the parameter values, the resonance as a function of x or ϵ can have either Lorentzian or dispersive shape or a linear combination thereof. The resonance arises due to the fact that destructive quantum interference results in a strongly reduced post-selection probability,

$$\langle \Pi_\phi \rangle_f \ \approx \ |\langle \phi | \psi \rangle|^2 [x^2 + \epsilon^2 + (\Delta F/\bar{F})^2]. \tag{4.67}$$

The resonance as a function of x and ϵ has one or two extrema, the extremum with the largest magnitude lying in the optimal region,

$$x^2 + \epsilon^2 \ \lesssim \ \left(\frac{\Delta F}{\bar{F}} \right)^2. \tag{4.68}$$

The extrema of the resonance can be obtained analytically. However, for simplicity, we provide here only an estimate of the maximum of the magnitude of the pointer deflection. This estimate has the same value (4.38) as in the case $|\bar{F}| \lesssim \Delta F$. Indeed, in the optimal region (4.68) we obtain from Eq. (4.64) that

$$\begin{aligned} |\bar{R}_s - \bar{R}| \ &\leq \ \frac{|\,\overline{F_c R_c F_c}\,| + |\bar{F}|\, |\epsilon\, \mathrm{Im}\, \overline{[R, F]} + 2\sigma_{FR}\, x|}{\bar{F}^2\, [x^2 + \epsilon^2 + (\Delta F/\bar{F})^2]} \ \leq \ \frac{|\,\overline{F_c R_c F_c}\,| + 2|\bar{F}|\, |\,\overline{R_c F}\,|\, \sqrt{x^2 + \epsilon^2}}{\bar{F}^2\, [x^2 + \epsilon^2 + (\Delta F/\bar{F})^2]} \\ &\lesssim \ \frac{|\,\overline{F_c R_c F_c}\,| + |\bar{F}|\, (\Delta F \Delta R)\, (\Delta F/|\bar{F}|)}{(\Delta F)^2} \ = \ \frac{|\,\overline{F_c R_c F_c}\,|}{(\Delta F)^2} + \Delta R. \end{aligned} \tag{4.69}$$

Here in the second relation we used the Cauchy-Schwarz inequality and the last equality in Eq. (4.19), whereas in the third relation we used the inequalities (4.19) and (4.68). The right-hand side of Eq. (4.69) provides the estimate of the maximum of the magnitude of the pointer deflection, which coincides with Eq. (4.38).

The amplification coefficient is given by Eq. (4.52) also for $|\bar{F}| \gg \Delta F$, as follows. To obtain the maximal amplification coefficient in the optimal region (4.68), we use Eqs. (4.46) and (4.47), yielding

$$a \ \sim \ \frac{|\bar{R}_s - \bar{R}|}{|\gamma A_{\phi\psi}|\, \Delta F\, \Delta R} \ \sim \ \frac{\Delta R}{|\langle \phi | \psi \rangle / \bar{F}|\, \Delta F\, \Delta R} \ = \ \frac{|\bar{F}|}{\Delta F\, |\langle \phi | \psi \rangle|}. \tag{4.70}$$

Here we took into account that, in view of Eqs. (4.63) and (4.62), $|\gamma A_{\phi\psi} \bar{F}| \ \approx \ |\langle \phi | \psi \rangle|$; we also assumed the typical situation (4.40)-(4.41). Since in the optimal region (4.68) Eq. (4.67) yields

$$\langle \Pi_\phi \rangle_f^{-1/2} \ = \ \frac{|\bar{F}|}{\Delta F\, |\langle \phi | \psi \rangle|} \ \sim \ a, \tag{4.71}$$

the amplification coefficient (4.70) satisfies Eq. (4.52). An estimation of the magnitude of Eq. (4.64) for $x^2 + \epsilon^2 \gg \Delta F^2/\overline{F}^2$ also can be shown to yield Eq. (4.52).

Note that in the present case when $|\overline{F}| \gg \Delta F$, the optimality condition (4.68) is much stricter than the condition for the strongly-nonlinear regime (4.27) [or, equivalently, (4.28)].

An advantage of the present case $|\overline{F}| \gg \Delta F$ is that the optimal regime occurs at a much smaller value of $|\gamma|$ than for $|\overline{F}| \lesssim \Delta F$ [cf. Eqs. (4.63) and (4.35), respectively]. Correspondingly, the amplification coefficient (4.71) is much higher than the value (4.48) obtained in the case $|\overline{F}| \lesssim \Delta F$, for a given overlap magnitude $|\langle\phi|\psi\rangle|$. This allows for an increase of the measurement precision in the present case as compared to the case $|\overline{F}| \lesssim \Delta F$, when, by some reason, the overlap $\langle\phi|\psi\rangle$ cannot be made too small.

Moreover, the fact that Eq. (4.64) is a narrow resonance as a function of a number of parameters makes this resonance very sensitive to small perturbations of the parameters of the problem. This sensitivity of the resonance can be used for precise measurements of these parameters.

4.9. The minimum size of the ensemble and the signal-to-noise ratio

Here we estimate the minimum size N_0 of the ensemble required for a weak PPS measurement. In Secs. 4.9.1 and 4.9.2 we consider the region (4.26), which includes the linear response and the intermediate nonlinear regime, whereas in Sec. 4.9.3 we discuss the inverted region.

4.9.1. The linear and intermediate regimes

We consider the typical case when the uncertainty ΔR does not vanish and is sufficiently large, so that the width of the distribution of R at $t > t_{\mathrm{f}}$ is of the order of ΔR. Consider an ensemble of N pairs consisting of a system and a meter. Only $\langle\Pi_\phi\rangle_f N$ of the N pairs are taken into account in a PPS measurement. A measurement produces a shift of the maximum of the distribution of the sum of $\langle\Pi_\phi\rangle_f N$ pointer values, equal to $\langle\Pi_\phi\rangle_f N\,(\overline{R}_s - \overline{R})$. We determine the minimum size of the ensemble by requiring that the square of the shift of the maximum of the above distribution is equal to the variance of this distribution. This yields the equation

$$[\langle\Pi_\phi\rangle_f\, N\,(\overline{R}_s - \overline{R})]^2 \;=\; \langle\Pi_\phi\rangle_f\, N\,(\Delta R_s)^2, \tag{4.72}$$

where ΔR_s if the pointer uncertainty after a PPS measurement. Equation (4.72) provides the minimum size

$$N_0 \;=\; \frac{(\Delta R_s)^2}{\langle\Pi_\phi\rangle_f\,(\overline{R}_s - \overline{R})^2}. \tag{4.73}$$

In the linear-response regime, ΔR_s approximately equals ΔR, and Eq. (4.73) becomes

$$N_0 \;=\; \frac{(\Delta R)^2}{\langle\Pi_\phi\rangle_f\,(\overline{R}_s - \overline{R})^2}, \tag{4.74}$$

whereas beyond the linear response in weak PPS measurements, $\Delta R_s \sim \Delta R$, and Eq. (4.73) yields the relation

$$N_0 \;\sim\; \frac{(\Delta R)^2}{\langle\Pi_\phi\rangle_f\,(\overline{R}_s - \overline{R})^2}. \tag{4.75}$$

Moreover, it is useful to consider the signal-to-noise ratio (SNR) $\mathcal{R}$ with respect to the quantum noise. It equals the ratio of the left-hand side of Eq. (4.72) (the modulus of the shift, i.e., the signal) to the right-hand side (the square root of the variance, which sets the noise level), yielding

$$\mathcal{R} = \sqrt{\frac{N}{N_0}}. \tag{4.76}$$

Thus, the quantity N_0 determines the SNR by Eq. (4.76).

To estimate the lower bound on N_0 in the region of interest (4.26), we note that, in view of Eq. (4.46),

$$|\overline{R}_s - \overline{R}| \;\sim\; a\,\mu_0\,\Delta R, \tag{4.77}$$

and insert Eq. (4.77) into Eq. (4.75), yielding $N_0 \sim (\langle \Pi_\phi \rangle_f \, a^2 \mu_0^2)^{-1}$ or, in view of Eqs. (4.52) and (4.9),

$$N_0 \sim \mu_0^{-2} = (\gamma \, |A_{\phi\psi}| \, \Delta F)^{-2}. \tag{4.78}$$

Hence, generally the ensemble size equals roughly the inverse square of the measurement strength. It is remarkable that the post-selection probability $\langle \Pi_\phi \rangle_f$ and the amplification coefficient a mutually *cancel* in Eq. (4.78). Equation (4.78) shows that, until the condition (4.26) holds, one can decrease $\langle \phi | \psi \rangle$, thus increasing A_w for a constant N_0 or, alternatively, increase the coupling strength γ, thus decreasing N_0 for a constant A_w.

The minimum ensemble size (for given pre- and post-selected states) is obtained in the intermediate nonlinear regime (4.27), when Eq. (4.78) yields

$$N_0 \sim \frac{1 + (\overline{F}/\Delta F)^2}{|\langle \phi | \psi \rangle|^2}. \tag{4.79}$$

In the case $|\overline{F}| \lesssim \Delta F$, the ensemble size is minimal when [cf. Eq. (4.79)]

$$N_0 \sim |\langle \phi | \psi \rangle|^{-2}. \tag{4.80}$$

In the optimal regime, Eq. (4.79) can be recast in two different ways, as follows. We note that in the optimal regime the following estimate of the post-selection probability can be used,

$$\langle \Pi_\phi \rangle_f \sim \frac{|\langle \phi | \psi \rangle|^2}{1 + (\overline{F}/\Delta F)^2}, \tag{4.81}$$

Eq. (4.81) being equivalent to $\langle \Pi_\phi \rangle_f \sim |\langle \phi | \psi \rangle|^2$ for $|\overline{F}| \lesssim \Delta F$ and to the first relation in Eq. (4.71) for $|\overline{F}| \gg \Delta F$. Comparing Eqs. (4.79) and (4.81) and using the relation (4.52) yields

$$N_0 \sim \langle \Pi_\phi \rangle_f^{-1} \sim a^2. \tag{4.82}$$

Thus, in the optimal regime the ensemble size equals roughly the inverse post-selection probability or, alternatively, the squared amplification coefficient.

4.9.2. Comparison of weak measurements with and without post-selection

Let us compare the ensemble sizes for weak measurements with and without post-selection in the region (4.26). If one uses an essentially quantum meter [Eq. (2.8)] for both types of measurements, then a comparison of Eqs. (4.78) and (2.11) shows that *weak measurements with and without post-selection require ensembles of comparable sizes* (for comparable magnitudes of $A_{\phi\psi}$ and $\overline{A}$). The peculiarity of weak PPS measurements is that they are performed on a subensemble of the relative size $\langle \Pi_\phi \rangle_f$, where the pointer deflection is amplified with the amplification coefficient $\langle \Pi_\phi \rangle_f^{-1/2}$. This amplification allows one to increase the measurement accuracy in the presence of technical (but not quantum) noise, as noted in Ref. [80]. Thus, meters which are efficient for standard measurements (i.e., essentially quantum meters) are also efficient for PPS measurements.

In contrast, when the meter is not essentially quantum, i.e., $|\overline{[R, F]}| \ll \Delta R \, \Delta F$, the ensemble size for measurements without post-selection is generally much greater than for weak PPS measurements; indeed, then Eq. (2.10) implies that $N_0 \gg (\gamma \overline{A} \Delta F)^{-2}$. Thus, meters which are not essentially quantum meters are not efficient for standard measurements, but are still efficient for PPS measurements. Typically, meters are not essentially quantum, when the covariance is large, $\sigma_{FR} \gg |\overline{[R, F]}|$, since then Eq. (4.19) implies that $|\overline{[R, F]}| \ll \Delta R \, \Delta F$. In this case, the enhancement coefficient f is large [see Eq. (4.54)], which explains why such meters are efficient for PPS measurements.

Finally, in the limiting case $\overline{[R, F]} = 0$ (non-standard meters), weak standard measurements cannot be performed at all, while weak PPS measurements are still generally efficient.

4.9.3. Inverted region

When the overlap $\langle \phi | \psi \rangle$ tends to zero, the pointer deflection tends to a nonzero value [cf. Eq. (4.24)]

$$\delta R_\infty = \frac{\overline{F \, R_c \, F}}{\overline{F^2}}, \tag{4.83}$$

which depends only on the meter but not on the system or the coupling. The relevant pointer deflection, which is directly related to the weak value, is now adjusted by

$$\bar{R}_s - \bar{R} \;\; \rightarrow \;\; \bar{R}_s - \bar{R} - \delta R_\infty. \tag{4.84}$$

Here the quantity $\bar{R}_s - \bar{R} - \delta R_\infty$ is the deflection of the pointer from the value $\bar{R} + \delta R_\infty$ the pointer acquires in the limit $\langle\phi|\psi\rangle \rightarrow 0$. When $\overline{FR_cF} = 0$, the adjusted pointer deflection $\bar{R}_s - \bar{R} - \delta R_\infty$ coincides with the usual pointer deflection $\bar{R}_s - \bar{R}$. Now the minimum size of the ensemble is given by Eq. (4.73) or (4.75) with the change (4.84).

We estimate N_0 in the important case $|\bar{F}| \lesssim \Delta F$. To this end, we estimate $|\bar{R}_s - \bar{R} - \delta R_\infty|$ by Eq. (4.24) with the help of Eqs. (4.21) and (4.33). We also assume that the third term on the rhs of Eq. (4.24) does not exceed significantly the second term, which happens when $\bar{F}$ is zero or sufficiently small and also happens, as a rule, when Eq. (4.40) holds. Then we obtain that

$$|\bar{R}_s - \bar{R} - \delta R_\infty| \;\sim\; \frac{|\,\overline{R_cF}\,|}{|\gamma A_w|\,(\Delta F)^2} \;\sim\; \frac{\Delta R}{|\gamma A_w|\,\Delta F} \;=\; \frac{\Delta R\,|\langle\phi|\psi\rangle|}{|\gamma A_{\phi\psi}|\,\Delta F}. \tag{4.85}$$

Furthermore, $\langle\Pi_\phi\rangle_f/|\langle\phi|\psi\rangle|^2$ is given by the denominator in Eq. (4.11), so that in the present limit

$$\begin{aligned}\langle\Pi_\phi\rangle_f \;&=\; |\langle\phi|\psi\rangle|^2\,(1 + 2\gamma\bar{F}\,\mathrm{Im}\,A_w + \gamma^2\,\overline{F^2}\,|A_w|^2) \;\approx\; |\langle\phi|\psi\rangle|^2\gamma^2\,\overline{F^2}\,|A_w|^2 \\ &=\; \gamma^2\,|A_{\phi\psi}|^2\,\overline{F^2} \;\sim\; \gamma^2\,|A_{\phi\psi}|^2\,(\Delta F)^2.\end{aligned} \tag{4.86}$$

Inserting Eqs. (4.84)-(4.86) into Eq. (4.75) yields the minimal ensemble size given by Eq. (4.80),

$$N_0 \;\sim\; |\langle\phi|\psi\rangle|^{-2}. \tag{4.87}$$

Note that in the present limit the overlap $\langle\phi|\psi\rangle$ is very small; Eq. (4.85) implies that the present regime is suitable for measuring the overlap. In view of Eqs. (4.76) and (4.87), for such a measurement the SNR is

$$\mathcal{R} \;\sim\; |\langle\phi|\psi\rangle|\,\sqrt{N}. \tag{4.88}$$

It is quite remarkable that the quantum SNR (4.88), which was obtained for weak PPS measurements, is of the same order as for *strong (projective) measurements* of a small overlap $|\langle\phi|\psi\rangle|$. Indeed, for a system in the state $|\psi\rangle$, the overlap can be determined by measuring the projection operator[5] $\Pi_\phi = |\phi\rangle\langle\phi|$. Such a measurement results in the eigenvalue 1 with the probability $P_1 = |\langle\phi|\psi\rangle|^2$ and the eigenvalue 0 with the probability $P_0 = 1 - |\langle\phi|\psi\rangle|^2$. After the measurement of an ensemble of N systems, the sum of the obtained eigenvalues is described by the binomial distribution and, correspondingly, has the average NP_1 and the square root of the variance $(NP_1P_0)^{1/2}$. The equality between the two latter quantities is attained for the minimal ensemble size

$$N_0 \;=\; \frac{P_0}{P_1} \;\approx\; |\langle\phi|\psi\rangle|^{-2}, \tag{4.89}$$

where the approximation holds for $|\langle\phi|\psi\rangle| \ll 1$. As follows from Eqs. (4.76) and (4.89), now the SNR is given by

$$\mathcal{R} \;=\; |\langle\phi|\psi\rangle|\,\sqrt{N}. \tag{4.90}$$

Thus, weak PPS measurements in the regime of very large weak values can be used to measure small overlaps with the same quantum SNR as the ideal measurements. Moreover, when the measurement accuracy is limited by technical noise, weak PPS measurements can provide a higher measurement accuracy than ideal measurements, since weak PPS measurements involve a strong amplification. Indeed, in Eq. (4.85), the factor

$$a' \;=\; (|\gamma\,A_{\phi\psi}\,|\,\Delta F)^{-1} \;\gg\; 1, \tag{4.91}$$

---

[5] The method considered here is not the only conceivable projective measurement of $|\langle\phi|\psi\rangle|$. Another projective-measurement scheme, a balanced homodyne detection, is discussed in Sec. 12.3; however for both schemes the SNR values are of the same order of magnitude.

provides the proper amplification for the measurement of the overlap; this factor is large in weak PPS measurements, as implied by Eq. (4.7a). As follows from Eqs. (4.86) and (4.91), the amplification coefficient a' satisfies the relation [cf. Eq. (4.52)]

$$a' \;\sim\; \langle \Pi_\phi \rangle_f^{-1/2}. \tag{4.92}$$

The factor a' describes the increase of the quantum-limited signal-to-noise ratio (per one measurement)

$$\frac{|\bar{R}_s - \bar{R} - \delta R_\infty|}{\Delta R} \tag{4.93}$$

relative to the case when the small parameter approaches the limit $|\gamma\, A_{\phi\psi}|\,\Delta F \sim 1$, where the measurement is not weak and hence the present theory breaks; in this case, Eq. (4.85) yields

$$\frac{|\bar{R}_s - \bar{R} - \delta R_\infty|}{\Delta R} \;\sim\; |\langle\phi|\psi\rangle| \qquad \text{when } \; |\gamma A_{\phi\psi}|\,\Delta F \sim 1. \tag{4.94}$$

Equation (4.91) shows that now, paradoxically, *the decrease of the measurement strength* $|\gamma A_{\phi\psi}|\,\Delta F$ *increases the magnitude of the average adjusted pointer deflection* $|\bar{R}_s - \bar{R} - \delta R_\infty|$ (for given ΔR and $|\langle\phi|\psi\rangle|$) and hence increases the measurement accuracy with respect to technical errors.

However, a' cannot be increased indefinitely, since Eq. (4.85) holds only until $a'|\langle\phi|\psi\rangle| \ll 1$ [cf. Eq. (4.23)]. When a' becomes so large that $a'|\langle\phi|\psi\rangle| \sim 1$, the inverted-region case (the limit of very large weak values) is not applicable any more. Instead, the measurement is performed in the strongly-nonlinear regime [cf. Eq. (4.27)], which provides the highest accuracy and hence is optimal, as mentioned above.

Since the average adjusted pointer deflection (4.85) is proportional to ΔR and hence increases with the covariance σ_{FR} for a given ΔF [cf. the generalized uncertainty relation (4.19)], the present regime involves also an enhancement by the factor f in Eq. (4.53). The enhancement factor f describes the increase of the signal (i.e., the average adjusted pointer deflection) due to the correlation between F and R in comparison to the case of uncorrelated F and R, when ΔF is kept constant. The total amplification coefficient is given by [cf. Eq. (4.55)]

$$a'_T \;=\; a' f. \tag{4.95}$$

For non-standard meters ($\overline{[R,F]} = 0$), the parameters f and a'_T are infinite and hence do not make much sense, but the proper amplification is still a meaningful notion.

An experiment on weak PPS measurements in the inverted region is discussed in Sec. 12.

5. Mixed preselected state

5.1. The general nonlinear formula

Here we extend the above results to take into account that the initial ("preselected") state of the system ρ can be mixed. Now Eqs. (3.13) and (3.14) imply that the expansions for $\langle \Pi_\phi R_c \rangle_f$ and $\langle \Pi_\phi \rangle_f$ have the same form as in Eq. (3.16) with the changes

$$|\langle\phi|\psi\rangle|^2 \;\to\; \rho_{\phi\phi}, \tag{5.1a}$$

$$(A^k)_w (A^l)^*_w \;\to\; A_w^{(k,l)} \;\equiv\; \frac{(A^k \rho A^l)_{\phi\phi}}{\rho_{\phi\phi}} \qquad (k, l \geq 0), \tag{5.1b}$$

where $A^0 = (A^0)_w = 1$. As a result, Eqs. (4.11) and (4.12) become now, respectively,

$$\bar{R}_s - \bar{R} \;=\; \frac{2\gamma\, \mathrm{Im}\,(\overline{R_c F A_w}) + \gamma^2\, \overline{F R_c F}\, A_w^{(1,1)}}{1 + 2\gamma\, \bar{F}\, \mathrm{Im}\, A_w + \gamma^2\, \overline{F^2}\, A_w^{(1,1)}} \tag{5.2}$$

and

$$\bar{R}_s \;=\; \frac{\bar{R} + 2\gamma\, \mathrm{Im}\,(\overline{R F A_w}) + \gamma^2\, \overline{F R F}\, A_w^{(1,1)}}{1 + 2\gamma\, \bar{F}\, \mathrm{Im}\, A_w + \gamma^2\, \overline{F^2}\, A_w^{(1,1)}}. \tag{5.3}$$

Formally, Eqs. (5.2) and (5.3) follow from Eqs. (4.11) and (4.12) on replacing the definition (1.36) of the weak value by Eq. (1.58) and replacing

$$|A_w|^2 \;\to\; A_w^{(1,1)} \;=\; \frac{(A\rho A)_{\phi\phi}}{\rho_{\phi\phi}}. \tag{5.4}$$

As shown by Eq. (5.2) or (5.3), in the case of a mixed initial state, the results of weak PPS measurements depend on *two weak-value parameters*, A_w [given now by Eq. (1.58)] and the associated weak value $A_w^{(1,1)}$, Eq. (5.4).

5.2. Validity conditions for weak PPS measurements

The validity conditions for weak PPS measurements with a mixed preselected state can be derived as in Sec. 4.1, the only difference being that the A-dependent factors in Eq. (4.1) are changed now, in view of Eqs. (5.1), as follows,

$$(A^k)_{\phi\psi}(A^{n-k})_{\psi\phi} \;\to\; (A^k\rho A^{n-k})_{\phi\phi} \qquad (0 \le k \le n). \tag{5.5}$$

As a prerequisite to an estimation of these factors, we need to derive several inequalities, as follows.

The spectral expansion of ρ has the form

$$\rho = \sum_i \lambda_i \, |\psi_i\rangle\langle\psi_i|, \tag{5.6}$$

where $\langle\psi_i|\psi_j\rangle = \delta_{ij}$, $\lambda_i \ge 0$, and $\sum_i \lambda_i = 1$. In view of Eq. (5.6), we can write that

$$\begin{aligned} |(A^k\rho\, A^{n-k})_{\phi\phi}|^2 \;&=\; \left|\sum_i \lambda_i\, (A^k)_{\phi\psi_i}\, (A^{n-k})_{\psi_i\phi}\right|^2 \;\le\; \sum_i \lambda_i\, |(A^k)_{\phi\psi_i}|^2 \sum_j \lambda_j\, |(A^{n-k})_{\psi_j\phi}|^2 \\ &=\; (A^k\rho A^k)_{\phi\phi}\, (A^{n-k}\rho A^{n-k})_{\phi\phi}, \end{aligned} \tag{5.7}$$

where the Cauchy-Schwarz inequality is used. Thus, we obtain the inequality

$$|(A^k\rho\, A^{n-k})_{\phi\phi}|^2 \;\le\; (A^k\rho\, A^k)_{\phi\phi}\, (A^{n-k}\rho\, A^{n-k})_{\phi\phi}. \tag{5.8}$$

In particular, for $n = k = 1$, Eq. (5.8) implies that

$$|(A\rho)_{\phi\phi}|^2 \;\le\; (A\rho\, A)_{\phi\phi}\, \rho_{\phi\phi} \tag{5.9}$$

or, in view of Eqs. (1.58) and (5.4),

$$|A_w|^2 \;\le\; A_w^{(1,1)}. \tag{5.10}$$

For a pure state ρ, Eqs. (5.8)-(5.10) become equalities. Moreover, for $k \ge 0$, we have the inequality

$$\begin{aligned} (A^k\rho A^k)_{\phi\phi} \;&=\; \sum_i \lambda_i\, |(A^k)_{\phi\psi_i}|^2 \\ &\le\; \lambda_{\max} \sum_i |(A^k)_{\phi\psi_i}|^2 \;=\; \lambda_{\max}\, (A^{2k})_{\phi\phi}, \end{aligned} \tag{5.11}$$

where $\lambda_{\max} = \max\{\lambda_i\}$.

To estimate the quantity on the rhs of Eq. (5.5), we assume that

$$(A^{2k})_{\phi\phi} \;\lesssim\; [(A^2)_{\phi\phi}]^k \tag{5.12}$$

and that the left and right sides in Eq. (5.11) (with $k = 1$) are comparable, i.e.,

$$(A\rho\, A)_{\phi\phi} \;\sim\; \lambda_{\max}\, (A^2)_{\phi\phi}. \tag{5.13}$$

Combining Eqs. (5.8), (5.11), and (5.12) yields that

$$|(A^k\,\rho\, A^{n-k})_{\phi\phi}| \;\lesssim\; \lambda_{\max}\, [(A^2)_{\phi\phi}]^{n/2}. \tag{5.14}$$

Using the relations (5.13), (5.14), and (C.12), we obtain that the omission of higher-order terms in the numerator and denominator of Eq. (5.2) is justified under the condition

$$\mu' \equiv |\gamma| \, [(A^2)_{\phi\phi}]^{1/2} \, (|\bar{F}| + \Delta F) \ll 1, \tag{5.15}$$

where μ' is the small parameter in the case of a mixed initial state.

The small parameter μ' in Eq. (5.15) differs from μ in Eq. (4.5) by the A-dependent factor. The latter is obtained under the assumptions (5.12) and (5.13). Note that Eq. (5.12) holds, e.g., when $(A^2)_{\phi\phi} \sim ||A||^2$. It is of interest to compare the present validity conditions (5.12), (5.13), and (5.15) with the respective conditions (4.2) and (4.5) obtained for the case of a pure initial state $\rho = |\psi\rangle\langle\psi|$. In this case $\lambda_{\max} = 1$, so that Eq. (5.13) becomes the relation

$$|A_{\phi\psi}| \sim [(A^2)_{\phi\phi}]^{1/2}, \tag{5.16}$$

which implies the equivalence of the conditions (5.15) and (4.5). Note that the conditions (5.12) and (5.16) are generally stricter than Eq. (4.2). However, this difference can be negligible in some cases, as, e.g., in the important case $|A_{\phi\psi}| \sim ||A||$.

5.3. *Different regimes*

The linear approximation to Eq. (5.2) has the above form (4.13a) or (4.13c), with A_w given now by Eq. (1.58). Consider the validity conditions of the linear approximation. The denominator in Eq. (5.2) is close to one and hence can be omitted, when

$$\gamma^2 A_w^{(1,1)} \, [(\Delta F)^2 + \bar{F}^2] \ll 1. \tag{5.17}$$

If, moreover, A_w is sufficiently large, $|A_w|^2 \sim A_w^{(1,1)}$ [cf. Eq. (5.10)], then generally also the quadratic term in the numerator of Eq. (5.2) can be neglected, i.e., the linear approximation holds; in this case the condition (5.17) is equivalent to Eq. (4.20).

In the present case of a mixed initial state, the weak-value parameters A_w and $A_w^{(1,1)}$ generally cannot be made infinitely large (see Sec. 9.3). Still, if $A_w^{(1,1)}$ is sufficiently large, the nonlinear Eq. (5.2) should be used. In particular, when the condition (5.17) is inverted,

$$\gamma^2 A_w^{(1,1)} \, [(\Delta F)^2 + \bar{F}^2] \gg 1, \tag{5.18}$$

Eq. (5.2) yields Eq. (4.24) with the change

$$A_w \rightarrow \frac{A_w^{(1,1)}}{A_w^*}, \tag{5.19}$$

so that we obtain

$$\bar{R}_s - \bar{R} \approx \frac{\overline{F R_c F}}{\overline{F^2}} + \frac{2 \, \mathrm{Im} \, (\overline{R_c F} \, A_w)}{\gamma \, \overline{F^2} \, A_w^{(1,1)}} - \frac{2\bar{F} \, \overline{F R_c F} \, \mathrm{Im} \, A_w}{\gamma \, (\overline{F^2})^2 \, A_w^{(1,1)}}. \tag{5.20}$$

5.4. *Measuring the coupling strength and weak values*

The dependence of $\bar{R}_s$ on γ in Eq. (5.2) is similar to that in the case of a pure initial state, though the peaks in $|\bar{R}_s - \bar{R}|$ are now generally lower and broader. The measurements of γ and the weak values A_w and $A_w^{(1,1)}$ are now performed similarly to the case of a pure initial state (see Sec. 4.7), the measurements being optimal in the strongly-nonlinear regime [cf. Eq. (4.27)],

$$\gamma^2 A_w^{(1,1)} \, \overline{F^2} \sim 1. \tag{5.21}$$

Since now there are three real weak-value parameters, $\mathrm{Re} \, A_w$, $\mathrm{Im} \, A_w$, and $A_w^{(1,1)}$, measuring them requires, at least, three weak PPS measurements with different values of the meter or coupling parameters, rather than two as for a pure initial state.

5.5. Large average input variable, $|\bar{F}| \gg \Delta F$

In the case $|\bar{F}| \gg \Delta F$, it is convenient to characterize the effects of the mixedness of the preselected state by the parameter

$$v \;=\; \frac{(A_w^{(1,1)} - |A_w|^2)^{1/2}}{|\mathrm{Im}\, A_w|}. \tag{5.22}$$

Note that for pure preselected states $v = 0$. When the preselected state is almost pure, $v \ll 1$, the pointer value is resonantly enhanced under the conditions (4.62)-(4.63), the resonance being approximately described by the expression

$$\bar{R}_s - \bar{R} \;=\; \frac{\overline{F_c R_c F_c} - \epsilon \bar{F}\,\mathrm{Im}\,\overline{[R,F]} - 2x\bar{F}\sigma_{FR}}{\bar{F}^2[x^2 + \epsilon^2 + (\Delta F/\bar{F})^2 + v^2]}, \tag{5.23}$$

which differs from Eq. (4.64) by the term v^2 in the denominator. The effect of $v \neq 0$ is to broaden the resonance (5.23) and to decrease its amplitude, so that the maximum possible pointer deflection (4.38) can be achieved only for

$$v \;\lesssim\; \frac{\Delta F}{|\bar{F}|} \;\ll\; 1, \tag{5.24}$$

whereas for $v \gg \Delta F/|\bar{F}|$ the maximum magnitude of Eq. (5.23) is much less than Eq. (4.38), decreasing with v. Equation (5.24) provides a limitation on the ratio $|\bar{F}|/\Delta F$ under which the optimal regime (4.38) is possible, namely, $|\bar{F}|/\Delta F \lesssim v^{-1}$. The sensitivity of the resonance (5.23) to the quantity v for $v \gtrsim \Delta F/|\bar{F}|$ can be used to measure v when v is very small.

5.6. The ensemble size needed for weak PPS measurements

Let us estimate the size of the ensemble needed for weak PPS measurements for the important case

$$\gamma^2 A_w^{(1,1)}\,[(\Delta F)^2 + \bar{F}^2] \;\lesssim\; 1, \tag{5.25}$$

which includes both the linear and nonlinear regimes. We start from Eq. (4.75). For the important case $|A_w|^2 \sim A_w^{(1,1)}$, in the region of interest (5.25) we can insert Eq. (4.34) into Eq. (4.75), yielding [cf. Eq. (4.78)]

$$N_0 \;\sim\; [\gamma^2\,(A\rho A)_{\phi\phi}\,(\Delta F)^2]^{-1}. \tag{5.26}$$

Similarly to Sec. 4.9, we obtain that N_0 is minimized in the intermediate nonlinear regime given by Eq. (5.21), when Eq. (5.26) becomes [cf. Eq. (4.79)]

$$N_0 \;\sim\; \frac{1 + (\bar{F}/\Delta F)^2}{\rho_{\phi\phi}}. \tag{5.27}$$

This equation implies that the minimum size of the ensemble is obtained in the important case, $|\bar{F}| \lesssim \Delta F$, where

$$N_0 \;\sim\; (\rho_{\phi\phi})^{-1} \;\sim\; \langle \Pi_\phi \rangle_f^{-1}. \tag{5.28}$$

6. Effects of the system and meter Hamiltonians on pre- and post-selected and standard measurements

The Hamiltonians of the system and meter, H_S and H_M, were neglected so far. Let us now discuss the effects of these Hamiltonians on PPS and standard measurements. The results in this section hold for PPS and standard measurements of *arbitrary strength*.

For simplicity, we consider only the cases when the coupling Hamiltonian (1.8) is the same in the Schrödinger and interaction pictures. This holds when H_S and H_M commute with the coupling Hamiltonian (1.8), so that in the interval $(0, t_\mathrm{f})$, $H_\mathrm{S}(t) = H_{\mathrm{S}1}$ [$H_\mathrm{M}(t) = H_{\mathrm{M}1}$] commutes with $\hat{A}$ ($\hat{F}$) or vanishes; however, for $t > t_\mathrm{f}$, $H_\mathrm{S}(t) = H_{\mathrm{S}2}$ and $H_\mathrm{M}(t) = H_{\mathrm{M}2}$ can be arbitrary. These assumptions are rather general, and they include, in particular, the case of time-independent Hamiltonians, $H_{i1} = H_{i2}$, $(i = \mathrm{S}, \mathrm{M})$. A measurement scheme with $H_{i1} \neq H_{i2}$ was discussed in Ref. [123].

6.1. Effects of the Hamiltonians on pre- and post-selected measurements

First, consider PPS measurements. Assume that the post-selection is made at $t_S > t_f$ and the measurement of the meter is performed at $t_M > t_f$. Then the effects of the system and meter Hamiltonians are taken into account by the change

$$U \to U_S U_M U \tag{6.1}$$

in Eq. (3.8), where

$$U_S = \exp[-iH_{S2}(t_S - t_f)] \exp[-iH_{S1}t_f], \tag{6.2a}$$

$$U_M = \exp[-iH_{M2}(t_M - t_f)] \exp[-iH_{M1}t_f]. \tag{6.2b}$$

Instead of changing U, one can equivalently make the following replacements,

$$\rho \to U_{S1}\, \rho\, U_{S1}^\dagger, \quad |\phi\rangle \to U_{S2}^\dagger |\phi\rangle \tag{6.3a}$$

to allow for a nonzero system Hamiltonian and

$$\rho_M \to U_{M1}\, \rho_M\, U_{M1}^\dagger, \quad \hat{R} \to U_{M2}^\dagger \hat{R}\, U_{M2} \tag{6.3b}$$

to allow for a nonzero meter Hamiltonian. In Eqs. (6.3), U_{S1}, U_{S2}, U_{M1}, and U_{M2} are any unitary operators such that U_{S1} (U_{M1}) commutes with $\hat{A}$ ($\hat{F}$), and

$$U_{S2}U_{S1} = U_S, \quad U_{M2}U_{M1} = U_M. \tag{6.4}$$

Thus, there is a freedom in selecting U_{S1}, U_{S2}, U_{M1}, and U_{M2}, which may be conveniently used.

6.2. Effects of the Hamiltonians on standard measurements

For standard measurements, the effects of the system and meter Hamiltonians are taken into account by Eqs. (6.1)-(6.3), with the exception of Eq. (6.3a) which should be substituted by

$$\rho \;\to\; U_S\, \rho\, U_S^\dagger. \tag{6.5}$$

6.3. Special cases for the meter Hamiltonian

Let us consider in more detail the effects of the meter Hamiltonian. The results shown below hold both for PPS and standard measurements. The effects of the system Hamiltonian can be similarly considered.

In the general case, when H_{M2} does not necessarily commute with $\hat{F}$, it may be convenient to ascribe all the effects of the meter Hamiltonian to the effective pointer given by the replacement

$$\hat{R} \;\to\; \hat{R}(t_M) = U_M^\dagger \hat{R}\, U_M, \tag{6.6}$$

where $R(t)$ is the quantity R in the Heisenberg representation, while ρ_M is left unchanged [see Eq. (6.3b) with $U_{M1} = I_M$]. Consider now several simple cases.

In the special case

$$H_{M1} = H_{M2} \equiv H_M, \tag{6.7}$$

Eq. (6.2b) simplifies to

$$U_M = \exp(-iH_M t_M). \tag{6.8}$$

In this case the operator $\hat{R}(t)$ obeys the equation

$$\frac{\partial \hat{R}(t)}{\partial t} = i[H_M, \hat{R}(t)] \tag{6.9}$$

with the initial condition

$$\hat{R}(0) = \hat{R}. \tag{6.10}$$

No.	Meter configuration	Moments of the meter variables: $\overline{R_cF}$	$\overline{FR_cF}$	$\overline{F_cR_cF_c}$
1	$\overline{F_c^3} = 0$	$(\Delta F)^2$	$2\overline{F}(\Delta F)^2$	0
2	General	$(\Delta F)^2$	$\overline{F_c^3} + 2\overline{F}(\Delta F)^2$	$\overline{F_c^3}$

Table 5: Moments of the meter variables used in the present theory, for an arbitrary meter with $R = F$ with different classes of initial states.

An alternative simplification exists in the special case, when not only H_{M1} but also H_{M2} commutes with $\hat{F}$,

$$[H_{\mathrm{M2}}, \hat{F}] = 0. \tag{6.11}$$

Then also U_{M}, Eq. (6.2b), and hence U_{M2} commute with $\hat{F}$. In this case, on setting in Eq. (6.3b) $U_{\mathrm{M1}} = U_{\mathrm{M}}$ and $U_{\mathrm{M2}} = I_{\mathrm{M}}$, the effect of the meter Hamiltonian can be taken into account without a change of R, by changing only ρ_{M} in Eq. (3.8),

$$\rho_{\mathrm{M}} \;\rightarrow\; \rho_{\mathrm{M}}(t_{\mathrm{M}}) \;=\; U_{\mathrm{M}}\,\rho_{\mathrm{M}}\,U_{\mathrm{M}}^{\dagger}. \tag{6.12}$$

Here $\rho_{\mathrm{M}}(t)$ is the meter state in the Schrödinger representation, which would be obtained in the absence of the system-meter coupling.

When both Eqs. (6.7) and (6.11) hold, Eq. (6.12) is independent of t_{f} [cf. Eq. (6.8)]. This means that now, as far as the measurement is concerned, it is not important in which part of the interval $(0, t_{\mathrm{M}})$ the coupling (1.8) is nonzero.

Finally, when $t_{\mathrm{M}}, t_{\mathrm{f}}, t_{\mathrm{i}} \rightarrow 0$, the measurement results are independent of the meter Hamiltonians H_{M1} and H_{M2}, since then $U_{\mathrm{M}} \rightarrow 1$ [see Eq. (6.2b)].

7. Examples of meters

The above theory is very general and holds for meters with finite- and infinite-dimensional Hilbert spaces. Below we consider the average pointer deflection for various types of meters. In particular, we will obtain formulas for the meter parameters which are important for weak PPS measurements. Such parameters, which are discussed below, include the following complicated mixed moments of the meter variables: $\overline{R_cF}$, $\overline{FR_cF}$, and $\overline{F_cR_cF_c}$ [compare, e.g., Eqs. (4.11), (4.38), (4.64), and (5.2)].

7.1. Non-standard meters

Consider two simple types of non-standard meters.

7.1.1. Coinciding input and output variables, R = F

The above theory significantly simplifies when R and F commute. For the simplest such case, $R = F$, the moments of meter variables used in the present theory are shown in Table 5 for different classes of the initial states of the meter. In particular, case 2 in Table 5 corresponds to an arbitrary initial state, whereas meter configuration 1 describes the special case $\overline{F_c^3} = 0$, which occurs, e.g., for a symmetric distribution $\Phi(F) = \langle F|\rho_{\mathrm{M}}|F\rangle$ (e.g., a Gaussian or a Lorentzian) centered at $\overline{F}$, so that $\Phi(F) = \Phi(2\overline{F} - F)$. In Table 5 we used Eq. (4.37).

Thus, configuration 2 in Table 5 implies that for $R = F$, Eq. (4.11) becomes

$$\overline{F}_s - \overline{F} \;=\; \frac{2\gamma\,(\Delta F)^2\,\mathrm{Im}\,A_w + \gamma^2[\overline{F_c^3} + 2\overline{F}(\Delta F)^2]\,|A_w|^2}{1 + 2\gamma\,\overline{F}\,\mathrm{Im}\,A_w + \gamma^2\,\overline{F^2}\,|A_w|^2}. \tag{7.1}$$

In the linear regime [Eq. (4.20)], Eq. (7.1) yields

$$\overline{F}_s - \overline{F} \;=\; 2\gamma\,(\Delta F)^2\,\mathrm{Im}\,A_w, \tag{7.2}$$

which is an extension of the second equality in Eq. (1.54) to the general meter state.

Finally, when the weak value is very large and $\bar{F} = \overline{F_c^3} = 0$, we obtain a simple expression [see Eq. (4.24) and Table 5, configuration 1],

$$\bar{F}_s \;=\; \frac{2}{\gamma}\,\mathrm{Im}\,\frac{1}{A_w^*} \qquad \text{for } \;|\gamma A_w|\,\Delta F \gg 1. \tag{7.3}$$

In particular, Eq. (7.3) provides an interpretation in terms of weak values of the result (9) in Ref. [133] (see Sec. 12).

7.1.2. Meters with zero pointer uncertainty, $\Delta R = 0$.

Furthermore, consider the case when $\Delta R = 0$ and $\hat{R}$ has a discrete spectrum.[6] In this case

$$\hat{R}\rho_{\mathrm{M}} \;=\; \rho_{\mathrm{M}}\,\hat{R} \;=\; \bar{R}\rho_{\mathrm{M}} \tag{7.4}$$

[cf. the remark after Eq. (3.10)], and hence

$$\hat{R}_c\,\rho_{\mathrm{M}} \;=\; \rho_{\mathrm{M}}\,\hat{R}_c \;=\; 0. \tag{7.5}$$

Now the linear approximation (4.13) vanishes since $\overline{R_c F} = \mathrm{Tr}\,(\rho_{\mathrm{M}}\hat{R}_c\hat{F}) = 0$, in view of Eq. (7.5); however the weak value is still measurable in the nonlinear regime. Indeed, now Eq. (4.11) becomes

$$\bar{R}_s - \bar{R} \;=\; \frac{\gamma^2\,\overline{F_c R_c F_c}\,|A_w|^2}{1 + 2\gamma\,\bar{F}\,\mathrm{Im}\,A_w + \gamma^2\,\overline{F^2}\,|A_w|^2}, \tag{7.6}$$

where we took into account Eq. (4.37). Note that Eq. (7.6) differs from zero only when $\hat{F}$ and $\hat{R}$ do not commute. Indeed, for commuting $\hat{F}$ and $\hat{R}$, we have $\overline{F_c\,R_c\,F_c} = \overline{F_c^2\,R_c} = \mathrm{Tr}\,(\hat{F}_c^2\,\hat{R}_c\,\rho_{\mathrm{M}}) = 0$, in view of Eq. (7.5).

In both cases (7.1) and (7.6) one can measure $\mathrm{Im}\,A_w$ and $|\mathrm{Re}\,A_w|$, as discussed in the end of Sec. 4.7.5.

7.2. Continuous-variable meters

The standard measurement theory [1, 24, 68] involves a continuous-variable meter and canonically conjugate variables. Correspondingly, the bulk of the literature on weak values involves such meters. Here we apply the above theory to the important case of continuous-variable meters.

First, we remind that meters with $R = F$ (including continuous-variable meters) were discussed in Sec. 7.1 (see, especially, Table 5). The case of commuting F and R is essentially similar to the case $R = F$. Consider now a continuous-variable meter with non-commuting F and R.

7.2.1. Canonically conjugate variables

The present theory is applicable to arbitrary meter variables, however here we focus on canonically conjugate variables given by Eq. (1.12). Since $[q, p] = i$, now Eq. (4.16) becomes

$$\overline{R_c F} \;\equiv\; \overline{q_c p} \;=\; \sigma_{pq} + i/2, \tag{7.7}$$

and the general linear-response formula (4.13c) reduces to the result of Ref. [110], which is a direct extension of Eq. (1.41),

$$\bar{q}_s - \bar{q} = \gamma\,(\mathrm{Re}\,A_w + 2\,\sigma_{pq}\,\mathrm{Im}\,A_w). \tag{7.8}$$

The covariance σ_{pq} is an important parameter, since it affects the result (7.8) of weak PPS measurements. Moreover, it enters the generalized uncertainty relation for the canonically conjugate meter variables p and q, which, as follows from Eq. (4.19), has the form

$$\Delta p\;\Delta q \;\geq\; \sqrt{1/4 + \sigma_{pq}^2}. \tag{7.9}$$

Therefore, it is of interest to obtain the conditions under which $\sigma_{pq} \neq 0$.

---

[6] When $\hat{R}$ has a continuous spectrum, we do not consider the case $\Delta R = 0$, since then states with $\Delta R = 0$ are generally unphysical.

Assume now for simplicity that at $t = 0$ the meter is in a pure state $|\psi_{\rm M}\rangle$. Presenting $\psi_{\rm M}(q) = \langle q|\psi_{\rm M}\rangle$ and $\psi_{\rm M}(p) = \langle p|\psi_{\rm M}\rangle$ in the forms

$$\psi_{\rm M}(q) = f_q(q)\,\exp[i\xi(q)], \tag{7.10}$$

$$\psi_{\rm M}(p) = f_p(p)\,\exp[-i\zeta(p)], \tag{7.11}$$

where $f_q(q)$, $\xi(q)$, $f_p(p)$, and $\zeta(p)$ are real, continuous functions, we obtain two equivalent expressions for the anticommutator of q and p (see Appendix D),

$$\overline{\{q,p\}} \;=\; 2\,\overline{q\,\xi'(q)} \;=\; 2\,\overline{p\,\zeta'(p)}, \tag{7.12}$$

where the prime denotes differentiation. The second equality in Eq. (7.12) is an interesting and nontrivial relation between the phases $\xi(q)$ and $\zeta(p)$. Combining Eqs. (4.15) and (7.12) yields two equivalent expressions for σ_{pq},

$$\sigma_{pq} \;=\; \overline{p\zeta'(p)} - \bar{q}\bar{p} \;=\; \overline{q\xi'(q)} - \bar{q}\bar{p}. \tag{7.13}$$

A consequence of Eq. (7.13) is that $\sigma_{pq} = 0$ if, at least, one of the phases $\zeta(p)$ and $\xi(q)$ is linear or constant. This result follows from Eq. (7.13) and the fact that linear $\zeta(p)$ and $\xi(q)$ imply, respectively,

$$\zeta'(p) = \bar{q}, \quad \xi'(q) = \bar{p}, \tag{7.14}$$

Eq. (7.14) resulting from the general expressions (see Appendix D)

$$\overline{\zeta'(p)} = \bar{q}, \tag{7.15}$$

$$\overline{\xi'(q)} = \bar{p}. \tag{7.16}$$

Thus, we obtain the following theorem. The covariance σ_{pq} for a coordinate q and the canonically conjugated moment p is nonzero if and only if one of the two equivalent conditions holds: (a) the phase $\zeta(p)$ is nonlinear in p and

$$\overline{p\,\zeta'(p)} \;\neq\; \bar{q}\,\bar{p} \tag{7.17}$$

or (b) the phase $\xi(q)$ is nonlinear in q and

$$\overline{q\,\xi'(q)} \;\neq\; \bar{q}\,\bar{p}. \tag{7.18}$$

On inserting Eq. (7.13) into Eq. (7.8), we obtain two equivalent expressions for the linear response,

$$\bar{q}_s - \bar{q} \;=\; \gamma\,\{{\rm Re}\,A_w + 2[\,\overline{p\zeta'(p)} - \bar{q}\bar{p}\,]\,{\rm Im}\,A_w\} \tag{7.19a}$$

$$\;=\; \gamma\,\{{\rm Re}\,A_w + 2[\,\overline{q\xi'(q)} - \bar{q}\bar{p}\,]\,{\rm Im}\,A_w\}. \tag{7.19b}$$

It is usually noted [24, 110, 114] that Eq. (7.8) reduces to Eq. (1.41) for a real $\psi_{\rm M}(q)$. The above discussion of σ_{pq} implies a more general result: namely, Eq. (1.41) holds whenever the phase of either $\psi_{\rm M}(q)$ or $\psi_{\rm M}(p)$ is a linear function (or, as a special case, a constant or zero). In contrast, a nonlinear phase $\zeta(p)$ or $\xi(q)$ generally results in a non-vanishing correlation between p and q, $\sigma_{pq} \neq 0$, so that both terms in Eqs. (7.8) do not vanish (see also Sec. 7.2.2).

When weak values are large, one should use the general nonlinear Eq. (4.11) [or (5.2), for a mixed preselected state] or Eqs. (4.64) and (5.23) for the case $|\bar{F}| \gg \Delta F$. In particular, Eq. (4.11) with the account of Eq. (7.7) now becomes

$$\bar{q}_s - \bar{q} \;=\; \frac{\gamma\,({\rm Re}\,A_w + 2\sigma_{pq}\,{\rm Im}\,A_w) + \gamma^2\,\overline{pq_cp}\,|A_w|^2}{1 + 2\gamma\bar{p}\,{\rm Im}\,A_w + \gamma^2\,\overline{p^2}\,|A_w|^2}, \tag{7.20}$$

whereas for a mixed preselected state one should replace $|A_w|^2 \to A_w^{(1,1)}$ in Eq. (7.20).

The expressions for the meter parameters entering the present theory for the meter (1.12) with an arbitrary initial state are shown in Table 6, case 4. To derive these expressions, we used Eqs. (4.15), (4.37), (7.12), (7.15), the equality

$$\overline{p\,q_c\,p} \;=\; \overline{p\,q\,p} - \bar{q}\,\overline{p^2}, \tag{7.21}$$

		Moments of the meter variables:		
No.	Meter configuration	σ_{pq}	$\overline{pq_cp}$	$\overline{p_cq_cp_c}$
1	Zero or linear $\zeta(p)$	0	0	0
2	Quadratic $\zeta(p)$, $\overline{p_c^3} = 0$	$b/2$	$b\overline{p}$	0
3	Quadratic $\zeta(p)$	$b/2$	$b\overline{p^2p_c}/2(\Delta p)^2$	$b\overline{p_c^3}/2(\Delta p)^2$
4	General	$\overline{p\zeta_c'(p)}$ or $\overline{q\xi_c'(q)}$	$\overline{p^2\zeta_c'(p)}$	$\overline{p_c^2\zeta_c'(p)}$

Table 6: Moments of meter variables used in the present theory, for a meter with $F = p$ and $R = q$ with different classes of initial states. Here, $\zeta_c'(p) = \zeta'(p) - \overline{q}$, and $\xi_c'(q) = \xi'(q) - \overline{p}$.

and the following relation obtained in Appendix D,

$$\overline{p\,q\,p} \;=\; \overline{p^2\,\zeta'(p)}. \tag{7.22}$$

The case when $\psi_{\mathrm{M}}(p)$ is real or has a linear phase $\zeta(p)$, is especially simple, since then the meter parameters listed in Table 6 vanish: see Table 6, configuration 1 (see also Sec. 7.2.3).

Consider now the simplest case of a nonlinear phase in the momentum representation: a quadratic $\zeta(p)$. Using Eq. (7.15), it is easy to show that in the general case a quadratic $\zeta(p)$ satisfies the equation

$$\zeta'(p) \;=\; \overline{q} + \frac{b\,(p-\overline{p})}{2(\Delta p)^2}, \tag{7.23}$$

where b is a real dimensionless parameter characterizing the quadratic phase modulation. Inserting Eq. (7.23) into the formulas for case 4 in Table 6 yields case 3 in Table 6. In particular, the linear-response result (4.13a) becomes

$$\overline{q}_s - \overline{q} \;=\; \gamma\,(\mathrm{Re}\,A_w + b\,\mathrm{Im}\,A_w). \tag{7.24}$$

Now we obtain $\sigma_{pq} = b/2$ (see Table 6, configuration 3), and the generalized uncertainty relation (7.9) now becomes

$$\Delta p\,\Delta q \;\geq\; \frac{\sqrt{1+b^2}}{2}. \tag{7.25}$$

When $\overline{p_c^3} = 0$, which holds, e.g., for the function $\Phi(p) = |\psi_{\mathrm{M}}(p)|^2$, which is symmetric with respect to $\overline{p}$, $\Phi(p) = \Phi(2\overline{p} - p)$, the formulas for the case of the quadratic $\zeta(p)$ simplify: see case 2 in Table 6.

An example of a state with a quadratic phase and a symmetric $\Phi(p)$ is a general complex Gaussian state given by Eqs. (1.49) and (1.50). The parameters Δp and Δq in Eqs. (1.49) and (1.50) are related by Eq. (1.51), which is essentially the generalized uncertainty relation (7.25) with the equals sign. A general Gaussian state implies the formulas in Table 6, case 2.

7.2.2. Invariance with respect to a meter gauge transformation

As mentioned above (see also Table 6), p and q are generally correlated (i.e., $\sigma_{pq} \neq 0$) whenever the phase $\zeta(p)$ is nonlinear. To understand better this result, we make the following remark.

The formulas in Table 6, cases 1 and 4, imply that the average pointer deflection in the presence of a nonlinear $\zeta(p)$ will not change if the meter is modified, as follows: (i) $\zeta(p)$ is replaced by a vanishing or at most linear in p phase $\tilde{\zeta}(p)$ and (ii) the pointer is changed according to

$$q \;\rightarrow\; \tilde{R} = q + \zeta'(p) + C, \tag{7.26}$$

where C is an arbitrary real constant. Equation (7.26) is a special case of the invariance property of the average pointer deflection under a gauge transformation of the meter, discussed in Appendix A.2 [see, in particular, Eq. (A.9)]. In the case of a quadratic $\zeta(p)$ (7.23), Eq. (7.26) becomes

$$q \;\rightarrow\; \tilde{R} = q + bp + C. \tag{7.27}$$

The modified pointer variable $\tilde{R}$ in Eq. (7.26) is obviously correlated with p when $\zeta(p)$ is nonlinear in p.

Note that $\tilde{R}$ is canonically conjugate to p, since $[\tilde{R}, p] = [q, p] = i$, for any $\zeta(p)$. This is not surprising, since the canonically conjugate variable is known to be determined not uniquely [146].

7.2.3. Measuring physical parameters

a. Measuring γ. As an application of the above results, let us discuss measuring the coupling strength γ, using a conjugate-variable meter with $|\bar{p}| \lesssim \Delta p$. We will consider two cases: (i) the phase $\zeta(p)$ in Eq. (7.11) is constant or linear and (ii) $\zeta(p)$ is nonlinear.

Case (i): a constant or linear $\zeta(p)$. In this case Eq. (7.20) is especially simple (cf. Table 6, case 1),

$$\bar{q}_s - \bar{q} \;=\; \frac{\gamma\,\mathrm{Re}\,A_w}{1 + 2\gamma\bar{p}\,\mathrm{Im}\,A_w + \gamma^2\,\overline{p^2}\,|A_w|^2}. \tag{7.28}$$

This quantity differs from zero only when $\mathrm{Re}\,A_w$ is nonvanishing. The magnitude of the pointer deflection (7.28) is maximal for

$$\gamma A_w \;=\; \frac{\pm\Delta p - i\bar{p}}{\overline{p^2}}, \tag{7.29}$$

when Eq. (7.28) becomes, respectively,

$$\bar{q}_s - \bar{q} \;=\; \pm\frac{1}{2\Delta p}. \tag{7.30}$$

Thus, for $\bar{p} = 0$ ($\bar{p} \neq 0$), the optimal A_w should be real (complex). The Heisenberg uncertainty relation [Eq. (7.9) with $\sigma_{pq} = 0$] and Eq. (7.30) imply that now

$$|\bar{q}_s - \bar{q}| \;\leq\; \Delta q, \tag{7.31}$$

in agreement with the general Eq. (4.41). The equality in Eq. (7.31) is achieved for a Gaussian initial state of the meter under the conditions (7.29).

Case (ii): a nonlinear $\zeta(p)$. This case can be analyzed similarly to case (i), though generally Eq. (7.20) is more complicated than Eq. (7.28). In contrast to case (i), this case shows the enhancement discussed in Sec. 4.6.2. In particular, in the optimal regime the maximum magnitude of the pointer deflection is of the order of Δq in both cases (i) and (ii), in agreement with the general result (4.41). However, for a given Δp, the quantity Δq in case (ii) is greater than in case (i) due to a non-zero covariance σ_{pq} [cf. Eq. (7.9)]. An increase of a nonlinear $\zeta(p)$ leads to an increase of $|\sigma_{pq}|$, which in turn yields an enhancement of the maximum pointer deflection and thus an increase of the measurement accuracy.

The enhancement of the pointer deflection occurs also in the linear-response regime, though, in contrast to the nonlinear regime, only when $\mathrm{Im}\,A_w \neq 0$ [see Eq. (7.8)], the increase being maximized when A_w is purely imaginary [80, 83–86, 89]. In both regimes, the increase of the pointer deflection is characterized by the enhancement coefficient f (4.53). However, the optimal conditions are obtained only in the nonlinear regime.

Let us consider two examples.

First, we consider the case of a quadratic $\zeta(p)$ with $\bar{p} = \overline{p^3} = 0$. Then, as follows from Eq. (7.20) and Table 6, case 2,

$$\bar{q}_s - \bar{q} \;=\; \frac{\gamma\,(\mathrm{Re}\,A_w + b\,\mathrm{Im}\,A_w)}{1 + \gamma^2\,(\Delta p)^2\,|A_w|^2}. \tag{7.32}$$

The magnitude of Eq. (7.32) is maximum for

$$\gamma A_w \;=\; \pm\frac{1 + ib}{\Delta p\,\sqrt{1 + b^2}}, \tag{7.33}$$

when Eq. (7.32) becomes, respectively,

$$\bar{q}_s - \bar{q} \;=\; \pm\frac{\sqrt{1 + b^2}}{2\Delta p}. \tag{7.34}$$

In view of Eq. (7.34) and the generalized uncertainty relation (7.25), we again arrive at Eq. (7.31), the equality where is achievable for a Gaussian ψ_{M}.

Note, however, that the pointer deflection in Eq. (7.34) is enhanced relative to Eq. (7.30) by the factor given *exactly* by Eq. (4.53), which now becomes

$$f = \sqrt{1+b^2}. \tag{7.35}$$

In particular, for $|b| \gg 1$ we obtain that

$$f = |b| \gg 1. \tag{7.36}$$

In the above example, just as in the linear case (7.8), the enhancement cannot be obtained with a real weak value, since then the b-dependent term disappears in Eq. (7.32). The following example shows that in the nonlinear case a strong enhancement is possible even for a real A_w, when $\overline{pq_cp} \neq 0$.

Let A_w be real, $\zeta(p)$ quadratic, and $\overline{p_c^3} = 0$. Then Eq. (7.20) and Table 6, case 2, yield

$$\bar{q}_s - \bar{q} = \frac{\gamma A_w + \gamma^2\, b\, \bar{p}\, A_w^2}{1 + \gamma^2\, \overline{p^2}\, A_w^2}. \tag{7.37}$$

Now the pointer-deflection magnitude is maximal when

$$\bar{q}_s - \bar{q} = \frac{b\,\bar{p}}{2\overline{p^2}} \left\{ 1 + \left[1 + \frac{\overline{p^2}}{(b\bar{p})^2} \right]^{1/2} \right\} = \gamma A_w. \tag{7.38}$$

In particular, for

$$|b| \gg 1, \qquad |\bar{p}| = \Delta p \tag{7.39}$$

Eq. (7.38) becomes

$$\bar{q}_s - \bar{q} = \mathrm{sgn}(\bar{p})\, \frac{b}{2\Delta p} = \gamma A_w. \tag{7.40}$$

Comparing Eqs. (7.40) and (7.34) shows that now one has the same enhancement (7.36) as in the previous example.

b. Tomography of weak values. Finally, we remark about tomography of weak values in case (i). In this case, in the linear regime, Eq. (1.41), obviously only $\mathrm{Re}\, A_w$ can be measured [24]. In contrast, as implied by Eq. (7.28), in the nonlinear regime generally both $\mathrm{Re}\, A_w$ and $\mathrm{Im}\, A_w$ can be obtained (cf. Table 4, cases 2 and 3).

7.2.4. Effects of the meter Hamiltonian

The meter Hamiltonian is often nonzero in experiments. Therefore, let us consider the effects of the meter Hamiltonian. For simplicity, we assume that the meter is described by the same Hamiltonian as a free particle [80, 111],

$$H_{\mathrm{M}} \equiv H_{\mathrm{M1}} = H_{\mathrm{M2}} = \frac{p^2}{2m_p}, \tag{7.41}$$

where m_p is the "particle" mass.

a. Effective initial state. First, we consider the case of the canonically conjugate meter variables (1.12). Now the Hamiltonian (7.41) commutes with $F = p$, therefore, as discussed in Sec. 6.3, the effects of the meter Hamiltonian can be taken into account by two equivalent ways: either through the effective initial state or through the effective pointer.

Here we describe the effects of the meter Hamiltonian by the effective initial state [see Eqs. (6.12) and (6.8)],

$$\psi_{\mathrm{M}}(p, t_{\mathrm{M}}) = \exp(-iH_{\mathrm{M}} t_{\mathrm{M}})\, \psi_{\mathrm{M}}(p). \tag{7.42}$$

Due to the Hamiltonian (7.41), there is a quadratic contribution to the phase of $\psi_{\mathrm{M}}(p, t_{\mathrm{M}})$, with b given by the quantity

$$b(t_{\mathrm{M}}) = \frac{2(\Delta p)^2\, t_{\mathrm{M}}}{m_p}, \tag{7.43}$$

which increases with t_{M}. Thus, the effective initial state can have a nonlinear phase modulation due to the free meter Hamiltonian, even when the phase of the initial meter state $\psi_{\mathrm{M}}(p)$ vanishes or is linear in p.

Generally, the initial state $\psi_{\rm M}(p)$ has a nonlinear phase $\zeta(p)$. As a result, the meter parameters for weak PPS measurements are the sums of the contribution due to $\zeta(p)$ (see Table 6, case 4) and the contribution due to the meter Hamiltonian, i.e., due to the quadratic phase modulation determined by the parameter b in Eq. (7.43) (see Table 6, case 3).

In particular, in the simple case, when the initial meter phase in the momentum space is constant or linear, the effect of the meter Hamiltonian is to change case 1 in Table 6 to case 2 or 3. For a sufficiently long $t_{\rm M}$, this results in a large pointer-deflection enhancement [cf. Eq. (7.36)],

$$f \;=\; \frac{2(\Delta p)^2 t_{\rm M}}{m_p} \;\gg\; 1, \tag{7.44}$$

When $\psi_{\rm M}(p)$ is a Gaussian, Eq. (7.44) can be recast also as

$$f \;=\; \frac{2(\Delta q_{\rm M})^2\, m_p}{t_{\rm M}}, \tag{7.45}$$

where $\Delta q_{\rm M}$ is the uncertainty of q at the moment $t_{\rm M}$. To derive Eq. (7.45), we took into account that $\Delta p \Delta q_{\rm M} = b(t_{\rm M})/2 \gg 1$ [cf. Eq. (1.51)], which yields, in view of Eq. (7.43),

$$\Delta q_{\rm M} \;=\; \frac{\Delta p\; t_{\rm M}}{m_p}. \tag{7.46}$$

Equations (7.44) and (7.45) were obtained and checked experimentally in Ref. [80] (where the enhancement factor f is denoted by F) for the special case of linear response (see also Ref. [111]).

Note, however, that the same enhancement is obtainable also in the optimal regime, as discussed in Sec. 4.6.2 and shown by a direct calculation in Sec. 7.2.3. It is advantageous to perform experiments in the optimal regime, since the proper amplification and hence the total amplification [Eq. (4.55)] are greater in the optimal regime by, at least, an order of magnitude than those in the linear regime.

b. Effective pointer variable. Consider the case when F is arbitrary, whereas $R = q$. Now the Hamiltonian $H_{\rm M}$ does not necessarily commute with $\hat{F}$. In this case, as discussed in Sec. 6.3, the effects of $H_{\rm M}$ can be taken into account through the effective pointer variable. From Eqs. (6.6), (6.9), (6.10) and (7.41) we obtain that the effective pointer variable is

$$q(t_{\rm M}) \;=\; q + \frac{t_{\rm M}}{m_p} p, \tag{7.47}$$

both for PPS and standard measurements. Correspondingly, now the pointer deflection equals (irrespective of the measurement strength)

$$\overline{q}_{s,f} - \overline{q} \;=\; (\overline{q}_{s,f} - \overline{q})_0 + \frac{t_{\rm M}}{m_p}(\overline{p}_{s,f} - \overline{p})_0. \tag{7.48}$$

Here the subscript s (f) corresponds to PPS (standard) measurements, whereas the two terms in the parentheses denoted by the subscript “0” are the unperturbed results of the measurements of the coordinate and the momentum, respectively, i.e., the results obtained in the absence of the meter Hamiltonian.

Equation (7.48) implies that, when $t_{\rm M}$ is very small, the effect of the meter Hamiltonian is negligible,

$$\overline{q}_{s,f} - \overline{q} = (\overline{q}_{s,f} - \overline{q})_0. \tag{7.49}$$

In the opposite limit, when $t_{\rm M}$ is sufficiently large, the unperturbed contribution from the coordinate can be neglected in Eq. (7.48), and the measurement of the coordinate provides the unperturbed momentum deflection,

$$\overline{q}_{s,f} - \overline{q} = \frac{t_{\rm M}}{m_p}(\overline{p}_{s,f} - \overline{p})_0. \tag{7.50}$$

In this case, the measurement of the momentum is “translated” into the measurement of the coordinate [67]. This is a very useful feature, since it is usually much easier to measure the position of a particle than its momentum.

Note that the factor $t_{\rm M}/m_p$ in Eq. (7.50) increases with $t_{\rm M}$ and hence can provide a strong enhancement. In the case (1.12), this enhancement is equivalent to that mentioned above, which is due to the correlation between F and

R. However, generally (e.g., for $F = q$) the enhancement due to the meter Hamiltonian in Eq. (7.50) differs from the enhancement discussed above (Sec. 4.6.2).

Let us discuss special cases.

(i) Consider measurements with

$$F = R = q, \tag{7.51}$$

such as the Stern-Gerlach experiments, both the standard one and that proposed by AAV [24], and some optical experiments [73, 83–86, 89]. Note a difference between standard and weak PPS measurements for the case (7.51). For standard measurements, the first term on the rhs of Eq. (7.48) vanishes [cf. Eq. (2.5) with $F = R = q$], i.e., the "translation" (7.50) is exact for any t_{M}. Hence, effectively the meter variables are given by [cf. the case (1.76)]

$$F = q, \quad R = \frac{t_{\mathrm{M}}}{m_p} p. \tag{7.52}$$

In comparison, for PPS measurements both terms in Eq. (7.48) are generally nonzero. Now the "translation" (7.50) is approximate; it occurs only when t_{M} is sufficiently long, whereas in the opposite limit of a short t_{M} Eq. (7.49) holds [86].

(ii) Consider the meter (1.12). Now for standard measurements, Eq. (7.49) is exact, i.e., effects of the meter Hamiltonian vanish. In contrast, for weak PPS measurements with the meter (1.12), effects of the meter Hamiltonian do not vanish. Now Eq. (7.48) yields the results discussed above in paragraph *a*. This can be checked by inserting Eq. (7.20) and Eq. (7.1) with $F = p$ on the rhs of Eq. (7.48) and using Table 6. Thus, the two seemingly different approaches developed for this case in paragraphs *a.* and *c.* are equivalent, in agreement with the discussion in Sec. 6.3. This equivalence implies that the quadratic phase characterized by the parameter (7.43) can be equivalently replaced by the effective pointer (7.47). In turn, the latter equivalence is a consequence of the invariance of PPS measurements with respect to gauge transformations of the meter (Appendix A.2, see also Sec. 7.2.2).

c. The covariance and the spatial spread.

Consider a meter modeled as a particle moving in a potential, and let $F = p$ and $R = q$. Due to nonzero meter Hamiltonian H_{M}, the meter state is changing in time. We now assume, for simplicity, that the system Hamiltonian is zero. In the special case of instantaneous (impulsive) measurements, $t_{\mathrm{M}}, t_{\mathrm{f}}, t_{\mathrm{i}} \to 0$, Jozsa [110] obtained Eq. (7.8), where the covariance σ_{pq} is related to the rate at which the meter distribution is spreading in space by the equality

$$\sigma_{pq} = \left. \frac{m_p}{2} \frac{d\{[\Delta q(t)]^2\}}{dt} \right|_{t=0}, \tag{7.53}$$

where $\Delta q(t)$ is calculated for the free-evolving meter state $\rho_{\mathrm{M}}(t) = e^{-iH_{\mathrm{M}}t} \rho_{\mathrm{M}} e^{iH_{\mathrm{M}}t}$. As mentioned in Sec. 6.3, in the present case $t_{\mathrm{M}}, t_{\mathrm{f}}, t_{\mathrm{i}} \to 0$, the measurement results are not modified by the meter Hamiltonian H_{M}; hence also Eq. (7.20) with σ_{pq} obeying Eq. (7.53) holds now.

Consider now whether it is possible to extend Eq. (7.53) to measurements with a finite duration, $t_{\mathrm{M}} - t_{\mathrm{i}} > 0$. For weak PPS measurements with a finite duration, even when the coupling is impulsive, $t_{\mathrm{f}} - t_{\mathrm{i}} \to 0$, the effects of the meter Hamiltonian generally cannot be taken into account by a relation of the form (7.53). Indeed, when the meter Hamiltonian H_{M} does not commute with the coupling Hamiltonian (1.8), the effects of H_{M} are equivalent to a change of the pointer variable (see Sec. 6.3).

An exception is the case of the free-particle meter Hamiltonian (7.41). Indeed, since the Hamiltonian (7.41) commutes with the coupling Hamiltonian (1.8), then, as shown in Sec. 6.3, the meter Hamiltonian can be taken into account in measurements with a finite duration ($0 \le t_{\mathrm{i}} \le t_{\mathrm{f}} \le t_{\mathrm{M}}$) simply by replacing the initial meter state ρ_{M} with the state $\rho_{\mathrm{M}}(t_{\mathrm{M}})$ [see Eq. (6.12)]. This means that now Eqs. (7.8) and (7.20) are not changed, but Eq. (7.53) should be modified by the substitution $t = 0 \to t = t_{\mathrm{M}}$, i.e.,

$$\sigma_{pq} = \left. \frac{m_p}{2} \frac{d\{[\Delta q(t)]^2\}}{dt} \right|_{t=t_{\mathrm{M}}}. \tag{7.54}$$

7.3. *Two-level meter*

Until recently, pre- and post-selected measurements were studied mainly employing a continuous-variable meter. In a number of recent papers, measuring weak values of a qubit with a qubit meter was discussed [109, 112, 123], whereas the case of an arbitrary system measured with a qubit meter was considered in Ref. [114]. A qubit (two-level) meter was used for weak PPS measurements of a qubit [71, 72, 77, 88] and a continuous-variable system [90, 91]. Here we discuss weak PPS measurements of an arbitrary system with a qubit meter, *beyond the linear-response regime*.

For a general two-level (qubit) meter, the operators $\hat{F}$ and $\hat{R}$ can be written in the form,

$$\hat{F} = \hat{F}_1 + f_0, \quad \hat{F}_1 = \vec{\sigma} \cdot \vec{n}_1, \tag{7.55}$$

$$\hat{R} = \vec{\sigma} \cdot \vec{n}_R, \tag{7.56}$$

where $\vec{n}_1$ and $\vec{n}_R$ are unit vectors and f_0 is a real number.[7]

The meter parameters in the formulas of the present theory [see, e.g., Eqs. (4.11), (4.38), (4.64), (5.2), and (5.23)] are now given by

$$\overline{F} = \overline{F}_1 + f_0, \quad \overline{F^2} = 1 + 2 f_0 \overline{F}_1 + f_0^2, \quad \Delta F = \sqrt{1 - \overline{F}_1^2}, \tag{7.60}$$

$$\Delta R = \sqrt{1 - \overline{R}^2}, \tag{7.61}$$

$$\begin{aligned} \overline{R_c F} &= M_R - \overline{R}\,\overline{F}_1 + i M_I, \\ \overline{F R_c F} &= M - \overline{R} + 2 f_0 (M_R - \overline{R}\,\overline{F}_1), \\ \overline{F_c R_c F_c} &= M - 2\overline{F}_1 M_R + \overline{R}(2\overline{F}_1^2 - 1), \end{aligned} \tag{7.62}$$

where

$$M_R = \mathrm{Re}\,\overline{R F_1}, \quad M_I = \mathrm{Im}\,\overline{R F_1}, \quad M = \overline{F_1 R F_1}. \tag{7.63}$$

From Eqs. (7.55), (7.56), and (7.63) we obtain that

$$M_R = \cos\eta, \quad M_I = \overline{F}_2 \sin\eta, \quad M = \overline{F}_1 \cos\eta - \overline{F}_3 \sin\eta. \tag{7.64}$$

Here

$$\overline{F}_i = \mathrm{Tr}\,[(\vec{\sigma} \cdot \vec{n}_i)\rho_{\mathrm{M}}] \tag{7.65}$$

and η ($0 \leq \eta \leq \pi$) is the angle between $\vec{n}_1$ and $\vec{n}_R$, whereas $\vec{n}_{2,3}$ are unit vectors defined by

$$\vec{n}_2 = \frac{\vec{n}_R \times \vec{n}_1}{\sin\eta}, \quad \vec{n}_3 = \vec{n}_1 \times \vec{n}_2. \tag{7.66}$$

Note that for noncommuting $\hat{R}$ and $\hat{F}$ (i.e., for $\eta \neq 0$), $\{\vec{n}_1, \vec{n}_2, \vec{n}_3\}$ is an orthonormal basis in the Bloch sphere of the meter.

The general initial condition for a two-level meter is

$$\rho_{\mathrm{M}} = (I + \vec{\sigma} \cdot \vec{s}_{\mathrm{M}})/2, \tag{7.67}$$

where $\vec{s}_{\mathrm{M}}$ is the pseudospin. Using Eq. (7.67), we obtain that in Eqs. (7.61)-(7.62) and (7.65)

$$\overline{R} = \vec{s}_{\mathrm{M}} \cdot \vec{n}_R, \quad \overline{F}_i = \vec{s}_{\mathrm{M}} \cdot \vec{n}_i, \tag{7.68}$$

---

[7] Note that in the most general case $\hat{R}$ has the form

$$\hat{R} = r_1 \vec{\sigma} \cdot \vec{n}_R + r_0, \tag{7.57}$$

where r_0 and r_1 are real. As implied by Eq. (3.9), replacing Eq. (7.56) by Eq. (7.57) results in multiplying the expression for $\overline{R}_s - \overline{R}$ by r_1.

Similarly, the most general $\hat{F}$ has the form

$$\hat{F} = f_1(\hat{F}_1 + f_0), \tag{7.58}$$

where f_1 is real. However, when the factor $f_1 \neq 1$, it can be absorbed in the parameter $g(t)$ in the Hamiltonian (1.8) and, hence, also in the coupling strength γ. Hence, using Eq. (7.58) instead of Eq. (7.55) results in the following substitution in the formulas of the present theory,

$$\gamma \to f_1 \gamma. \tag{7.59}$$

No.	Meter configuration	Moments of the meter variables: $\bar{R}$	$\bar{F}_1$	$\overline{R_cF}$	$\overline{FR_cF}$	$\overline{F_cR_cF_c}$
1	$\vec{n}_1 \perp \vec{n}_R,\ \vec{s}_\mathrm{M} = \vec{n}_2$	0	0	i	0	0
2	$\vec{n}_1 = \vec{n}_R,\ \vec{s}_\mathrm{M} \cdot \vec{n}_1 = 0$	0	0	1	$2 f_0$	0
3	$\vec{s}_\mathrm{M} = \vec{n}_2$	0	0	$e^{i\eta}$	$2 f_0 \cos\eta$	0
4	$\vec{n}_1 = \vec{n}_R$	$\vec{s}_\mathrm{M} \cdot \vec{n}_1$	$\vec{s}_\mathrm{M} \cdot \vec{n}_1$	f_2	$2 f_0 f_2$	$-2\bar{F}_1 f_2$
5	$\vec{s}_\mathrm{M} = \vec{n}_R$	1	$\cos\eta$	0	$-\sin^2\eta$	$-\sin^2\eta$
6	$\vec{s}_\mathrm{M} = \vec{n}_R,\ \vec{n}_1 \perp \vec{n}_R$	1	0	0	-1	-1
7	$\vec{s}_\mathrm{M} = 0$	0	0	$\cos\eta$	$2 f_0 \cos\eta$	0

Table 7: Moments of meter variables used in the present theory, for various configurations of a two-level meter. The parameter $\bar{F}_1$ determines $\bar{F}$, $\overline{F^2}$, and ΔF by Eq. (7.60), whereas $f_2 = 1 - (\vec{s}_\mathrm{M} \cdot \vec{n}_1)^2 = (\Delta F)^2$.

the quantities $\bar{F}_i$ being the components of the pseudospin in the orthonormal basis $\{\vec{n}_1, \vec{n}_2, \vec{n}_3\}$.

When $\hat{R}$ and $\hat{F}$ commute, then $\eta = 0$ or π, i.e., $\vec{n}_1 = \pm\vec{n}_R$. In this case, the quantities $\bar{F}_{2,3}$ are not defined, but they drop from the expressions, and Eqs. (7.64) and (7.68) yield that

$$M_R = \pm 1, \quad M_I = 0, \quad M = \bar{R} = \pm\bar{F}_1, \tag{7.69}$$

where the choice of the sign on the right-hand sides of the equations coincides with that in the equality $\vec{n}_1 = \pm\vec{n}_R$.

In the present case of a two-level meter there are a number of free parameters, variation of which allows one to obtain desirable values of the meter moments. Several possible configurations of the qubit meter are listed in Table 7. To obtain the values of the moments of the meter variables shown in Table 7, we used Eqs. (7.62), (7.64), (7.66), (7.68), and (7.69).

A simple, but important, case is obtained when $\{\vec{n}_R, \vec{n}_1, \vec{s}_\mathrm{M}\}$ is a right-handed basis in the Bloch sphere of the meter, see meter configuration 1 in Table 7. This situation is similar to case 1 in Table 6. To obtain the explicit expression, we combine the data of configuration 1 in Table 7 with Eqs. (7.60) and (4.11), yielding

$$\bar{R}_s^{(1)} = \frac{2\gamma \operatorname{Re} A_w}{1 + 2\gamma f_0 \operatorname{Im} A_w + \gamma^2 (1 + f_0^2) |A_w|^2}. \tag{7.70}$$

Another simple situation, which is especially suitable for the case of an imaginary weak value, is given by configuration 2 in Table 7, when we obtain

$$\bar{R}_s^{(2)} = \frac{2\gamma \operatorname{Im} A_w + 2\gamma^2 f_0 |A_w|^2}{1 + 2\gamma f_0 \operatorname{Im} A_w + \gamma^2 (1 + f_0^2) |A_w|^2}. \tag{7.71}$$

The superscripts "(1)" and "(2)" remind that Eqs. (7.70) and (7.71) relate to cases 1 and 2 in Table 6. Equations (7.70) and (7.71) simplify in the linear regime, where γA_w is small, yielding respectively [cf. Eqs. (1.41) and (1.42)]

$$\bar{R}_s^{(1)} = 2\gamma \operatorname{Re} A_w, \tag{7.72}$$

$$\bar{R}_s^{(2)} = 2\gamma \operatorname{Im} A_w. \tag{7.73}$$

Note that in configuration 2 in Table 7, the meter may be in a pure or mixed state with $\vec{s}_\mathrm{M} \perp \vec{n}_1$ or *even in the completely mixed state*, $\vec{s}_\mathrm{M} = 0$. The fact that the purity of the meter state is not important in this case may be used to simplify experiments on weak PPS measurements, which employ configuration 2 in Table 7.

When the weak value is complex, joint measurements with meter configurations 1 and 2 allow one to perform weak-value tomography (i.e., to obtain the real and imaginary parts of the weak value). One can work in the linear-response regime, using Eqs. (7.72) and (7.73), or in the strongly-nonlinear regime, using Eqs. (7.70) and (7.71) (see

Sec. 4.7). The linear-response version of this method was demonstrated[8] experimentally in Ref. [91].

Table 7 lists also several other possible meter configurations. In particular, case 3 resembles cases 2 and 4 in Table 6, case 1 in Table 7 being a special case of case 3 for $\eta = \pi/2$. Configurations 2 and 4-7 in Table 7 are examples of non-standard meters. In configurations 2 and 4, $\hat{R}$ and $\hat{F}$ commute, configuration 2 being a special case of configuration 4. In configurations 5 and 6, $\Delta R = 0$ since then ρ_M is a pure state which is an eigenstate of $\hat{R}$ (see also Sec. 7.1); case 6 is a special case of case 5. Finally, configuration 7 is the case of a completely mixed state of the meter; this demonstrates the possibility of weak PPS measurements with meters in a completely mixed state. A special case of configuration 7 with $\vec{n}_1 = \vec{n}_R$ is included in case 2.

The above results show that for weak PPS measurements, the qubit meter is at least as versatile as the continuous-variable meter. One or more of the parameters entering Table 7 can be varied in experiments in order to perform tomography of weak values or optimize the measurements.

7.4. Experiments where the average input variable is nonzero, $\bar{F} \neq 0$

In previous theoretical and experimental studies of weak PPS measurements, $\bar{F}$ has been always set to zero, exactly or effectively. In the present theory we do not make this assumption, i.e., now generally $\bar{F} \neq 0$. Still, as shown above, the linear response does not depend on $\bar{F}$ [see Eq. (4.13)]; however, its validity condition generally does depend on $\bar{F}$ [see Eq. (4.61)].

What is more important, as shown above, in the nonlinear regime, weak PPS measurements depend significantly on the value of $\bar{F}$. In particular, a nonzero $\bar{F}$ can facilitate measurements of A_w and γ (Secs. 4.7.5 and 7.2.3), whereas the optimal regime for $|\bar{F}| \gg \Delta F$ has some advantages, as discussed in Secs. 4.8 and 5.5. Here we mention some systems for which the above effects can be checked experimentally.

Qubit meter is a simple example of a meter for which generally $\bar{F} \neq 0$ (Sec. 7.3). As follows from Eq. (7.60), for qubit meters the ratio $\bar{F}/\Delta F$ can be easily tuned by changing $\bar{F}_1$, i.e., by changing the initial meter state ρ_M (for specific examples, see the values of $\bar{F}_1$ in Table 7). Moreover, $\bar{F}$ is always nonzero when $\hat{F}$ is a projector; it can also be shown that this is the case for the experiments [72, 78].

The quantity $|\bar{F}|$ can be very large, as in the proposed Stern-Gerlach experiment [24] and in the actual optical experiments using birefringent elements [70, 72, 73, 75, 78, 87]. In this case, under certain conditions the effects of $\bar{F}$ can be often eliminated [24], using the invariance of PPS measurements under gauge transformations of the system, see Appendix A.1, especially Eqs. (A.4) and (A.5). Indeed, in a typical case of a two-level system with $\hat{A} = \sigma_z$, Eqs. (A.4) and (A.5) imply that $\bar{F}$ is effectively zero in PPS measurements when [24]

$$\gamma\bar{F} = n\pi \qquad \text{for } \ n = 0, \pm 1, \pm 2, \ldots. \tag{7.75}$$

In the above optical experiments γ was not varied, since it was fixed by the condition (7.75) with some value of n.

As discussed above, a nonzero $\bar{F}$ can be useful in the nonlinear regime. In the case of very large $\bar{F}$, one can obtain an effective $\bar{F}$ of an arbitrary magnitude by making the value of γ or $\bar{F}$ slightly differing from that fixed by Eq. (7.75). Then, in view of Eqs. (7.75) and (A.5), in the results for PPS measurements obtained in the present paper, the average of F should be substituted by its effective value,

$$\bar{F} \ \rightarrow \ \bar{F} - \frac{n\pi}{\gamma}, \tag{7.76}$$

where n is the integer minimizing $|\bar{F} - n\pi/\gamma|$. In particular, inserting Eq. (7.76) into the validity conditions of the present theory and of different regimes, such as, e.g., Eqs. (4.7) and (5.15), provides the limits for the allowed values of the quantity $\bar{F} - n\pi/\gamma$.

---

[8] More specifically, in Ref. [91] in both configurations 1 and 2, $\hat{F}$ is the operator of a spin component, so that the parameters in Eq. (7.58) are given by $f_0 = 0$ and $f_1 = 1/2$. As a result, Eq. (7.59) implies that Eqs. (7.72) and (7.73) become now, respectively,

$$\bar{R}_s^{(1)} = \gamma \,\mathrm{Re}\, A_w, \qquad \bar{R}_s^{(2)} = \gamma \,\mathrm{Im}\, A_w. \tag{7.74}$$

Finally, we note that $\bar{F}$ can be tuned also by performing in any part of the interval $(0, t_S)$ an additional unitary transformation $U' = \exp(-i\alpha\hat{A})$ on the system, where α is a real number. This will replace the transformation U (1.10) by UU', which is equivalent to the replacement

$$\bar{F} \;\to\; \bar{F} + \frac{\alpha}{\gamma}. \tag{7.77}$$

8. Distribution of the pointer values

Higher-order moments $\overline{R^n_s}$ of R can be obtained by substituting $\hat{R} \to \hat{R}^n$ in Eq. (4.11) or (5.2). These moments can be written in the form

$$\overline{R^n_s} \;=\; \sum_R R^n\,\Phi_s(R), \tag{8.1}$$

where $\Phi_s(R)$ is the distribution of the eigenvalues R of $\hat{R}$ for $t \geq t_f$. Hence, the maximum information is provided by the distribution $\Phi_s(R)$, discussed in this section.

8.1. General meter

Here we discuss the case of a general meter which can be a system with a finite number of states or a continuous-variable system. For simplicity, we will consider $\Phi_s(R)$ for a nondegenerate $\hat{R}$; then

$$\Phi_s(R) \;=\; \overline{|R\rangle\,\langle R|}_s, \tag{8.2}$$

where $|R\rangle$ is the eigenvector of $\hat{R}$ with the eigenvalue R. Substituting $\hat{R} \to |R\rangle\langle R|$ into Eq. (4.12) yields

$$\Phi_s(R) \;=\; \{\Phi(R) + 2\gamma\,\mathrm{Im}\,[A_w\Phi_1(R)] + \gamma^2\,|A_w|^2\,\Phi_2(R)\}/Q_0, \tag{8.3}$$

where $\Phi(R) = \langle R|\rho_M|R\rangle$ is the initial distribution of R, $\Phi_1(R) = \langle R|\hat{F}\rho_M|R\rangle$ is generally complex, and $\Phi_2(R) = \langle R|\hat{F}\rho_M\hat{F}|R\rangle$ is real, whereas

$$Q_0 \;=\; 1 + 2\gamma\,\bar{F}\,\mathrm{Im}\,A_w + \gamma^2\,\overline{F^2}\,|A_w|^2. \tag{8.4}$$

Here and below in Sec. 8 we assume that the initial state of the system is pure; if this is not the case, the results obtained still hold under the replacement (5.4). Consider several important cases.

When the meter is initially in a pure state $|\psi_M\rangle$, then in Eq. (8.3)

$$\Phi(R) = |\psi_M(R)|^2, \qquad \Phi_1(R) = \psi^*_M(R)\,d_R, \qquad \Phi_2(R) = |d_R|^2, \tag{8.5}$$

where

$$\psi_M(R) = \langle R|\psi_M\rangle, \qquad d_R = \langle R|\hat{F}|\psi_M\rangle. \tag{8.6}$$

The dependence $\Phi_s(R)$ (8.3) simplifies when F is a function of R, $F = h(R)$, which implies that $[\hat{F}, \hat{R}] = 0$. (For nondegenerate $\hat{F}$ and $\hat{R}$, the equality $F = h(R)$ holds if and only if $[\hat{F}, \hat{R}] = 0$.) Then in Eq. (8.3)

$$\Phi_n(R) \;=\; h^n(R)\,\Phi(R) \quad (n = 1, 2), \tag{8.7}$$

$\Phi_1(R)$ now being real.

Note that in the case $F = h(R)$ the final pointer distribution (8.3) depends on the initial probability distribution $\Phi(R)$ but not on the coherent properties of the initial state ρ_M [cf. Eq. (8.7)], whereas for noncommuting $\hat{F}$ and $\hat{R}$, Eq. (8.3) generally depends on the phase of the initial state [cf. Eq. (8.5)].

8.2. Continuous-variable meter

Consider now in more detail the distribution of the values of a continuous pointer variable (e.g., p or q). In the previous studies, it was assumed that the initial meter state is a real Gaussian in the F or R representation [24]. Here we only assume that the initial pointer distribution $\Phi(R)$ has a bell-like shape (e.g., Lorentzian or Gaussian).

Note that the validity condition for the result (8.3) for $\Phi_s(R)$ generally depends on R. In the main part of the peak $\Phi_s(R)$, i.e., in the interval within the peak width, the validity condition is the same as for $\overline{R}_s$ (see Secs. 4.1 and 5.2). However, for far tails of $\Phi_s(R)$ the present theory can fail, as illustrated by examples shown below. This is explained by the fact that the validity conditions of the present theory can become much stricter for the tails than for the central part of $\Phi_s(R)$. Since far tails of $\Phi_s(R)$ are of little interest, we do not go further into this point.

A weak PPS measurement can change the distribution of R significantly or slightly, depending on the values of the parameters, as discussed below. When the effect of the measurement is not too strong, an initially bell-shaped distribution can remain bell-shaped with the maximum generally shifted from the initial position. This shift is important in some applications, such as superluminal propagation and slow light [67, 74, 75, 78, 104, 128]. If this shift is sufficiently small, simple formulas for the shift can be derived, as shown below. These formulas hold regardless of whether the shape of the distribution changes or remains the same. Recall that some cases where the distribution is shifted practically without a change of the shape are listed in Sec. 1.4.2.

8.2.1. Coinciding meter variables, $R = F$

We begin with the simple case $R = F$. Then Eqs. (8.3) and (8.7) yield

$$\Phi_s(F) \;=\; \Phi(F)\,[1 + 2\gamma\,(\mathrm{Im}\,A_w)F + \gamma^2\,|A_w|^2F^2]/Q_0, \tag{8.8}$$

where $\Phi(F) = \langle F|\rho_{\mathrm{M}}|F\rangle$ is the distribution of F before the measurement (at $t = 0$). Thus, $\Phi_s(F)/\Phi(F)$ is a quadratic polynomial in F.

Note that the linear-response approximation provides a wrong result for the tails of the distribution (8.8) even in the linear-response regime (4.22), since for large $|F|$ the nonlinear term dominates in Eq. (8.8). This is an indication that for the case $R = F$ the present theory does not describe the far tails of $\Phi_s(F)$, as discussed above.

The quantity $\Phi_s(F)/\Phi(F)$ is minimal at

$$F_{\min} \;=\; -\frac{\mathrm{Im}\,A_w}{\gamma\,|A_w|^2}, \tag{8.9}$$

where

$$\frac{\Phi_s(F_{\min})}{\Phi(F_{\min})} \;=\; \frac{(\mathrm{Re}\,A_w)^2}{|A_w|^2 Q_0}. \tag{8.10}$$

Thus, $\Phi_s(F)$ is always positive, except for the case of a purely imaginary weak value, $\mathrm{Re}A_w = 0$, when

$$\Phi_s(F_{\min}) = 0, \qquad F_{\min} \;=\; -(\gamma\,\mathrm{Im}\,A_w)^{-1}. \tag{8.11}$$

Consider now the typical case $|\overline{F}| \lesssim \Delta F$ (the other case $|\overline{F}| \gg \Delta F$ is discussed in the last paragraph of this subsection). In the linear regime [Eq. (4.20) or (5.17)] the main part of $\Phi_s(F)$, except for the far tails, is given by

$$\Phi_s(F) \;\approx\; \Phi(F)\,[1 + 2\gamma\,(\mathrm{Im}\,A_w)F] \qquad \text{for } |F - \overline{F}| \lesssim \Delta F. \tag{8.12}$$

This equation implies that, like $\Phi(F)$, the function $\Phi_s(F)$ (8.12) has a bell-like shape with the maximum of $\Phi_s(F)$ shifted from the maximum $F_{\max}$ of $\Phi(F)$ by

$$\Delta F_{\max} \;=\; \beta\,(\overline{F}_s - \overline{F}) \;=\; 2\beta\gamma\,(\Delta F)^2\,\mathrm{Im}\,A_w. \tag{8.13}$$

Here $\overline{F}_s$ is given by Eq. (7.2) and

$$\beta \;=\; \frac{\Phi(R_{\max})}{|\Phi''(R_{\max})|\,(\Delta R)^2}, \tag{8.14}$$

where now $R = F$, the primes denoting the second derivative. In the derivation of Eq. (8.13) we assumed that the peak top has a parabolic shape,

$$\Phi(F) \;\approx\; \Phi(F_{\max}) - |\Phi''(F_{\max})|(F - F_{\max})^2/2 \qquad \text{for } |F - F_{\max}| \ll \Delta F. \tag{8.15}$$

When $\Phi(F)$ is Gaussian, then $\beta = 1$ in Eq. (8.13), and we again obtain Eq. (1.54). However, for a general non-Gaussian $\Phi(F)$, Eq. (8.13) shows that the shift of the maximum $\Delta F_{\max}$ differs from the average pointer deflection $(\bar{F}_s - \bar{F})$ by a dimensionless factor β, which depends on the shape of $\Phi(F)$.

In the opposite limit $A_w \to \infty$, i.e., for mutually orthogonal $|\psi\rangle$ and $|\phi\rangle$, Eq. (8.8) yields

$$\Phi_s(F) = \frac{F^2 \Phi(F)}{\overline{F^2}}. \tag{8.16}$$

This equality holds approximately also for $\gamma^2 |A_w|^2 \gg 1/\overline{F^2}$. Now the function $\Phi_s(F)$ has two peaks of comparable heights, at least, for $|\bar{F}| \lesssim \Delta F$.

In contrast, when $|\bar{F}| \gg \Delta F$, $\Phi_s(F)$ is a bell-shaped function, except for the case (4.62)-(4.63), where the narrow resonance (4.64) occurs. The shift of the maximum of this bell-shaped function from the maximum of $\Phi(F)$ can be shown to be given approximately by the first equality in Eq. (8.13). However, now the average pointer deflection $(\bar{F}_s - \bar{F})$ is described by a *nonlinear formula*, so that

$$\Delta F_{\max} = \beta(\bar{F}_s - \bar{F}) = \beta \frac{2\gamma (\Delta F)^2 (\,\mathrm{Im}\, A_w + \gamma \bar{F} |A_w|^2)}{1 + 2\gamma \bar{F}\, \mathrm{Im}\, A_w + \gamma^2 \bar{F}^2 \, |A_w|^2}, \tag{8.17}$$

which follows from Eq. (7.1) for $|\bar{F}| \gg \Delta F$. In Eq. (8.17) we took into account that for $|\bar{F}| \gg \Delta F$ one has

$$\overline{F^2} = (\Delta F)^2 + \bar{F}^2 \approx \bar{F}^2 \tag{8.18}$$

and [cf. Eq. (4.3)]

$$\overline{F^3} - \overline{F^2}\bar{F} = 2(\Delta F)^2 \bar{F} + \overline{F_c^3} \approx 2(\Delta F)^2 \bar{F}. \tag{8.19}$$

This result is obtained if the condition (8.15) holds and if $\Phi(F)$ is not too asymmetric, so that $F_{\max} \sim \bar{F}$. Note that for a Gaussian $\Phi(F)$, $\beta = 1$ in Eq. (8.17).

Finally, we note that the general Eq. (8.8) simplifies for an imaginary weak value,

$$\Phi_s(F) = \Phi(F)[1 + \gamma\, (\mathrm{Im}\, A_w) F]^2 / Q_0. \tag{8.20}$$

In particular, the intensity distribution of the "split-Gaussian mode" obtained in Ref. [133] can be interpreted quantum-mechanically as a quantity proportional to a special case of Eq. (8.20) (see Sec. 12).

8.2.2. Canonically conjugate R and F

Here we study a meter with canonically conjugate variables R and F. For such a meter, the shift of the pointer distribution is known to be proportional to $\mathrm{Re}\, A_w$, at least, when the initial meter state in the pointer representation is a real Gaussian [24, 69, 80, 118]. However, for the general case the shift has not been discussed yet.

Here we assume that the meter is initially in a pure state $|\psi_{\mathrm{M}}\rangle$, the pointer distribution possessing an *arbitrary* bell-like shape. In particular, we will show that for a complex Gaussian and for non-Gaussian states, the shift of the maximum of the pointer distribution generally depends on both the real and imaginary parts of the weak value.

For the canonically conjugate variables (1.12), the second Eq. (8.6) yields $d_q = -i\psi'_{\mathrm{M}}(q)$, where the prime denotes differentiation. Then Eqs. (8.3)-(8.5) yield that

$$\Phi_s(q) = \frac{\Phi(q) - 2\gamma\, \mathrm{Re}[A_w \psi^*_{\mathrm{M}}(q) \psi'_{\mathrm{M}}(q)] + \gamma^2 |A_w|^2 \, |\psi'_{\mathrm{M}}(q)|^2}{1 + 2\gamma \bar{p}\, \mathrm{Im}\, A_w + \gamma^2 \, \overline{p^2} \, |A_w|^2}. \tag{8.21}$$

This expression depends on the phase of the initial state, unlike the results in Sec. 8.2.1.

For $|\gamma A_w| \ll (\overline{p^2})^{-1/2}$ [cf. Eq. (4.20)] and $|q - \bar{q}| \lesssim \Delta q$ one can use in Eq. (8.21) the approximation linear in γ, yielding

$$\begin{aligned} \Phi_s(q) &\approx \Phi(q) - 2\gamma\, \mathrm{Re}[A_w \psi^*_{\mathrm{M}}(q) \psi'_{\mathrm{M}}(q)] \\ &= \Phi(q) - \gamma\, (\mathrm{Re}\, A_w)\, \Phi'(q) + 2\gamma\, (\mathrm{Im}\, A_w)\, \xi'(q) \Phi(q), \end{aligned} \tag{8.22}$$

where in the last equality Eq. (7.10) is taken into account. We assume that $\Phi(q)$ is a bell-shaped function with the maximum at $q_{\max}$, so that for $|q - q_{\max}| \ll \Delta q$,

$$\Phi(q) \ \approx\ \Phi(q_{\max}) - |\Phi''(q_{\max})|(q - q_{\max})^2/2. \tag{8.23}$$

Moreover, in some interval $|q - q_{\max}| \ll \Delta_\xi$, we have

$$\xi'(q) \approx \xi'(q_{\max}) + \xi''(q_{\max})(q - q_{\max}), \tag{8.24}$$

where the double primes denote the second derivative. Then $\Phi_s(q)$ is also a bell-shaped function with the maximum at $q_{\max} + \Delta q_{\max}$, where

$$\Delta q_{\max} \ =\ \gamma\, [\mathrm{Re}\, A_w + 2\beta\, \xi''(q_{\max})\, (\Delta q)^2\, \mathrm{Im}\, A_w]. \tag{8.25}$$

Here β is given by Eq. (8.14) with $R = q$. Equation (8.25) holds when

$$|\Delta q_{\max}| \ll \min\{\Delta q, \Delta_\xi\}. \tag{8.26}$$

Equation (8.25) shows that generally *the shift of the maximum of the distribution of q depends on both the real and imaginary parts of the weak value*. Generally, the shift does not coincide with the average pointer deflection, $\Delta q_{\max} \neq \overline{q}_s - \overline{q}$.

However, there are cases when Eq. (8.25) possesses the convenient property (1.45), which now has the form

$$\Delta q_{\max} = \overline{q}_s - \overline{q}. \tag{8.27}$$

In particular, Eq. (8.27) holds in the following cases.
(a) The weak value is real. In this case Eq. (1.48) holds, as shown above.
(b) The phase of $\psi_{\mathrm{M}}(q)$ is vanishing or linear in q. In this case, Eq. (8.25) simplifies and becomes equal to the average pointer deflection (1.41),

$$\Delta q_{\max} = \overline{q}_s - \overline{q} = \gamma\, \mathrm{Re}\, A_w. \tag{8.28}$$

Previously [24] Eq. (8.28) was obtained for the special case when $\psi_{\mathrm{M}}(q)$ is a real Gaussian [see Eq. (1.50) with $\overline{p} = b = 0$].
(c) $\psi_{\mathrm{M}}(q)$ is a general complex Gaussian state. For this state we obtained above Eq. (1.52). Here we can derive Eq. (1.52) in a different way. Namely, taking into account that for a general Gaussian state, $\beta = 1$ and the phase $\xi(q)$ is [see Eq. (1.50)]

$$\xi(q) \ =\ \frac{b(q - \overline{q})^2}{4(\Delta q)^2} + \overline{p}q, \tag{8.29}$$

we obtain that Eq. (8.25) coincides with Eq. (7.24).

For orthogonal states $|\psi\rangle$ and $|\phi\rangle$ (when $A_w = \infty$), Eq. (8.21) yields

$$\Phi_s(q) \ =\ \frac{|\psi'_{\mathrm{M}}(q)|^2}{\overline{p^2}} \ =\ \frac{[f'_q(q)]^2 + [\xi'(q)]^2\Phi(q)}{\overline{p^2}}, \tag{8.30}$$

where Eq. (7.10) was used. In particular, for a real $\psi_{\mathrm{M}}(q)$, the function (8.30) becomes

$$\Phi_s(q) \ =\ [f'_q(q)]^2 \,/\, \overline{p^2}; \tag{8.31}$$

it has two peaks of comparable heights with the minimum $\Phi_s(q_{\max}) = 0$ at the maximum of $\Phi(q)$. However, for a complex $\psi_{\mathrm{M}}(q)$, Eq. (8.30) generally does not vanish at any point.

As an example, for a real Gaussian state Eq. (8.31) becomes

$$\Phi_s(q) \ =\ \frac{Z_q^2(q - \overline{q})^2}{(\Delta q)^2} \exp\left[-\frac{(q - \overline{q})^2}{2(\Delta q)^2}\right]. \tag{8.32}$$

This is a two-peak function, symmetric with respect to $\overline{q}$ and vanishing at $q = \overline{q}$. Previously, an unnormalized distribution proportional to Eq. (8.32) was obtained numerically (Fig. 4(b) in Ref. [103]) and experimentally (Fig. 2(c) in Ref. [70]). In contrast to Eq. (8.32), for the complex Gaussian meter state (1.50) the distribution (8.30) vanishes nowhere and is generally not symmetric.

Note that the general Eq. (8.21) can be written in an explicit form for the complex Gaussian state (1.50). In this case $\Phi_s(q)/\Phi(q)$ is a quadratic function of q, where

$$\Phi(q) \;=\; Z_q^2 \exp\left[-\frac{(q-\bar{q})^2}{2(\Delta q)^2}\right]. \tag{8.33}$$

In particular, for a real Gaussian state, Eq. (1.50) with $\bar{p} = \bar{q} = b = 0$, and a real A_w we obtain a simple result,

$$\Phi_s(q) \;=\; \frac{\Phi(q)[1 + (\gamma A_w \Delta p)(q/\Delta q)]^2}{1 + (\gamma A_w \Delta p)^2}, \tag{8.34}$$

where $\Delta p = (2\Delta q)^{-1}$ [cf. Eq. (1.51) with $b = 0$].

In the case of a complex Gaussian state, as in Sec. 8.2.1, the present theory is not applicable for the far tails of $\Phi_s(q)$. An indication to this is the fact that the far tails in Eq. (8.34) cannot be described by the linear-response approximation, irrespective of how weak the coupling is, since the term $\propto \gamma^2 q^2$ in the numerator of Eq. (8.34) always dominates for sufficiently large $|q|$.

9. Weak values for a qubit

Weak values A_w for a qubit were calculated previously for a number of special cases, usually with a pure preselected state [24, 80, 83, 111, 114]. Here we provide a general study of the standard and associated weak values A_w and $A_w^{(1,1)}$ for a qubit, with an arbitrary preselected state.

9.1. General formulas

We assume that the measured system operator is

$$\hat{A} = \vec{\sigma} \cdot \vec{n}_A, \tag{9.1}$$

where $\vec{\sigma} = (\sigma_x, \sigma_y, \sigma_z)$ is the vector of the Pauli matrices and $\vec{n}$ is a unit vector in the Bloch sphere. The operator (9.1) has the eigenvalues ±1. Generally, the pre- and post-selected states of the qubit are, respectively,

$$\begin{aligned} \rho \;&=\; (I + P_{\rm in}\, \vec{\sigma} \cdot \vec{n}_{\rm in})/2 \qquad (0 \le P_{\rm in} \le 1), \\ \Pi_\phi \;&\equiv\; |\phi\rangle\langle\phi| \;=\; (I + \vec{\sigma} \cdot \vec{n}_f)/2. \end{aligned} \tag{9.2}$$

Here $\vec{n}_{\rm in}$ and $\vec{n}_f$ are unit vectors, $P_{\rm in}\, \vec{n}_{\rm in}$ and $\vec{n}_f$ being the pseudospins of ρ and $|\phi\rangle$, respectively, whereas $P_{\rm in}$ is the length of the initial-state pseudospin.

$P_{\rm in}$ characterizes the purity of the initial state; $P_{\rm in}$ varies from 1, corresponding to a pure state, to 0 for a maximally mixed state. The initial state ρ can also be written in the form of the spectral expansion (5.6),

$$\rho \;=\; \frac{1 + P_{\rm in}}{2}\, |\vec{n}_{\rm in}\rangle\langle\vec{n}_{\rm in}| + \frac{1 - P_{\rm in}}{2}\, |-\vec{n}_{\rm in}\rangle\langle-\vec{n}_{\rm in}|, \tag{9.3}$$

where $|\vec{n}_{\rm in}\rangle$ is a state with the pseudospin given by the unit vector $\vec{n}_{\rm in}$. Equation (9.3) implies that $P_{\rm in}$ is expressed through the eigenvalues of ρ by the relation

$$P_{\rm in} = |\lambda_1 - \lambda_2|. \tag{9.4}$$

Taking into account that $O_{\phi\phi} = {\rm Tr}\,(O\Pi_\phi)$ for any operator O of a qubit, we obtain from Eqs. (1.58), (5.4), and (9.2) that

$$\begin{aligned} A_w \;&=\; \frac{\vec{n}_A \cdot \vec{n}_f + P_{\rm in}(\vec{n}_A \cdot \vec{n}_{\rm in} + i\vec{n}_A \cdot \vec{n}_{\rm in} \times \vec{n}_f)}{1 + P_{\rm in}\vec{n}_{\rm in} \cdot \vec{n}_f}, \\ A_w^{(1,1)} \;&=\; \frac{1 - \vec{n}_{\rm in} \cdot \vec{n}_f + P_{\rm in}(\vec{n}_A \cdot \vec{n}_{\rm in})(\vec{n}_A \cdot \vec{n}_f)}{1 + P_{\rm in}\vec{n}_{\rm in} \cdot \vec{n}_f}. \end{aligned} \tag{9.5}$$

According to Eq. (9.5), A_w is generally complex. A_w is real if the vectors $\vec{n}_A$, $\vec{n}_{\rm in}$, and $\vec{n}_f$ lie in the same plane or for $P_{\rm in} = 0$ (the completely mixed initial state), whereas A_w is purely imaginary when $\vec{n}_A$ is perpendicular to the sum of the pre- and post-selected pseudospins $P_{\rm in}\, \vec{n}_{\rm in} + \vec{n}_f$ and, in addition, the vectors $\vec{n}_{\rm in}$ and $\vec{n}_f$ are not collinear.

9.2. Conditions for maximizing weak values

Equation (9.5) shows that a necessary condition for $|A_w|$ to be large is $P_{\text{in}}\vec{n}_{\text{in}} \cdot \vec{n}_f \simeq -1$ or, equivalently, the simultaneous relations

$$\vec{n}_{\text{in}} \simeq -\vec{n}_f, \quad P_{\text{in}} \simeq 1. \tag{9.6}$$

The conditions (9.6) ensure that the overlap between the initial and final states is small,

$$\rho_{\phi\phi} \ll 1. \tag{9.7}$$

In the case of a pure preselected state, $P_{\text{in}} = 1$, the condition (9.6) or (9.7) requires that the pre- and post-selected states be almost orthogonal. In the case of a mixed preselected state, the condition (9.6) requires that the preselected state ρ be almost pure and that its eigenstate corresponding to the greater eigenvalue, i.e., $|\vec{n}_{\text{in}}\rangle$ [cf. Eq. (9.3)], be almost (or completely) orthogonal to the post-selected state.

The condition (9.6) is necessary but not sufficient to maximize the weak value. In the further study of conditions under which the weak value is maximal, we consider separately the cases of pure and mixed preselected states. As mentioned above, in the case of a pure preselected state, Eq. (9.7) means that the initial and final states are almost orthogonal, $|\langle\phi|\psi\rangle| \ll 1$. This condition is equivalent to

$$|\psi\rangle \simeq |\phi_1\rangle, \quad |\phi\rangle \simeq |\phi_2\rangle, \tag{9.8}$$

where $\{|\phi_1\rangle, |\phi_2\rangle\}$ is an orthonormal basis,

$$|\phi_1\rangle = |\vec{n}_0\rangle, \quad |\phi_2\rangle = |-\vec{n}_0\rangle. \tag{9.9}$$

Here $\vec{n}_0$ is a unit vector in the Bloch sphere. Note that the pseudospin $\vec{n}_0$ is not uniquely determined by the condition (9.8), and actually there is a narrow cone of possible values of $\vec{n}_0$.

Anyhow, in the case (9.8) for any allowed value of $\vec{n}_0$, Eq. (1.36) yields

$$A_w \approx \frac{A_{\phi_2\phi_1}}{\langle\phi|\psi\rangle}. \tag{9.10}$$

For a given magnitude of the overlap $|\langle\phi|\psi\rangle|$, the magnitude of the weak value $|A_w|$ is maximal when $|A_{\phi_2\phi_1}|$ is maximal. For the operator $\hat{A}$ in Eq. (9.1), the following equality can be shown to hold,

$$|A_{\phi_2\phi_1}| = \sin\eta_1, \tag{9.11}$$

where η_1 is the angle between $\vec{n}_A$ and $\vec{n}_0$. Hence, the maximal $|A_{\phi_2\phi_1}| = 1$ is obtained for any basis $\{|\phi_1\rangle, |\phi_2\rangle\}$ corresponding to a vector $\vec{n}_0$ perpendicular to $\vec{n}_A$,

$$\vec{n}_0 \perp \vec{n}_A. \tag{9.12}$$

Accordingly, the value of $|A_w|$ is maximum for a given $|\langle\phi|\psi\rangle| \ll 1$, when the pre- and post-selected states satisfy Eqs. (9.8) with the states (9.9) obeying Eq. (9.12); the above maximum of $|A_w|$ equals [cf. Eq. (9.10)]

$$|A_w|_{\max} = |\langle\phi|\psi\rangle|^{-1}. \tag{9.13}$$

In the case of a mixed preselected state, Eq. (9.13) does not hold, however the conditions for maximizing $|A_w|$ are the same as above, with the only difference that now in Eq. (9.8) $|\psi\rangle$ should be replaced by $|\vec{n}_{\text{in}}\rangle$. In the next subsection, we provide explicit formulas for weak values of a qubit.

9.3. Explicit formulas for a typical case

Let us consider in detail a typical case. First, we recall that a unit vector in the Bloch sphere has the form

$$\vec{n} = (\sin\kappa\cos\nu, \sin\kappa\sin\nu, \cos\kappa), \qquad \text{where } 0 \le \kappa < \pi,\ -\pi < \nu \le \pi. \tag{9.14}$$

Here κ and ν are the usual spherical coordinates of the pseudospin, i.e., κ is the angle between the pseudospin and the z axis, whereas the projection of $\vec{n}$ on the xy plane forms the polar angle ν with $\vec{x}$. A pure state with the pseudospin $\vec{n}$ is given by

$$|\vec{n}\rangle = \cos(\kappa/2)|0\rangle + \exp(i\nu)\sin(\kappa/2)|1\rangle. \tag{9.15}$$

We assume here that $\hat{A} = \sigma_x$, i.e., $\vec{n}_A = \vec{x}$. Moreover, we set $\vec{n}_{\text{in}} = \vec{n}$ and $\vec{n}_f = -\vec{z}$; the latter equality implies $|\phi\rangle = |1\rangle$. Note that the angle κ is a measure of the overlap of the pre- and post-selected states, since

$$|\langle\phi|\psi\rangle| = \sin\frac{\kappa}{2}. \tag{9.16}$$

In particular, for small κ,

$$\kappa = 2|\langle\phi|\psi\rangle| \qquad \text{for } \kappa \ll 1. \tag{9.17}$$

Then Eq. (9.5) yields

$$A_w = \frac{P_{\text{in}}\sin\kappa}{1 - P_{\text{in}}\cos\kappa}\exp(-i\nu), \qquad A_w^{(1,1)} = \frac{1+\cos\kappa}{1 - P_{\text{in}}\cos\kappa}. \tag{9.18}$$

For a pure initial state ($P_{\text{in}} = 1$) Eq. (9.18) yields

$$A_w = \cot\left(\frac{\kappa}{2}\right)\exp(-i\nu). \tag{9.19}$$

Note that, as shown by Eqs. (9.18) and (9.19), the phase of A_w can be chosen at will by an appropriate choice of the initial and final states. In particular, the weak value in Eqs. (9.18) and (9.19) is real (imaginary) when $\vec{n}$, Eq. (9.14), lies in the xz (yz) plane.

For $\kappa \ll 1$ the weak value in Eq. (9.19) is large, tending to infinity for $\kappa \to 0$. Now the expression for A_w simplifies,

$$A_w \approx \frac{2}{\kappa}\exp(-i\nu) \qquad (\kappa \ll 1). \tag{9.20}$$

For a mixed initial state, the necessary conditions for a large weak value (9.6) become now $P_{\text{in}} \approx 1$ and $\kappa \ll 1$. In this case Eq. (9.18) becomes approximately

$$A_w = \frac{2\kappa\exp(-i\nu)}{\kappa^2 + 2(1-P_{\text{in}})}, \qquad A_w^{(1,1)} = \frac{4}{\kappa^2 + 2(1-P_{\text{in}})}. \tag{9.21}$$

Now $|A_w|$ and $A_w^{(1,1)}$ as functions of κ have dispersive and Lorentzian shapes, respectively. Equation (9.21) shows explicitly that the weak values for a qubit with a mixed preselected state are always finite.

The conditions, under which the above results (9.20) and (9.21) have been obtained, satisfy the above requirements for maximizing weak values, Eqs. (9.6) and (9.12); in particular, now $\vec{n}_0 = \vec{z}$ and $\vec{n}_A = \vec{x}$. Correspondingly, Eq. (9.20) yields the same $|A_w|$ as in Eq. (9.13), in view of Eq. (9.17).

In Fig. 6 the weak values A_w for pure and mixed preselected states with $\nu = 0$ as well as the quantity $[A_w^{(1,1)}]^{1/2}$ for a mixed state with an arbitrary ν [see Eq. (9.19) and (9.18)] are plotted versus the angle κ, i.e., essentially versus the overlap $|\langle\phi|\psi\rangle|$ [cf. Eqs. (9.16) and (9.17)]. Note that the quantity A_w corresponding to $\nu = 0$ coincides with $|A_w|$ corresponding to an arbitrary ν; indeed, Eq. (9.18) implies that

$$|A_w| = A_w|_{\nu=0} = \frac{P_{\text{in}}\sin\kappa}{1 - P_{\text{in}}\cos\kappa}. \tag{9.22}$$

Hence, the solid and and dot-dashed curves in Fig. 6 show both A_w and $|A_w|$.

For

$$\kappa^2 \gg 2(1-P_{\text{in}}), \tag{9.23}$$

the weak values for the pure and mixed preselected states [Eqs. (9.19) and (9.18), respectively] are approximately equal, whereas $A_w^{(1,1)} \approx |A_w|^2$ (cf. Fig. 6). However, for

$$\kappa^2 \lesssim 2(1-P_{\text{in}}) \tag{9.24}$$

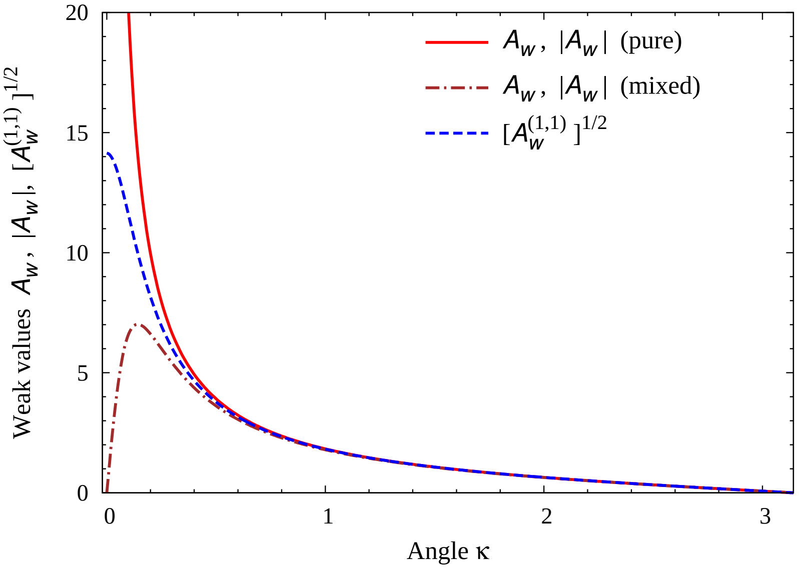

Figure 6: (color online). Weak values for a qubit versus the angle κ. We show A_w and $|A_w|$ for a pure preselected state, Eq. (9.19), and A_w, $|A_w|$, and $[A_w^{(1,1)}]^{1/2}$ for a mixed preselected state with $P_{\rm in} = 0.99$, Eq. (9.18). The quantity A_w is shown for $\nu = 0$. Since $|A_w|$ corresponding to an arbitrary ν equals A_w corresponding to $\nu = 0$, the solid and and dot-dashed curves show both A_w and $|A_w|$.

the magnitude of the weak value for a mixed preselected state is significantly less than that for a pure preselected state and also than $[A_w^{(1,1)}]^{1/2}$ (cf. Fig. 6). Both $|A_w|$ and $A_w^{(1,1)}$ have large but *finite* maxima:

$$|A_w| \;=\; [2(1-P_{\rm in})]^{-1/2} \quad \text{at} \;\; \kappa = [2(1-P_{\rm in})]^{1/2} \tag{9.25}$$

and

$$A_w^{(1,1)} \;=\; \frac{2}{1-P_{\rm in}} \quad \text{at} \;\; \kappa = 0. \tag{9.26}$$

It is interesting that now $\lim_{\kappa\to 0} A_w \;=\; 0$ for a mixed preselected state. In contrast, for a pure preselected state, $\lim_{\kappa\to 0} A_w = \infty$, as one would expect.

Equation (9.25) shows that the maximum weak-value magnitude increases with the purity of the preselected state. This dependence is rather slow; e.g., for a rather pure state with $P_{\rm in} = 0.99$, the maximum $|A_w|$ is only $\sqrt{50} \approx 7.1$ (see the dot-dashed curve in Fig. 6). Generally, to achieve the weak-value magnitude A_{w1}, the parameter $P_{\rm in}$ should satisfy the condition

$$1 - P_{\rm in} \leq (2A_{w1}^2)^{-1}. \tag{9.27}$$

For example, to obtain $|A_w| = 100$, it is necessary that $1 - 5 \times 10^{-5} \leq P_{\rm in} \leq 1$.

Here we assume that the post-selection measurement is ideal. However, a non-ideal post-selection measurement can effect PPS measurements in the same manner as a mixed preselected state, as shown below in Sec. 13.5.

10. PPS measurements of arbitrary strength: Exact solution for a qubit

Here we obtain exact results for pre- and post-selected measurements of arbitrary strength in the case of a two-level system (qubit). First we consider the case of a general meter and then discuss three specific examples of the meter.

10.1. Formulas for a general meter

10.1.1. Average pointer value

As above, we assume that the measured operator $\hat{A}$ of the qubit has the form (9.1). Taking into account that $\hat{A}^2 = I$, where I is the unity operator, Eq. (1.10) yields

$$U = \cos(\gamma\hat{F}) - i\hat{A}\sin(\gamma\hat{F}). \tag{10.1}$$

On inserting Eq. (10.1) into Eqs. (3.8) and (3.4), we obtain from Eq. (3.7) that

$$\overline{R}_s \;=\; [G_{\rm cc} + 2{\rm Im}(A_w G_{\rm cs}) + A_w^{(1,1)} G_{\rm ss}]/Q_1, \tag{10.2a}$$

where

$$Q_1 \;=\; [1 + M_c + 2M_s{\rm Im}\,A_w + (1 - M_c)A_w^{(1,1)}]/2. \tag{10.2b}$$

In Eqs. (10.2) we denoted

$$\begin{aligned} &G_{\rm cc} = \overline{\cos(\gamma F)R\cos(\gamma F)}, \qquad G_{\rm cs} = \overline{\cos(\gamma F)R\sin(\gamma F)}, \qquad G_{\rm ss} = \overline{\sin(\gamma F)R\sin(\gamma F)},\\ &M_c = \overline{\cos(2\gamma F)}, \qquad M_s = \overline{\sin(2\gamma F)} \end{aligned} \tag{10.3}$$

It is interesting that the qubit parameters enter the exact Eqs. (10.2) through the same weak values A_w and $A_w^{(1,1)}$ (see Sec. 9) as in the weak-coupling case, Eq. (5.3). Equation (5.3) results on expanding Eqs. (10.2) in powers of γ up to γ^2 and neglecting small terms as discussed in Sec. 4.3.

10.1.2. Pointer distribution

An exact expression for the pointer-value distribution is obtained from Eq. (10.2a) under the substitution $\hat{R} \to |R\rangle\langle R|$, using Eq. (8.2). This yields

$$\Phi_s(R) \;=\; \{\Phi_{\rm cc}(R) + 2{\rm Im}[A_w\Phi_{\rm sc}(R)] + A_w^{(1,1)}\Phi_{\rm ss}(R)\}/Q_1, \tag{10.4}$$

where

$$\Phi_{\rm cc}(R) = \langle R|\cos(\gamma F)\rho_{\rm M}\cos(\gamma F)|R\rangle, \quad \Phi_{\rm sc}(R) = \langle R|\sin(\gamma F)\rho_{\rm M}\cos(\gamma F)|R\rangle, \quad \Phi_{\rm ss}(R) = \langle R|\sin(\gamma F)\rho_{\rm M}\sin(\gamma F)|R\rangle. \tag{10.5}$$

When the initial state of the meter is pure, $|\psi_{\rm M}\rangle$, then Eq. (10.5) becomes,

$$\Phi_{\rm cc}(R) = |\psi_c(R)|^2, \qquad \Phi_{\rm sc}(R) = \psi_s(R)\psi_c^*(R), \qquad \Phi_{\rm ss}(R) = |\psi_s(R)|^2, \tag{10.6}$$

where

$$\psi_c(R) = \langle R|\cos(\gamma F)|\psi_{\rm M}\rangle, \qquad \psi_s(R) = \langle R|\sin(\gamma F)|\psi_{\rm M}\rangle. \tag{10.7}$$

The above results in Sec. 10.1 are exact, being applicable for arbitrary coupling strength and an arbitrary meter. Below we discuss specific examples of the meter.

10.2. Specific types of meters

10.2.1. Coinciding meter variables, $F = R$

Equations (10.2a) and (10.4) simplify when F is a function of R. For example, when $F = R$, Eq. (10.3) implies that

$$G_{\rm cc} \;=\; \overline{F\cos^2(\gamma F)} \;=\; [\overline{F} + \overline{F\cos(2\gamma F)}]/2 \;=\; \overline{F}/2 + M_s'/4, \tag{10.8}$$

where $M_{s(c)}' = dM_{s(c)}/d\gamma$. Similarly,

$$G_{\rm cs} \;=\; -M_c'/4, \qquad G_{\rm ss} \;=\; \overline{F}/2 - M_s'/4. \tag{10.9}$$

As a result, Eq. (10.2a) becomes

$$\overline{R}_s \;=\; [2\overline{F} + M_s' - 2M_c'\,{\rm Im}\,A_w + (2\overline{F} - M_s')A_w^{(1,1)}]/(4Q_1). \tag{10.10}$$

In the present case $F = R$, the exact pointer distribution (10.4) with the account of Eq. (10.5) becomes

$$\Phi_s(F) \;=\; \Phi(F)\,[\cos^2(\gamma F) + ({\rm Im}\,A_w)\sin(2\gamma F) + A_w^{(1,1)}\sin^2(\gamma F)]/Q_1. \tag{10.11}$$

10.2.2. Two-level meter

Consider now a two-level meter (qubit). Using Eq. (7.55) and taking into account that $\hat{F}_1^2 = I$, we obtain that

$$\cos\gamma\hat{F} = \cos\gamma\cos\gamma f_0 - \hat{F}_1\sin\gamma\sin\gamma f_0, \qquad \sin\gamma\hat{F} = \cos\gamma\sin\gamma f_0 + \hat{F}_1\sin\gamma\cos\gamma f_0. \tag{10.12}$$

Inserting Eq. (10.12) into Eq. (10.3) yields

$$\begin{aligned} G_{\mathrm{cc}} &= C_{10}^2 C_{11}^2 \overline{R} - S_{20}S_{21}M_R/2 + S_{10}^2 S_{11}^2 M, \\ G_{\mathrm{cs}} &= [C_{10}^2 S_{21}\overline{R} + S_{20}(C_{21}M_R + iM_I) - S_{10}^2 S_{21}M]/2, \\ G_{\mathrm{ss}} &= C_{10}^2 S_{11}^2 \overline{R} + S_{20}S_{21}M_R/2 + S_{10}^2 C_{11}^2 M, \\ M_c &= C_{20}C_{21} - S_{20}S_{21}\overline{F}_1, \quad M_s = C_{20}S_{21} + S_{20}C_{21}\overline{F}_1. \end{aligned} \tag{10.13}$$

Here $M_R,\ M_I$, and M are given by Eqs. (7.64), (7.68), and (7.69), whereas ($m = 1, 2$)

$$C_{m0} = \cos(m\gamma), \quad S_{m0} = \sin(m\gamma), \quad C_{m1} = \cos(m\gamma f_0), \quad S_{m1} = \sin(m\gamma f_0). \tag{10.14}$$

10.2.3. Continuous-variable meter

Consider a meter with continuous variables.

a. Arbitrary meter state. The case $F = R$ was discussed in Sec. 10.2.1. For the case of the canonically conjugate variables (1.12) and a pure meter state, as shown in Appendix D,

$$\begin{aligned} G_{\mathrm{cc}} &= \overline{\cos(\gamma p)\, q\, \cos(\gamma p)} = [\overline{q} + \overline{\zeta'(p)\cos(2\gamma p)}]/2, \\ G_{\mathrm{ss}} &= \overline{\sin(\gamma p)\, q\, \sin(\gamma p)} = [\overline{q} - \overline{\zeta'(p)\cos(2\gamma p)}]/2, \\ G_{\mathrm{cs}} &= \overline{\cos(\gamma p)\, q\, \sin(\gamma p)} = [i\gamma + \overline{\zeta'(p)\sin(2\gamma p)}]/2. \end{aligned} \tag{10.15}$$

In this case, using the expression $\hat{F} = p = -i\partial/\partial q$, we obtain that Eq. (10.7) becomes

$$\psi_c(q) = [\psi_{\mathrm{M}}(q+\gamma) + \psi_{\mathrm{M}}(q-\gamma)]/2, \qquad \psi_s(q) = [\psi_{\mathrm{M}}(q+\gamma) - \psi_{\mathrm{M}}(q-\gamma)]/(2i). \tag{10.16}$$

b. Gaussian meter state. When the meter initial state is a general complex Gaussian state (1.49), all the relevant averages can be expressed in a simple form. Taking into account Eq. (7.23), we obtain that in Eq. (10.15)

$$\begin{aligned} \overline{\zeta'(p)\cos(2\gamma p)} &= [\overline{q}\cos(2\gamma\overline{p}) - \gamma b\sin(2\gamma\overline{p})]\, \exp[-2(\gamma\Delta p)^2], \\ \overline{\zeta'(p)\sin(2\gamma p)} &= [\overline{q}\sin(2\gamma\overline{p}) + \gamma b\cos(2\gamma\overline{p})]\, \exp[-2(\gamma\Delta p)^2], \end{aligned} \tag{10.17}$$

whereas in Eqs. (10.3) and (10.8) for $F = p$ we have

$$\begin{aligned} M_c &= \cos(2\gamma\overline{p})\, \exp[-2(\gamma\Delta p)^2], \qquad M_s = \sin(2\gamma\overline{p})\, \exp[-2(\gamma\Delta p)^2], \\ M_c' &= -2[\overline{p}\sin(2\gamma\overline{p}) + 2\gamma\Delta p^2\cos(2\gamma\overline{p})]\, \exp[-2(\gamma\Delta p)^2], \\ M_s' &= 2[\overline{p}\cos(2\gamma\overline{p}) - 2\gamma\Delta p^2\sin(2\gamma\overline{p})]\, \exp[-2(\gamma\Delta p)^2]. \end{aligned} \tag{10.18}$$

11. Numerical results and discussion

Here we present results of calculations for weak PPS measurements of a qubit with two types of a continuous-variable meter. We assume that for both meters, $F = p$ and $\overline{p_c^3} = 0$. For meter 1, $R = p$, whereas for meter 2, $R = q$ and the phase $\zeta(p)$ is quadratic. In this section we set $\Delta p = 1$.

For the measured qubit we take $\hat{A} = \sigma_x$, $|\psi\rangle = |\vec{n}\rangle$, Eq. (9.15), and $|\phi\rangle = |-\vec{z}\rangle$. Correspondingly, in Figs. 7-11, A_w is given by Eq. (9.19), whereas in Fig. 12, A_w and $A_w^{(1,1)}$ are given by Eq. (9.18). Equations (9.18) and (9.19) imply that now the weak-value phase $\theta = -\nu$. Note that $|A_{\phi\psi}| \leq 1$, and hence the validity condition (4.5) of Eq. (4.11) certainly holds for

$$|\gamma| \ll (1 + |\overline{p}|)^{-1}. \tag{11.1}$$

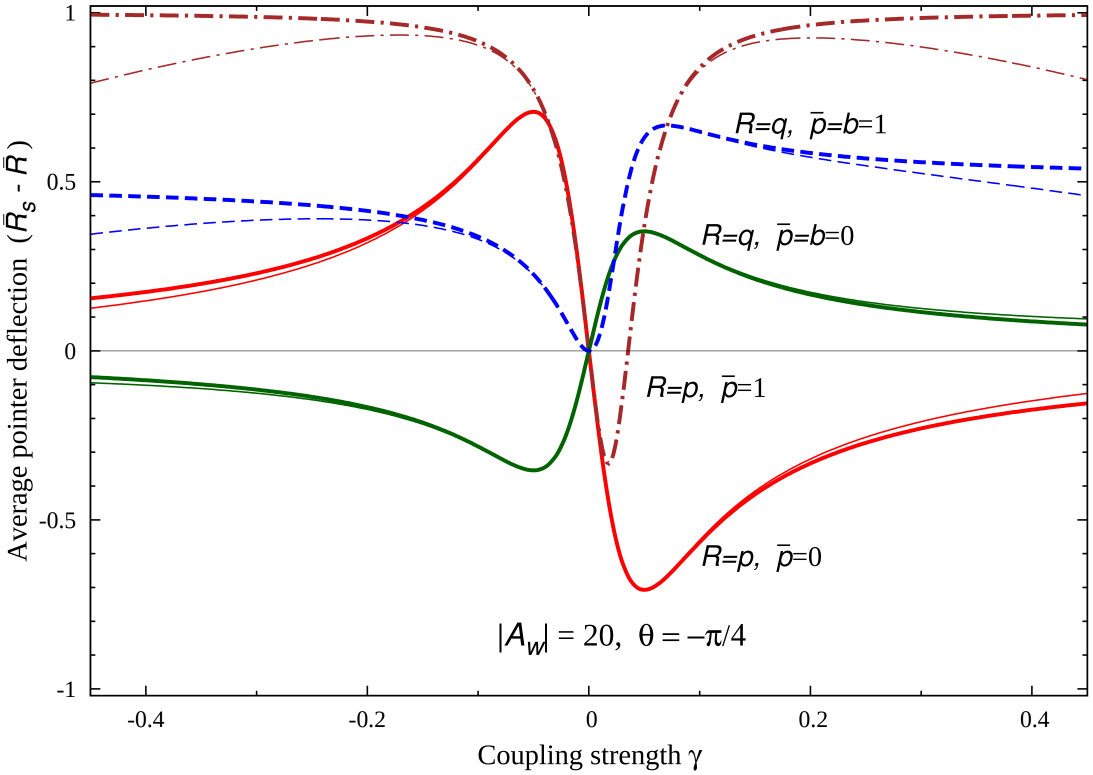

Figure 7: (color online). The average pointer deflection $(\bar{R}_s - \bar{R})$ versus the coupling strength γ. Here $\Delta p = 1$, $P_{\rm in} = 1$ (a pure initial state); thick lines: Eqs. (11.2); thin lines: the exact solution (10.2). Solid red lines: $R = p$, $\bar{p} = 0$; dot-dashed brown lines: $R = p$, $\bar{p} = 1$; solid dark-green lines: $R = q$, $\bar{p} = b = 0$; dashed blue lines: $R = q$, $\bar{p} = b = 1$. The figure shows several lineshapes which are possible in weak PPS measurements. Notice that our general approximate formulas (11.2) approximate very well the exact solutions in the region where the measurements are weak, see the inequality (11.1), which now is $|\gamma| \ll 1$.

To get a better understanding of weak PPS measurements, below we show plots of our general formulas (4.11), (4.64), and (5.2) versus various parameters. The values of the meter parameters in Eqs. (4.11), (4.64), and (5.2) are given by case 1 in Table 5 and case 2 in Table 6 for meters 1 and 2, respectively. In particular, Eq. (4.11) becomes for meters 1 and 2, respectively,

$$\bar{p}_s - \bar{p} = \frac{2\gamma\,(\Delta p)^2\,(\mathrm{Im}\,A_w + \gamma\bar{p}\,|A_w|^2)}{1 + 2\gamma\bar{p}\,\mathrm{Im}\,A_w + \gamma^2(1+\bar{p}^2)\,|A_w|^2}, \tag{11.2a}$$

$$\bar{q}_s - \bar{q} = \frac{\gamma\,\mathrm{Re}\,A_w + \gamma b\,\mathrm{Im}\,A_w + \gamma^2 b\bar{p}\,|A_w|^2}{1 + 2\gamma\bar{p}\,\mathrm{Im}\,A_w + \gamma^2(1+\bar{p}^2)\,|A_w|^2}. \tag{11.2b}$$

Equation (5.2) reduces now to Eqs. (11.2) with the accuracy to the substitution (5.4). In Figs. 7-12 the plots of Eqs. (11.2) are shown by thick lines. These results are verified against the exact solution (10.2) with a Gaussian meter state (Sec. 10.2.3), which is plotted by thin lines.

Figure 7 presents the average pointer deflection $(\bar{R}_s - \bar{R})$ versus the coupling strength for different values of $\bar{p}$ and b. One can see that Eqs. (11.2) approximate the exact solutions very well when the condition (11.1) holds (i.e., now for $|\gamma| \ll 1$). In this interval, Fig. 7 shows a variety of lineshapes, which, as discussed above, include Lorentzian-like, dispersive-like, as well as similar, though more complicated, lineshapes. The main features of the curves agree with the analysis in Sec. 4. Namely, when γ is very close to zero, the dependence is described by the linear Eq. (7.2) (for $R = p$) or (7.24) ($R = q$). The exception is the case $R = q$, $\bar{p} = b = 1$ (the blue dashed lines),when the linear response vanishes; this plot shows clearly that weak PPS measurements are possible even in the absence of a linear response. With a further increase of $|\gamma|$, the quantity $|\bar{R}_s - \bar{R}|$ increases to a value of the order of the maximum, i.e., of order ΔR

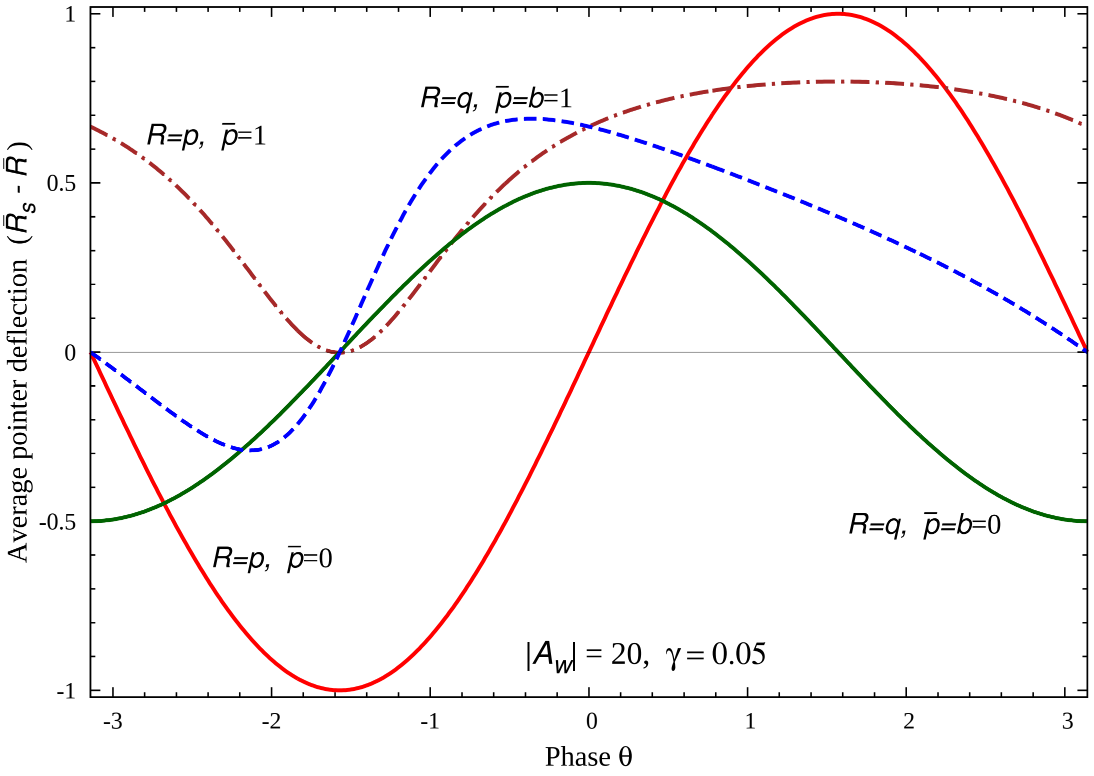

Figure 8: (color online). The average pointer deflection $(\overline{R}_s - \overline{R})$ versus the phase θ of A_w. Here $\Delta p = 1$, $P_{\text{in}} = 1$; thick lines: Eqs. (11.2); thin lines: the exact solution (10.2). The thin lines are not seen since they practically coincide with the thick lines. The four cases are plotted with the same line styles as in Fig. 7.

[see Eq. (4.41)], for

$$|\gamma A_w| \sim (1 + |\overline{p}|)^{-1} \tag{11.3}$$

[cf. Eq. (4.27)], i.e., now for $|\gamma| \sim 0.05/(1 + |\overline{p}|)$. Note that in the present case

$$\Delta R = \Delta p = 1 \qquad \text{for} \quad R = p, \tag{11.4a}$$

$$\Delta R = \Delta q = \frac{\sqrt{1+b^2}}{2} \qquad \text{for} \quad R = q, \tag{11.4b}$$

where Eq. (11.4b) follows from Eq. (1.51).

Figure 8 shows the dependence of the average pointer deflection $(\overline{R}_s - \overline{R})$ on the phase of the weak value for $\gamma = 0.05$, the other parameters being as in Fig. 7. Now the coupling strength γ satisfies the condition (11.1); correspondingly, there is no discernable difference between the exact and approximate formulas. Moreover, now we set $|\gamma A_w| = 1$ to satisfy the condition (11.3); hence Fig. 8 corresponds to a significantly nonlinear regime. Therefore, the maximum values of $|\overline{R}_s - \overline{R}|$ in Fig. 8 are of order ΔR. For curves with $\overline{p} = 0$, the θ dependence is sinusoidal, and the maxima and zeros of $|\overline{R}_s - \overline{R}|$ occur at the same values of θ as for the linear response, Eqs. (4.17) and (4.18), since the last term in the numerator and the second term in the denominator of Eqs. (11.2) disappear now. Note that for meter 1, $\theta_0 = 0$, whereas for meter 2, $\theta_0 = \pi/2$ for $\overline{p} = 0$ and $\theta_0 = \pi/4$ for $\overline{p} = 1$. For curves with $\overline{p} \neq 0$, the θ dependence is not sinusoidal, and the positions of the maxima and zeros of $|\overline{R}_s - \overline{R}|$ differ from those for the linear response, since then, in contrast to the case $\overline{p} = 0$, generally all the terms in Eqs. (11.2) are nonzero.

Figure 9 demonstrates the dependence of $(\overline{R}_s - \overline{R})$ on the angle κ which determines $|A_w| = \cot(\kappa/2)$, see Eq. (9.19). Actually for $\kappa \ll 2$, Fig. 9 shows the dependence on the quantity $2/|A_w|$ ($\approx \kappa$). In Fig. 9, the exact and approximate

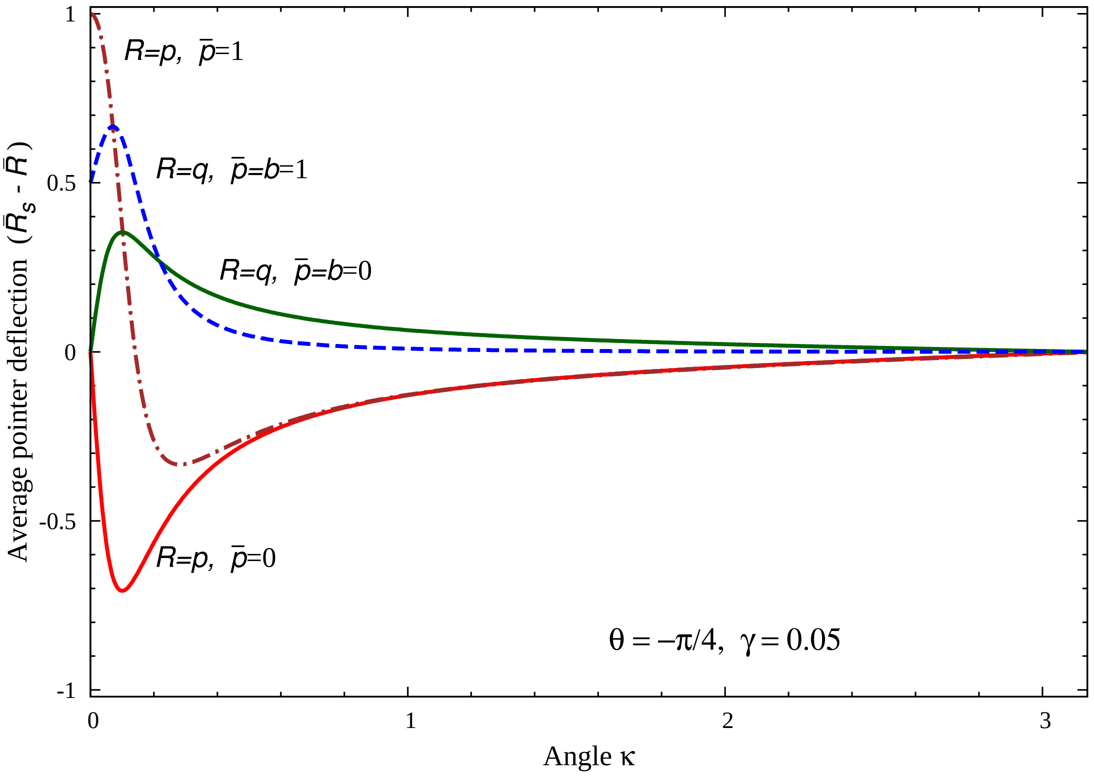

Figure 9: (color online). The average pointer deflection $(\bar{R}_s - \bar{R})$ versus the angle κ in Eq. (9.19). Here $\Delta p = 1$, $P_{\text{in}} = 1$; thick lines: Eqs. (11.2); thin lines: the exact solution (10.2). The thin lines are not seen since they practically coincide with the thick lines. The four cases are plotted with the same line styles as in Fig. 7.

formulas practically coincide. Figure 9 illustrates the fact that $|\bar{R}_s - \bar{R}|$ becomes significant, i.e., of order ΔR, when A_w is sufficiently large to satisfy Eq. (11.3). The latter condition is now equivalent to $\kappa \sim 0.1(1 + |\bar{p}|)$.

In Figs. 7-9 above we illustrated the behavior of the average pointer deflection $(\bar{R}_s - \bar{R})$ for the case $\bar{F} \lesssim \Delta F$ ($\bar{p} \lesssim 1$ now). Consider now the case $\bar{F} \gg \Delta F$ (i.e., $\bar{p} \gg 1$ in this section), which, as mentioned in Sec. 4, is quite different from the case $\bar{F} \lesssim \Delta F$. In this case $(\bar{R}_s - \bar{R})$ is significant only when the parameters x and ϵ in Eqs. (4.65)-(4.66) are small. Thus, as shown by Figs. 10 and 11, $(\bar{R}_s - \bar{R})$ is a narrow resonance as a function of different parameters in the problem. This case is approximated by Eq. (4.64), which for meters 1 and 2 becomes, respectively,

$$\bar{p}_s - \bar{p} = \frac{-2(\Delta p)^2 x}{\bar{p}\,(x^2 + \epsilon^2 + \bar{p}^{-2})}, \tag{11.5a}$$

$$\bar{q}_s - \bar{q} = \frac{-\epsilon - bx}{\bar{p}\,(x^2 + \epsilon^2 + \bar{p}^{-2})}. \tag{11.5b}$$

Figures 10 and 11 show that the simple Eqs. (11.5) describe well the resonance in the pointer deflection. In Fig. 10, $\epsilon = 0$, whereas the varied parameter γ is linearly related to x. In contrast, in Fig. 11, x is negligibly small, whereas θ is linearly related to ϵ. In this case, as shown by Eq. (11.5b), $(\bar{q}_s - \bar{q})$ is practically independent of b; correspondingly, the plots for $b = 0$ and $b = 1$ practically coincide in Fig. 11. One can see that $(\bar{R}_s - \bar{R})$ is almost zero for the case $R = q,\ b = 0$, when $\text{Re}\,A_w = \epsilon = 0$ (Fig. 10), and for $R = p$ when x practically vanishes (Fig. 11). The reason for this is clear from the simplified Eqs. (11.5b) and (11.5a), respectively.

Note that there is a slight discrepancy between Eqs. (11.2a) and (10.2) for $R = p$ when $\theta \approx -\pi/2$ (see the thick and thin red solid lines in Fig. 11). This is explained by the fact that in this case the two terms in the numerator of Eq. (11.2a) practically cancel, so the higher-order terms neglected in Eq. (4.11) become noticeable. However, this

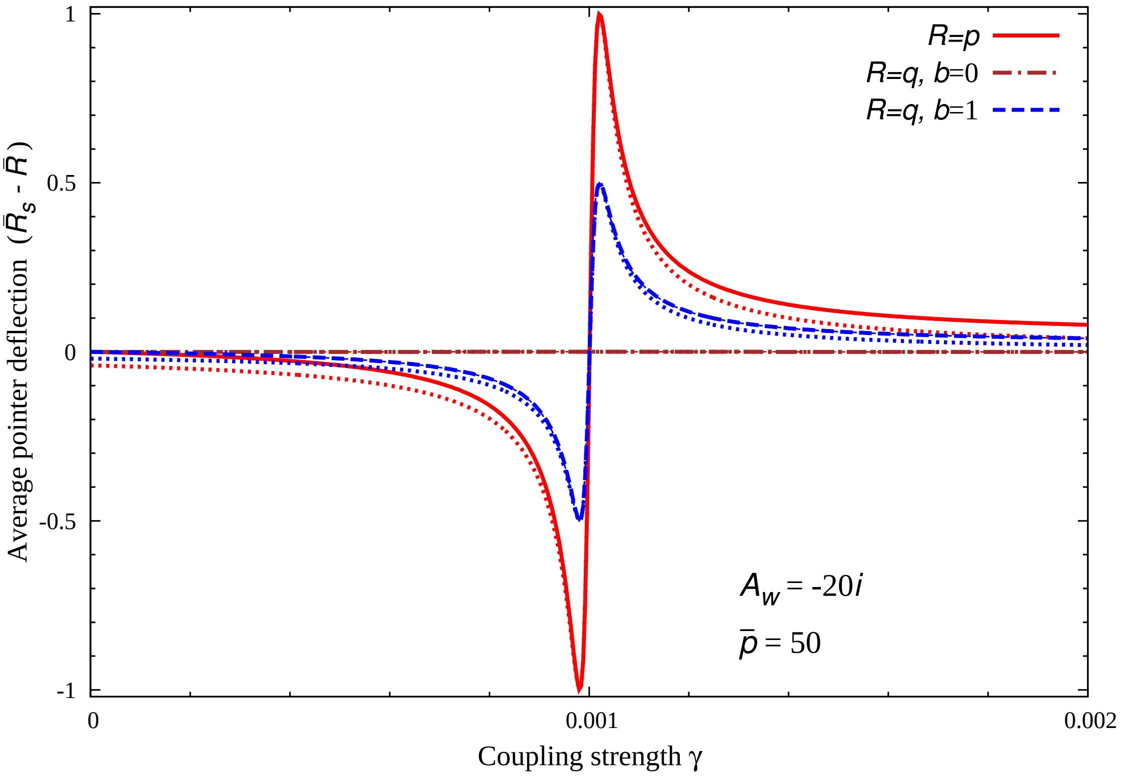

Figure 10: (color online). The average pointer deflection $(\bar{R}_s - \bar{R})$ versus the coupling strength γ. Here $\Delta p = 1$, $P_{\rm in} = 1$; thick lines: Eqs. (11.2); thin lines: the exact solution (10.2); dotted lines: the simplified Eqs. (11.5). The thin lines are not seen since they practically coincide with the thick lines. The figure shows the regime of a narrow resonance obtainable for $\bar{F} \gg \Delta F$, i.e., now for $\bar{p} \gg 1$.

discrepancy is rather insignificant, since it occurs for the not very interesting case of a small $(\bar{R}_s - \bar{R})$ [see the remark after Eq. (4.11)].

The effect of a mixed initial state is illustrated by Fig. 12, where $P_{\rm in} = 0.99$. A comparison of Figs. 9 and 12 shows that even a small impurity of the initial state can significantly decrease the maximum magnitude of the average pointer deflection.

12. Discussion of two recent interferometric experiments

Starling et al. [133] experimentally demonstrated an optical-phase measurement technique based on phase amplification. Similar sensitivity to balanced homodyne detection was obtained. In Ref. [133], the experiment was explained on the basis of classical wave optics. A similar experiment was performed also in Ref. [83], but there the explanation was given in terms of the weak value. Below we provide a unified description of both experiments on the basis of the present nonperturbative theory of weak PPS measurements. In particular, we show that the results of Refs. [83, 133] are described by two different limits of the same nonlinear formula.

The correspondence between the notation here and in Refs. [83, 133] is presented in Table 8.

12.1. Unified theory of two interferometric measurement schemes

We begin with a brief description of the schematic of the weak PPS measurement in Refs. [83, 133] shown in Fig. 13 (the details can be found in Refs. [83, 133]). A photon enters a Sagnac interferometer, composed of a 50/50 beam splitter and mirrors, and eventually exits the same beam splitter. The measured quantum system consists of the clockwise and counterclockwise paths of a photon in the interferometer, denoted by $|1\rangle$ and $|2\rangle$, respectively. The

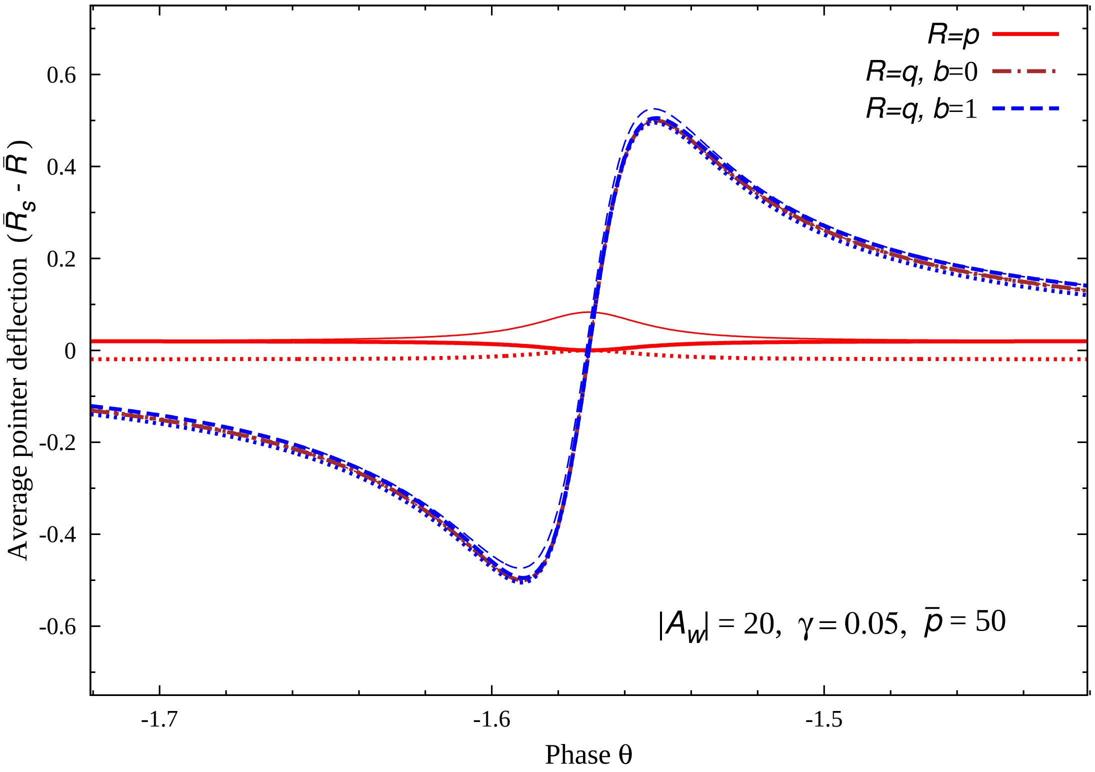

Figure 11: (color online). The average pointer deflection $(\bar{R}_s - \bar{R})$ versus the phase θ of A_w. Here $\Delta p = 1$, $P_{\text{in}} = 1$; thick lines: Eqs. (11.2); thin lines: the exact solution (10.2); dotted lines: the simplified Eqs. (11.5). The figure shows the regime of narrow resonance obtainable for $|\bar{p}| \gg 1$.

	γ	q	Δq	φ
[83]	k	x	a	$-\phi$
[133]	k	x	σ	ϕ

Table 8: The correspondence between the notation used here and the one used in Refs. [83, 133].

system is coupled to the meter (a transverse degree of freedom of the photon) by a controlled tilt given to the piezo-driven mirror (PDM), resulting in the transverse-momentum shifts γ and $-\gamma$ of the photon in the paths $|1\rangle$ and $|2\rangle$, respectively. The coupling unitary operator is given [83] by Eq. (1.10), where $\hat{F} = q$ is the transverse coordinate and

$$\hat{A} = |1\rangle\langle 1| - |2\rangle\langle 2|. \tag{12.1}$$

Moreover, due to the polarizer and the half-wave plate (HWP), the photon passes the Soleil-Babinet compensator (SBC) in the polarization state depending on the path. As a result, after passing the SBC, the photon acquires different phases φ_1 and φ_2 in the paths $|1\rangle$ and $|2\rangle$, respectively, so that a relative phase

$$\varphi = \varphi_1 - \varphi_2 \tag{12.2}$$

is introduced between the paths. In the clockwise (counterclockwise) path the photon passes the SBC before (after) the PDM, therefore the photon state before the exit of the photon from the interferometer is

$$U_2 U U_1 |\psi_0\rangle \psi_{\text{M}}(q) \ = \ U U_2 U_1 |\psi_0\rangle \psi_{\text{M}}(q). \tag{12.3}$$

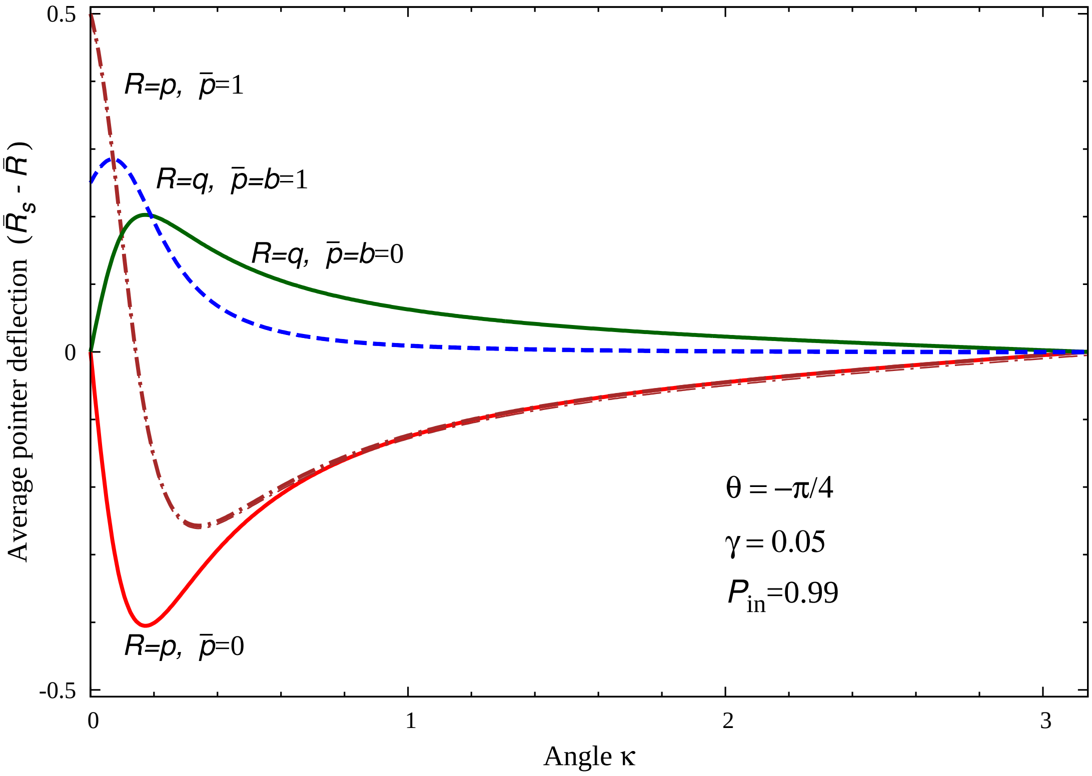

Figure 12: (color online). The average pointer deflection $(\bar{R}_s - \bar{R})$ versus the angle κ in Eq. (9.19), for a mixed initial state. Here $\Delta p = 1$; thick curves: Eqs. (11.2) with the substitution (5.4); thin lines: the exact solution (10.2). The thin curves are not seen since they practically coincide with the thick lines. The four cases are plotted with the same line styles as in Fig. 7. The figure shows that adding a small impurity in the preselected state can result in a significant decrease of the maximum magnitude of the average pointer deflection.

Here $|\psi_0\rangle$ is the photon state immediately after the photon enters the interferometer,

$$|\psi_0\rangle = \frac{1}{\sqrt{2}}(|1\rangle + i|2\rangle), \qquad U_j = \exp(i\varphi_j|j\rangle\langle j|). \tag{12.4}$$

In Eq. (12.3) we changed the order of the operators U_2 and U, since U_2 commutes with $\hat{A}$ and hence with U. Equation (12.3) implies that the effective preselected state is [83]

$$|\psi\rangle \;=\; U_2U_1|\psi_0\rangle \;=\; \frac{1}{\sqrt{2}}(e^{i\varphi}|1\rangle + i|2\rangle). \tag{12.5}$$

Here the last equality holds with the accuracy to an irrelevant total phase.

The post-selection is performed by detecting (with the split detector) the photons exiting only the “dark port” of the beam splitter, the post-selected state being [83]

$$|\phi\rangle = \frac{1}{\sqrt{2}}(|1\rangle - i|2\rangle). \tag{12.6}$$

Equations (12.1), (12.5), and (12.6) imply that

$$\langle\phi|\psi\rangle \;=\; \frac{e^{i\varphi} - 1}{2} \;\approx\; \frac{i\varphi}{2}, \qquad A_{\phi\psi} \;=\; \frac{e^{i\varphi} + 1}{2} \;\approx\; 1. \tag{12.7}$$

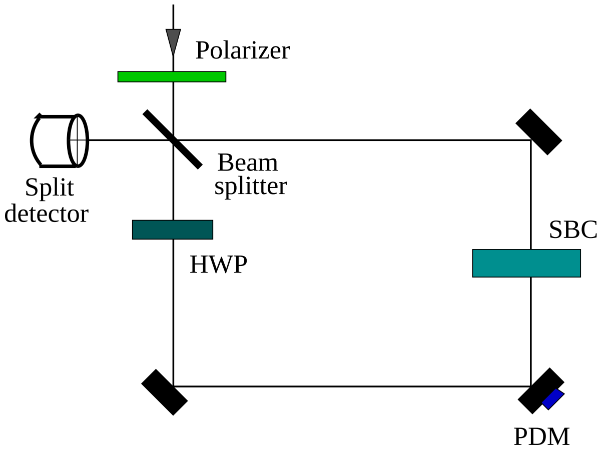

Figure 13: (color online). Schematic diagram of the Sagnac interferometer for weak PPS measurements used in Refs. [83, 133]. Here HWP is a half-wave plate, SBC is a Soleil-Babinet compensator, and PDM is a piezo-driven mirror.

Here and below the approximations hold for $|\varphi| \ll 1$. Using Eq. (12.7) in Eq. (1.36) yields the weak value [83]

$$A_w = -i\cot\left(\frac{\varphi}{2}\right) \approx -\frac{2i}{\varphi}. \tag{12.8}$$

The split detector measures the average transverse coordinate of the photon, which means that $R = F = q$. Moreover, in Refs. [83, 133] the initial meter state is a Gaussian with $\overline{q} = 0$, whereas the beam divergence is negligible, i.e., the meter Hamiltonian is zero. Hence, from Eq. (4.11) and case 1 in Table 5 we obtain that

$$\overline{q}_s = \frac{2\gamma(\Delta q)^2 \operatorname{Im} A_w}{1 + \gamma^2(\Delta q)^2 |A_w|^2} \approx -\frac{4\gamma(\Delta q)^2\varphi}{\varphi^2 + 4\gamma^2(\Delta q)^2}, \tag{12.9}$$

where the approximation (12.8) is used in the second equality.

The formula (12.9) simplifies in two limits. In the linear-response regime,

$$|\gamma A_w|\,\Delta q \ll 1, \quad \text{i.e.,} \quad 2\gamma(\Delta q) \ll |\varphi|, \tag{12.10}$$

Eq. (12.9) yields ([83], Eq. (5))

$$\overline{q}_s = 2\gamma(\Delta q)^2 \operatorname{Im} A_w \approx -\frac{4\gamma(\Delta q)^2}{\varphi} \tag{12.11}$$

and in the inverted region,

$$|\gamma A_w|\,\Delta q \gg 1, \quad \text{i.e.,} \quad 2|\gamma|\,\Delta q \gg |\varphi|, \tag{12.12}$$

Eq. (12.9) yields ([133], Eq. (9))

$$\overline{q}_s = -\frac{2}{\gamma}\operatorname{Im}\frac{1}{A_w} \approx -\frac{\varphi}{\gamma}. \tag{12.13}$$

The above results (12.9), (12.11), and (12.13) hold under the condition (4.7a), which now becomes

$$|\gamma|\,\Delta q \ll 1. \tag{12.14}$$

Equations (12.11) and (12.13) constitute the central results of Refs. [83] and [133], respectively.[9] As shown above, these two experiments were performed in different regimes of weak PPS measurements, described by two limits of our general nonlinear formula, which now has the form (12.9).

---

[9] Dixon et al. [83] demonstrated also an enhancement of the pointer deflection due to propagation effects, see the discussion in Ref. [84]. These propagation effects are completely analogous to the time evolution due to a meter Hamiltonian [80]. Hence, they can be explained also with the help of the present theory of the effects of the meter Hamiltonian (Secs. 6 and 7.2.4).

It is of interest also to consider the distribution of the pointer values. It is given by Eq. (8.20) taking into account Eqs. (8.4) and (12.8),

$$\Phi_s(q) \; = \; \frac{[\gamma q - \tan(\varphi/2)]^2 \, \Phi(q)}{\tan^2(\varphi/2) + \gamma^2 \, (\Delta q)^2}. \tag{12.15}$$

In particular, in the limit (12.12)

$$\Phi_s(q) \; \approx \; \left[\frac{q}{\Delta q} - \frac{\tan(\varphi/2)}{\gamma \Delta q} \right]^2 \Phi(q). \tag{12.16}$$

For a Gaussian $\Phi(q)$, Eq. (12.16) coincides, up to a constant factor, with the intensity at the dark port (i.e., the unnormalized pointer distribution) given by Eq. (7) in Ref. [133] (cf. Table 8). In Ref. [133] the light with the intensity distribution (12.16) is called the "split-Gaussian mode", since this distribution has a slightly asymmetric two-peak shape, shown in Fig. 2 in Ref. [133].

Thus, we have derived the results of Ref. [133] quantum-mechanically. We have shown that the experiment in Ref. [133] is a weak PPS measurement in the inverted region.

12.2. Amplification coefficient for phase measurements

Starling et al. [133] showed that their experiment is well suited for precision measurements of the phase φ. They claimed that their technique involves phase amplification with the coefficient proportional to γ^{-1}, but they did not provide the exact value of the amplification coefficient. Let us obtain the latter. Note that, in view of Eq. (12.7),

$$|\varphi| = 2|\langle\phi|\psi\rangle|. \tag{12.17}$$

As follows from the general discussion in Sec. 4.9.3, in measurements of the overlap the proper amplification coefficient is [cf. Eq. (4.91)]

$$a' \; = \; (|\gamma| \, \Delta q)^{-1}, \tag{12.18}$$

where we took into account the second Eq. (12.7). The amplification coefficient a_φ for the phase φ is obtained from the relation $a'|\langle\phi|\psi\rangle| = a_\varphi|\varphi|$, i.e., in view of the first Eq. (12.7),

$$a_\varphi = \frac{a'}{2} \; = \; (2|\gamma| \, \Delta q)^{-1}. \tag{12.19}$$

This can be compared with the linear-response result (12.11), which was used in Ref. [83] for an amplification of the pointer deflection (i.e., the beam deflection) or for measuring γ, the proper amplification coefficient being [cf. Eqs. (4.48) and (12.17)]

$$a \; \sim \; |\varphi|^{-1}. \tag{12.20}$$

In the case (12.10) [(12.12)] the magnitude of the pointer deflection (12.11) [(12.13)] increases, when the ratio γ/φ increases (decreases). For both cases, the amplification is maximal in the strongly-nonlinear regime,

$$|\gamma A_w| \, \Delta q \sim 1, \quad \text{i.e.,} \quad 2|\gamma| \, \Delta q \sim |\varphi|, \tag{12.21}$$

where, in view of Eqs. (12.19) and (12.20),

$$a_\varphi \; \sim \; a \; \sim \; |\varphi|^{-1}. \tag{12.22}$$

In this regime, the nonlinear Eq. (12.9) should be used.

12.3. A comparison of the phase-amplification technique with projective measurements

In Sec. 4.9.3, we obtained an estimation of the SNR with respect to the quantum noise for weak PPS measurements in the regime of very large weak values [see Eq. (4.88)]. The above estimation holds for the general case. However, for the special case of the phase-amplification technique [133] (i.e., the weak PPS measurement described above), the quantum SNR can be obtained exactly. Indeed, in view of the third equality in Eq. (4.86) and the second equation in Eq. (12.7), we obtain that now the post-selection probability is given by the value [133]

$$\langle\Pi_\phi\rangle_f \; = \; \gamma^2(\Delta q)^2 \ll 1, \tag{12.23}$$

which is small due to Eq. (12.14). Taking into account also that the pointer deflection is given by Eq. (12.13), we obtain from Eqs. (4.73) and (4.76) that the quantum SNR is given by

$$\mathcal{R} \; = \; 3^{-1/4}|\varphi| \sqrt{N} \; \approx \; 0.76\,|\varphi| \sqrt{N}. \tag{12.24}$$

Here we took into account that Eq. (12.16) with a Gaussian $\Phi(q)$ implies the pointer uncertainty $\Delta R_s \approx 3^{1/4}\Delta R$. Equation (12.24) is derived assuming that the average position is obtained by a statistical analysis of the measurement results. For comparison, in the split-detection method the average position is deduced from the difference between the integrated intensities on the left and right sides of the detector, resulting in a somewhat higher SNR than Eq. (12.24) [133],

$$\mathcal{R} = \sqrt{\frac{2}{\pi}}\,|\varphi| \sqrt{N} \approx 0.80\,|\varphi| \sqrt{N}. \tag{12.25}$$

The phase φ can be measured also with the help of strong (projective) quantum measurements. The projective measurement described in Sec. 4.9.3 can be implemented in the present case by setting $\gamma = 0$ and measuring the statistics of photons exiting the dark and bright output ports of the beam splitter in Fig. 13, since the exit probabilities equal $P_1 = |\langle\phi|\psi\rangle|^2 \approx \varphi^2/4$ and $P_0 = 1 - P_1$, respectively. As follows from Eqs. (4.90), for this method, the SNR with respect to the quantum noise is

$$\mathcal{R}_1 = \frac{|\varphi| \sqrt{N}}{2}. \tag{12.26}$$

In fact, in Ref. [133] a more sophisticated version of strong measurements was implemented, the so called balanced homodyne detection. In this scheme a unitary transformation of $|\psi\rangle$ is performed, so that $\varphi \to \pi/2 + \varphi$ in Eq. (12.5), and then the integrated intensities of both output ports are subtracted, resulting in the homodyne signal per one photon $\sin\varphi \approx \varphi$. As shown in Ref. [133], the quantum SNR for the balanced homodyne detection is

$$\mathcal{R}_2 = |\varphi| \sqrt{N}, \tag{12.27}$$

two times greater than for the above simple scheme of projective measurements [cf. Eq. (12.26)].

A comparison of Eq. (12.27) with Eqs. (12.24) and (12.25) shows that the phase-amplification technique has similar sensitivity to balanced homodyne detection with respect to quantum noise [133]. This is in agreement with the discussion in Sec. 4.9.3, where the quantum SNR was shown to be generally of the same order for projective and weak PPS measurements.

As noted in Ref. [133], the phase-amplification technique is a robust, low-cost alternative to balanced homodyne phase detection. In particular, as a split detector one can use a low-cost detector with a low saturation intensity owing to the large attenuation [cf. Eq. (12.23)]. Note that the increase of the attenuation does not decrease the quantum SNR (12.25) [or (12.24)] owing to the simultaneous increase of the amplification coefficient (12.19).

13. PPS measurements with a general post-selection measurement

13.1. General formulas

Until now, we considered PPS measurements in which the post-selection is performed by a measurement projecting the system state on a discrete, nondegenerate eigenstate of some variable B. In this section, we discuss the general case, where the post-selection is performed by means of a general measurement described by a POVM (see Sec. 1.3.1). This case includes different possible situations, such as, e.g., a projection on a degenerate eigenvalue of B. Another situation, where this case may be relevant, arises when one takes into account errors in the post-selection measurement. Indeed, in the presence of measurement errors, a projective measurement can be described as a general measurement characterized by a POVM [3, 23, 147].

In the general case, a PPS ensemble consists of systems for which the post-selection measurement yields a specific outcome. The POVM operator corresponding to this measurement outcome is denoted here by E. By repeating the derivation in Sec. 3.1 with the change

$$\Pi_\phi \; \to \; E, \tag{13.1}$$

it is easy to obtain that in the general case [cf. Eqs. (3.7) and (3.9)]

$$\bar{R}_s = \frac{\langle ER\rangle_f}{\langle E\rangle_f} \tag{13.2}$$

and

$$\bar{R}_s - \bar{R} = \frac{\langle ER_c\rangle_f}{\langle E\rangle_f}, \tag{13.3}$$

where $\langle E\rangle_f$ is the post-selection probability and the averages are given by [cf. Eqs. (3.8) and (3.4)]

$$\langle ER\rangle_f = \mathrm{Tr}\,[(E\otimes\hat{R})\rho_f], \qquad \langle E\rangle_f = \mathrm{Tr}\,[(E\otimes I_{\mathrm{M}})\rho_f]. \tag{13.4}$$

13.2. Relation between PPS and standard measurements of any strength

Equation (13.2) allows us to connect PPS and standard quantum measurements of arbitrary strength. In the limiting case when E is just the unity operator I_{S}, we obtain that $\langle E\rangle_f = \langle I_{\mathrm{S}}\rangle_f = 1$ and hence Eq. (13.2) reduces to Eq. (2.1). Thus, in this case PPS measurements coincide with standard measurements for any measurement strength and any preselected state. This statement extends the similar results obtained for the special cases of strong and weak measurements with a pure preselected state in Ref. [67] (cf. Sec. 1.3.1).

The above statement is a limiting case of a more general relation between PPS and standard quantum measurements of any strength, as follows. If ρ or E commutes with $\hat{A}$, then a measurement of A in a PPS ensemble provides the same results as in an ensemble preselected in the state

$$\rho' = \frac{E\rho + \rho E}{2\,\mathrm{Tr}\,(E\rho)}. \tag{13.5}$$

To prove this statement, we use Eq. (13.4) and the third equality in Eq. (3.2) to write

$$\langle ER\rangle_f = \mathrm{Tr}\,[(E\otimes\hat{R})\,U\,(\rho\otimes\rho_{\mathrm{M}})\,U^\dagger] = \frac{1}{2}\mathrm{Tr}\,[(I_s\otimes\hat{R})\,U\,((E\rho+\rho E)\otimes\rho_{\mathrm{M}})\,U^\dagger], \tag{13.6}$$

$$\langle E\rangle_f = \mathrm{Tr}\,[(E\otimes I_{\mathrm{M}})\,U\,(\rho\otimes\rho_{\mathrm{M}})\,U^\dagger] = \mathrm{Tr}\,[U\,(E\rho\otimes\rho_{\mathrm{M}})\,U^\dagger] = \mathrm{Tr}\,(E\rho\otimes\rho_{\mathrm{M}}) = \mathrm{Tr}\,(E\rho)\,\mathrm{Tr}\,\rho_{\mathrm{M}} = \mathrm{Tr}\,(E\rho). \tag{13.7}$$

In the second equalities in Eqs. (13.6) and (13.7) we used Eqs. (B.11) and (B.10), respectively. Inserting Eqs. (13.6) and (13.7) into Eq. (13.2) yields Eq. (2.1) with ρ given by Eq. (13.5). This proves the statement in question.

Note that ρ' in Eq. (13.5) does not exist when $\mathrm{Tr}\,(E\rho) = 0$. However, in this case PPS measurements are not possible, since the postselection probability (13.7) is zero.

Now let us apply the above relation between PPS and standard measurements to prove the time-symmetry property, mentioned in Sec. 1.5.2, that measurements in a preselected (only) ensemble and a post-selected (only) ensemble with the same pre- or post-selected state, respectively, produce the same results, irrespective of the measurement strength. Consider measurements in a post-selected ensemble, i.e., an ensemble with the completely mixed preselected state $\rho_{\mathrm{c.m.}}$, Eq. (1.18), and a post-selected state $|\phi\rangle$. Since $\rho_{\mathrm{c.m.}}$ commutes with any $\hat{A}$, a measurement in a post-selected ensemble is equivalent to a measurement in a preselected ensemble with the preselected state ρ', Eq. (13.5). Now $E = \Pi_\phi \equiv |\phi\rangle\langle\phi|$, and, in view of Eq. (1.18), Eq. (13.5) yields

$$\rho' = \frac{\Pi_\phi\,\rho_{\mathrm{c.m.}} + \rho_{\mathrm{c.m.}}\Pi_\phi}{2\,\mathrm{Tr}\,(\Pi_\phi\,\rho_{\mathrm{c.m.}})} = \frac{2\Pi_\phi/d}{2d^{-1}} = \Pi_\phi. \tag{13.8}$$

This proves the statement in question.

13.3. Weak PPS measurements

Now the expansions in the coupling parameter can be obtained in the form [cf. Eqs. (3.13)-(3.15)],

$$\langle ER_c\rangle_f = \sum_{n=1}^{\infty}\frac{i^n\gamma^n}{n!}\sum_{k=0}^{n}(-1)^k\binom{n}{k}\mathrm{Tr}\,(A^{n-k}EA^k\rho)\,\overline{F^{n-k}R_cF^k}, \tag{13.9}$$

$$\langle E\rangle_f = \sum_{n=0}^{\infty}\frac{i^n\gamma^n\,\overline{F^n}}{n!}\sum_{k=0}^{n}(-1)^k\binom{n}{k}\mathrm{Tr}\,(A^{n-k}EA^k\rho), \tag{13.10}$$

$$\langle ER\rangle_f = \sum_{n=0}^{\infty}\frac{i^n\gamma^n}{n!}\sum_{k=0}^{n}(-1)^k\binom{n}{k}\mathrm{Tr}\,(A^{n-k}EA^k\rho)\,\overline{F^{n-k}RF^k}. \tag{13.11}$$

Correspondingly, the expansions (3.16) hold now with the changes [cf. Eq. (5.1)]

$$|\langle\phi|\psi\rangle|^2 \rightarrow \mathrm{Tr}\,(E\rho), \tag{13.12a}$$

$$(A^k)_w(A^l)^*_w \rightarrow A_w^{(k,l)} \equiv \frac{\mathrm{Tr}\,(A^lEA^k\rho)}{\mathrm{Tr}\,(E\rho)} \qquad (k,l\geq 0). \tag{13.12b}$$

In the first order in γ, Eqs. (13.3), (13.9), and (13.10) yield the linear-response result (4.13), where in the present general case the weak value is given by

$$A_w = \frac{\mathrm{Tr}\,(EA\rho)}{\mathrm{Tr}\,(E\rho)}. \tag{13.13}$$

Equation (13.13) follows from Eq. (13.12b), on taking into account that $A_w = A_w^{(1,0)}$. The real part of the weak value (13.13) was obtained in Ref. [106]. Note, however, that the real part of A_w is generally not sufficient to describe the linear response (4.13). Equation (13.13) was obtained in Ref. [92] and discussed in Ref. [114].

It is easy to show that A_w is a usual value, when any two of the operators $\hat{A}$, ρ, and E commute, since then A_w is an average of $\hat{A}$,

$$A_w = \mathrm{Tr}\,(A\rho'), \tag{13.14}$$

where ρ' is given by Eq. (13.5). This situation involves two different cases:
(a) When E or ρ commutes with $\hat{A}$, the results of PPS and standard measurements coincide (see Sec. 13.2), Eq. (13.14) being a consequence of this fact. This case involves paragraphs *c.*, *e.*, and *f.* in Sec. 1.5.2 as its special cases.
(b) The case, when E and ρ commute, is an extension of paragraphs *a.* and *b.* in Sec. 1.5.2.

As shown above, in the nonlinear theory of weak PPS measurements, in addition to the weak value, one needs another parameter related to A, the associated weak value $A_w^{(1,1)}$. As follows from Eq. (13.12b), in the general case

$$A_w^{(1,1)} = \frac{\mathrm{Tr}\,(AEA\rho)}{\mathrm{Tr}\,(E\rho)}. \tag{13.15}$$

13.4. Time-symmetry properties for PPS measurements of any strength

A time-symmetry relation for measurements in ensembles of special types was discussed in the last paragraph of Sec. 13.2. Here we consider a more general time-symmetry property.

The expansions (3.16) with the changes (13.12) imply a time-symmetry property for PPS measurements of any strength. Namely, it is easy to see that

$$A_w^{(k,l)} \rightarrow (A_w^{(k,l)})^* = A_w^{(l,k)}, \tag{13.16}$$

under the simultaneous substitutions

$$\rho \rightarrow \frac{E}{\mathrm{Tr}\,E}, \qquad E \rightarrow e_1\rho. \tag{13.17}$$

Here e_1 is any positive number such that $e_1\rho$ is an allowed POVM operator. As implied by Eq. (1.6), this means that the maximal eigenvalue of $e_1\rho$ should not exceed one; hence,

$$0 < e_1 \leq \lambda_{\max}^{-1}, \tag{13.18}$$

where $\lambda_{\max}$ is the maximal eigenvalue of ρ.

Consider the important case when the pre- and post-selected states are pure. Then $\rho = \Pi_\psi \equiv |\psi\rangle\langle\psi|$ and $E = e_0\Pi_\phi$ $(0 < e_0 \leq 1)$ and the time-symmetry relation (13.17) becomes

$$\rho = \Pi_\psi \;\rightarrow\; \Pi_\phi, \qquad E = e_0\Pi_\phi \;\rightarrow\; e_1\Pi_\psi. \tag{13.19}$$

Strictly speaking, when $e_0 \neq 1$, the POVM operator $E = e_0\Pi_\phi$ is not a projector, but still the post-selection state is $|\phi\rangle$. In other words, generally there is no one-to-one correspondence between the pure state of the system after a measurement and the POVM operator, unless it is stipulated that the POVM operator is a projector. Equation (13.19) is equivalent to the relation

$$|\psi\rangle \;\leftrightarrow\; |\phi\rangle. \tag{13.20}$$

Thus, in the case of pure pre- and post-selected states, the time-symmetry relation is conceptually simple: Eq. (13.16) holds under the exchange of the pre- and post-selected states. This is an extension of the time-symmetry relation for strong PPS measurements [66–68] (see Sec. 1.3.2).

When the preselected state is mixed and/or $E \neq e_0\Pi_\phi$, then the quantities which are exchanged in the time-symmetry relation (13.17) are, with the accuracy to numerical factors, the preselected state ρ and the post-selection POVM operator E, rather than pre- and post-selected states, as one might expect. To understand this, we note that the density matrix ρ, on one hand, and the final-measurement outcome corresponding to the post-selection together with the respective POVM operator E, on the other hand, provide the complete information about the preselection and the post-selection, respectively, which is needed to determine a given PPS ensemble. In contrast, the state of the system after the post-selection generally cannot be used to characterize a PPS ensemble, since for a general post-selection measurement it depends on the evolution (e.g., a measurement) in the interval between the preselection and postselection.

For weak PPS measurements the above time-symmetry property means that the weak value and the associated weak value satisfy the relations [cf. Eq. (13.16)]

$$A_w \;\rightarrow\; A_w^*, \qquad A_w^{(1,1)} \;=\; \text{invariant} \tag{13.21}$$

under the simultaneous substitutions (13.17). Consider a simple example. When both pre- and post-selected states are pure, the symmetry relations (13.21) and (13.20) yield

$$A_w \;\rightarrow\; A_w^* \qquad \text{for} \quad |\psi\rangle \;\leftrightarrow\; |\phi\rangle. \tag{13.22}$$

This relation follows also from Eq. (1.36).

Equation (13.16) shows that the substitutions (13.17) generally change the results of PPS measurements. Still, strong PPS measurements are not affected by the change (13.17), as implied by Eq. (1.20). In contrast, Eq. (13.21) implies that the results of weak PPS measurements generally are changed by the substitutions (13.17), unless A_w is real.

13.5. A pure preselected state

Consider an important situation when in a weak PPS measurement the preselected state is pure, $\rho = |\psi\rangle\langle\psi|$, but the post-selection measurement is general. As mentioned above, such a situation may arise, e.g., when measurement errors are to be taken into account.

Now the weak values (13.13) and (13.15) become

$$A_w = \frac{(EA)_{\psi\psi}}{E_{\psi\psi}}, \qquad A_w^{(1,1)} = \frac{(AEA)_{\psi\psi}}{E_{\psi\psi}}. \tag{13.23}$$

There is an important relation between the present situation and the case of a mixed preselected state and a pure post-selected state. Indeed, the weak values (1.58) and (5.4) are connected to the formulas (13.23) by the relation (13.21) under the substitutions

$$\rho \;\rightarrow\; \frac{E}{\operatorname{Tr} E}, \qquad |\phi\rangle \;\rightarrow\; |\psi\rangle. \tag{13.24}$$

This relation allows one to use results of preceding sections in the present case. Namely, in the present situation the nonlinear equations (5.2) and (5.3) hold provided the definitions (13.23) are used. Moreover, the other results obtained above for the case of a mixed preselected state (see especially Secs. 5 and 9 and Fig. 12) are also valid now, with the accuracy to the substitutions (13.24).

14. Conclusion

Weak pre- and post-selected measurements are important for studies of the fundamentals of quantum mechanics. They also hold promise for precision metrology, since they provide significant amplification of the pointer deflection in comparison to standard weak measurements. This paper starts with a review of strong and weak PPS measurements (Sec. 1). Afterwards, we present original contributions, which generalize previous theoretical work.

In particular, a nonperturbative theory of weak PPS measurements is developed. The theory is applicable to an arbitrary quantum system and an arbitrary meter, with arbitrary initial states for both of them. The results are expressed in a simple analytical form. We have shown that weak values and the coupling strength can be measured not only in the linear regime, as was done previously, but also in two other regimes: the strongly-nonlinear regime and the inverted region (i.e., the limit of very large weak values, where the overlap of the pre- and post-selected states is very small). We have verified our theory by showing that the optical experiment in Ref. [133] can be described quantum-mechanically as a weak PPS measurement in the regime of large weak values.

Optimal conditions for measurements are obtained in the strongly nonlinear regime, since there the pointer deflection is generally of the order of the maximum value. Correspondingly, under optimal conditions, the amplification is stronger than in the linear regime by at least an order of magnitude. The nonlinear regime can be achieved only for anomalously large weak values, which implies the requirement that the overlap of the pre- and post-selected states is small. The optimal conditions are obtained when the above overlap is of the order of the small parameter of the theory.

We have revealed that in the nonlinear regime weak PPS measurements significantly depend on the value of $\bar{F}$. In particular, a nonzero $\bar{F}$ may facilitate measurements of weak values (Sec. 4.7.5) and the coupling strength γ (Sec. 7.2.3). Moreover, the optimal regime of measurements is qualitatively different for $|\bar{F}| \lesssim \Delta F$ and for $|\bar{F}| \gg \Delta F$. In the latter case, the optimal conditions are much stricter, but the amplification is much stronger, than for $|\bar{F}| \lesssim \Delta F$. This increase of the amplification may result in an increased measurement precision. The optimal regime for $|\bar{F}| \gg \Delta F$ is very sensitive to small perturbations of several parameters; this property can be used for various precision measurements. We have indicated experimental schemes where $\bar{F}$ is nonzero and tunable.

We have derived exact solutions for PPS measurements of a qubit with several types of meters and, using these solutions, verified the present theory by numerical calculations. The present theory can be verified experimentally in many types of physical systems, including optical experiments and experiments with qubits. Moreover, the present results can be applied to improve the accuracy of precision measurements. In particular, the present theory can be applied to existing experimental setups, such as those in Refs. [80, 83–86, 133], where using the optimal regime can increase the amplification by, at least, an order of magnitude.

In recent years, research on weak PPS measurements and weak values has been expanding with an increasing rate. In spite of an initial controversy, weak values have demonstrated to be a fruitful concept both for fundamental studies and for designing novel experimental techniques. Potential applications of weak values include such diverse topics as optical communications and quantum information processing. The general theory of weak PPS measurements developed here will hopefully provide insights and a useful guide for further applications of weak values.

Acknowledgements

We thank S. A. Gurvitz for fruitful discussions. FN gratefully acknowledges partial support from the Laboratory of Physical Sciences, National Security Agency, Army Research Office, DARPA, AFOSR, National Science Foundation under Grant No. 0726909, JSPS-RFBR under Contract No. 09-02-92114, Grant-in-Aid for Scientific Research (S), MEXT Kakenhi on Quantum Cybernetics, and the Funding Program for Innovative R&D on S&T (FIRST).

Appendix A Gauge invariance of PPS measurements

Here we discuss the invariance properties of PPS measurements (with arbitrary measurement strength) under unitary transformations of the system and meter.

A.1 System transformations

Equation (3.9) shows that $\bar{R}_s - \bar{R}$ is independent of $\bar{R}$ (at least, for $R \neq F$). In contrast, as shown by Eq. (4.11) or (5.2), $\bar{R}_s - \bar{R}$ depends on $\bar{F}$. However, it is easy to see that $\bar{R}_s$ in Eqs. (3.7) and (3.9) is invariant under a "gauge" transformation

$$\hat{F} \;\to\; \hat{F}' = \hat{F} - F_0, \tag{A.1}$$

where F_0 is a real number, if simultaneously the pre- and post-selected states undergo unitary transformations,

$$\rho \;\to\; \exp(-i\gamma' F_0 \hat{A})\,\rho\,\exp(i\gamma' F_0 \hat{A}), \tag{A.2}$$

$$|\phi\rangle \;\to\; |\phi'\rangle = \exp(i\gamma'' F_0 \hat{A})\,|\phi\rangle, \tag{A.3}$$

where γ' and γ'' are real numbers satisfying $\gamma' + \gamma'' = \gamma$. Note that one can choose $\gamma' = \gamma$ (or $\gamma'' = \gamma$) and $\gamma'' = 0$ ($\gamma' = 0$), leaving thus $|\phi\rangle$ (or ρ) without a change. In particular, for $\gamma' = \gamma$ and $\gamma'' = 0$ the transformation (A.2)-(A.3) reduces to the change of the initial state,

$$\rho \;\to\; \exp(-i\gamma F_0 \hat{A})\,\rho\,\exp(i\gamma F_0 \hat{A}). \tag{A.4}$$

The transformation (A.1)-(A.3) allows one to change $\bar{F}$ according to

$$\bar{F} \;\to\; \bar{F}' = \bar{F} - F_0, \tag{A.5}$$

where F_0 is an arbitrary real number.

A.2 Meter transformations

Consider the invariance of the average pointer deflection under a "gauge" transformation of the meter. It is easy to see that Eq. (3.9) yields

$$\bar{R}_s - \bar{R} \;=\; \bar{\tilde{R}}_s - \bar{\tilde{R}} \tag{A.6}$$

under the transformation of the initial state and the pointer variable,

$$\rho_{\mathrm{M}} \;\to\; \tilde{U}_{\mathrm{M}}\,\rho_{\mathrm{M}}\,\tilde{U}^{\dagger}_{\mathrm{M}}, \qquad \hat{R} \;\to\; \hat{\tilde{R}} = \tilde{U}^{\dagger}_{\mathrm{M}}\,\hat{R}\,\tilde{U}_{\mathrm{M}} + C, \tag{A.7}$$

where $\tilde{U}_{\mathrm{M}}$ is a unitary operator commuting with $\hat{F}$ and C is a real constant. When $C = 0$, then not only $\bar{R}_s - \bar{R}$ but also $\bar{R}_s$ and $\bar{R}$ individually are invariant under the change (A.7).

For example, if $F = p$ and $R = q$, one can use in Eq. (A.7) operators of the form

$$\tilde{U}_{\mathrm{M}} = \exp[-i\zeta_0(p)], \tag{A.8}$$

where $\zeta_0(p)$ is an arbitrary real function of p. In this case, Eq. (A.7) implies

$$\tilde{R} = q + \zeta_0'(p) + C, \tag{A.9}$$

where the prime denotes the differentiation with respect to p.

Appendix B Operator identities

Here we prove several operator identities used in the present paper. To begin with, we derive a formula for n consecutively embedded commutators,

$$\underbrace{[D, \ldots [D,}_{n} C \underbrace{\,] \ldots]}_{n} = \sum_{k=0}^{n} a_{nk}\, D^{n-k} C D^{k}, \tag{B.1}$$

where the coefficients a_{nk} are to be determined. It is easy to see that the latter satisfy the recursive formula $a_{n+1,k} = a_{nk} - a_{n,k-1}$, which by the change

$$a_{nk} = (-1)^k\, a'_{nk} \tag{B.2}$$

becomes

$$a'_{n+1,k} = a'_{nk} + a'_{n,k-1} \qquad (0 \le k \le n+1;\ n \ge 1) \tag{B.3}$$

with $a'_{n,-1} = a'_{n,n+1} = 0$. As follows from Eq. (B.1) with $n = 1$ and Eq. (B.2),

$$a'_{10} = a'_{11} = 1. \tag{B.4}$$

Equation (B.3) with the initial conditions (B.4) has a unique solution given by the binomial coefficients [148], $a'_{nk} = \binom{n}{k}$. Combining the latter formula with Eqs. (B.2) and (B.1) yields finally Eq. (3.12).

Now let us prove the following operator identities. Let O_S and O'_S (O_M and O'_M) be arbitrary operators in the Hilbert space $\mathcal{H}_\mathrm{S}$ ($\mathcal{H}_\mathrm{M}$) of system S (M), whereas O and O' are operators in the Hilbert space $\mathcal{H}_\mathrm{S} \otimes \mathcal{H}_\mathrm{M}$. If O and O' can be written as the sums

$$O = \sum_i O_{\mathrm{S}i} \otimes O_{\mathrm{M}i}, \quad O' = \sum_j O'_{\mathrm{S}j} \otimes O'_{\mathrm{M}j}, \tag{B.5}$$

where $O_{\mathrm{S}i}$, $O'_{\mathrm{S}j}$, and either $O_\mathrm{S} \otimes I_\mathrm{M}$ or $O'_\mathrm{S} \otimes I_\mathrm{M}$ commute pairwise for all i and j, then the following identities hold

$$\begin{aligned}\mathrm{Tr}\,[(O_\mathrm{S} \otimes O_\mathrm{M})O(O'_\mathrm{S} \otimes O'_\mathrm{M})O'] &= \mathrm{Tr}\,[(I_\mathrm{S} \otimes O_\mathrm{M})O(O_\mathrm{S}O'_\mathrm{S} \otimes O'_\mathrm{M})O'] \\ &= \mathrm{Tr}\,[(I_\mathrm{S} \otimes O_\mathrm{M})O(O'_\mathrm{S}O_\mathrm{S} \otimes O'_\mathrm{M})O'], \\ &= \frac{1}{2}\mathrm{Tr}\,[(I_\mathrm{S} \otimes O_\mathrm{M})O((O_\mathrm{S}O'_\mathrm{S} + O'_\mathrm{S}O_\mathrm{S}) \otimes O'_\mathrm{M})O'].\end{aligned} \tag{B.6}$$

Note that the above validity conditions for Eq. (B.6) imply that either $O_\mathrm{S} \otimes I_\mathrm{M}$ or $O'_\mathrm{S} \otimes I_\mathrm{M}$ commutes with O and O'. When $O_\mathrm{S} \otimes I_\mathrm{M}$ commutes with O, the first equality in Eq. (B.6) is obvious. Now let us prove the first equality in Eq. (B.6) for the case when O'_S, $O_{\mathrm{S}i}$, and $O'_{\mathrm{S}j}$ commute pairwise. The left-hand side of Eq. (B.6) can be recast as

$$\begin{aligned}&\mathrm{Tr}\,[(O_\mathrm{S} \otimes O_\mathrm{M})O(O'_\mathrm{S} \otimes O'_\mathrm{M})O'] = \sum_{i,j} \mathrm{Tr}\,[(O_\mathrm{S}O_{\mathrm{S}i}O'_\mathrm{S}O'_{\mathrm{S}j}) \otimes (O_\mathrm{M}O_{\mathrm{M}i}O'_\mathrm{M}O'_{\mathrm{M}i'})] \\ &= \sum_{i,i'} \mathrm{Tr}\,(O_\mathrm{S}O_{\mathrm{S}i}O'_\mathrm{S}O'_{\mathrm{S}j})\mathrm{Tr}\,(O_\mathrm{M}O_{\mathrm{M}i}O'_\mathrm{M}O'_{\mathrm{M}i'}) = \sum_{i,i'} \mathrm{Tr}\,(O_{\mathrm{S}i}O_\mathrm{S}O'_\mathrm{S}O'_{\mathrm{S}j})\mathrm{Tr}\,(O_\mathrm{M}O_{\mathrm{M}i}O'_\mathrm{M}O'_{\mathrm{M}i'}).\end{aligned} \tag{B.7}$$

Here in the last equality we used the fact that $O_{\mathrm{S}i}$ commutes with O'_S and $O'_{\mathrm{S}j}$. The substitutions $O_\mathrm{S} \to I_\mathrm{S}$, $O'_\mathrm{S} \to O_\mathrm{S}O'_\mathrm{S}$ change the left-hand side of Eq. (B.7) into the rhs of the first equality in Eq. (B.6) but do not change the rhs of Eq. (B.7), which proves the first equality in Eq. (B.6). The second equality in Eq. (B.6) follows from the fact that either $O_\mathrm{S} \otimes I_\mathrm{M}$ or $O'_\mathrm{S} \otimes I_\mathrm{M}$ commutes with O and O'. For example, when $O'_\mathrm{S} \otimes I_\mathrm{M}$ commutes with O and O', we obtain that

$$\begin{aligned}&\mathrm{Tr}\,[(I_\mathrm{S} \otimes O_\mathrm{M})O(O_\mathrm{S}O'_\mathrm{S} \otimes O'_\mathrm{M})O'] = \mathrm{Tr}\,[(I_\mathrm{S} \otimes O_\mathrm{M})O(O_\mathrm{S} \otimes O'_\mathrm{M})O'(O'_\mathrm{S} \otimes I_\mathrm{M})] \\ &= \mathrm{Tr}\,[(O'_\mathrm{S} \otimes I_\mathrm{M})(I_\mathrm{S} \otimes O_\mathrm{M})O(O_\mathrm{S} \otimes O'_\mathrm{M})O'] = \mathrm{Tr}\,[(I_\mathrm{S} \otimes O_\mathrm{M})O(O'_\mathrm{S}O_\mathrm{S} \otimes O'_\mathrm{M})O'].\end{aligned} \tag{B.8}$$

Finally, the third equality in Eq. (B.6) follows from the previous equality.

As an example, consider the case when $O = U$, $O' = U^\dagger$, and O_S or O'_S commutes with $\hat{A}$. Here U is given by Eq. (1.10). In this case, the sums of the form (B.5) are obtained by expanding U and $U^\dagger$ in powers of γ, yielding

$$O'_{\mathrm{M}j} = O_{\mathrm{M}j} = \hat{A}^j \qquad (j \ge 0). \tag{B.9}$$

Thus, the validity conditions for Eq. (B.6) hold now. Consequently, when either O_S or O'_S commutes with $\hat{A}$, we obtain the identities

$$\mathrm{Tr}\,[(O_\mathrm{S} \otimes O_\mathrm{M})U(O'_\mathrm{S} \otimes O'_\mathrm{M})U^\dagger] = \mathrm{Tr}\,[(I_\mathrm{S} \otimes O_\mathrm{M})U(O_\mathrm{S}O'_\mathrm{S} \otimes O'_\mathrm{M})U^\dagger], \tag{B.10}$$

$$\mathrm{Tr}\,[(O_\mathrm{S} \otimes O_\mathrm{M})U(O'_\mathrm{S} \otimes O'_\mathrm{M})U^\dagger] = \frac{1}{2}\mathrm{Tr}\,[(I_\mathrm{S} \otimes O_\mathrm{M})U((O_\mathrm{S}O'_\mathrm{S} + O'_\mathrm{S}O_\mathrm{S}) \otimes O'_\mathrm{M})U^\dagger]. \tag{B.11}$$

Appendix C Estimation of moments of meter variables

In the present Appendix, Sec. C.2, we estimate the magnitude of the moments $\overline{F^k R_c F^{n-k}}$ $(0 \le k \le n)$ for a system in a mixed state [cf. Eq. (5.6)]

$$\rho_{\mathrm{M}} = \sum_i \tilde{\lambda}_i \, |\tilde{\psi}_i\rangle \, \langle\tilde{\psi}_i|, \tag{C.1}$$

where $\langle\tilde{\psi}_i|\tilde{\psi}_j\rangle = \delta_{ij}$, $\tilde{\lambda}_i \ge 0$, and $\sum_i \tilde{\lambda}_i = 1$. Before this, in Sec. C.1, we derive the generalized uncertainty relation for a quantum system in a mixed state and prove several inequalities required in Sec. C.2.

C.1 Generalized uncertainty relation

First, we prove the following useful inequality for arbitrary operators O_1 and O_2,

$$|\,\overline{O_1 O_2}\,|^2 \;\le\; \overline{O_1 O_1^\dagger}\;\, \overline{O_2^\dagger O_2}. \tag{C.2}$$

When the averages here are taken over a pure state, Eq. (C.2) was shown to be a direct consequence of the Cauchy-Schwarz inequality for Hermitian O_1 and O_2 in Ref. [146] and for general non-Hermitian O_1 and O_2 in Ref. [23]. Here we extend Eq. (C.2) to the case of a general mixed state (C.1), by writing

$$\begin{aligned}
|\,\overline{O_1 O_2}\,|^2 \;&=\; |\mathrm{Tr}\,(O_1 O_2 \,\rho_{\mathrm{M}})|^2 \;=\; \left|\sum_i \tilde{\lambda}_i \langle\tilde{\psi}_i|O_1 O_2|\tilde{\psi}_i\rangle\right|^2 \;\le\; \left(\sum_i \tilde{\lambda}_i |\langle\tilde{\psi}_i|O_1 O_2|\tilde{\psi}_i\rangle|\right)^2 \\
&\le\; \left[\sum_i \tilde{\lambda}_i (\langle\tilde{\psi}_i|O_1 O_1^\dagger|\tilde{\psi}_i\rangle \langle\tilde{\psi}_i|O_2^\dagger O_2|\tilde{\psi}_i\rangle)^{1/2}\right]^2 \;\le\; \sum_i \tilde{\lambda}_i \langle\tilde{\psi}_i|O_1 O_1^\dagger|\tilde{\psi}_i\rangle \sum_j \tilde{\lambda}_j \langle\tilde{\psi}_j|O_2^\dagger O_2|\tilde{\psi}_j\rangle \\
&=\; \overline{O_1 O_1^\dagger}\;\, \overline{O_2^\dagger O_2},
\end{aligned} \tag{C.3}$$

which proves Eq. (C.2) for the general case. In Eq. (C.3) the second inequality follows from Eq. (C.2) for a pure state, and the third inequality results from the Cauchy-Schwarz inequality.

The inequality (C.2) implies that

$$|\,\overline{R_c F_c^l}\,|^2 \;\le\; \overline{R_c^2}\;\overline{F_c^{2l}} \qquad (l \ge 1). \tag{C.4}$$

Equation (C.4) with $l = 1$ yields the generalized uncertainty relation for the variables F and R [see also Eq. (4.19)]

$$|\,\overline{R_c\, F_c}\,| \;\le\; \Delta R\, \Delta F. \tag{C.5}$$

The generalized uncertainty relation (C.5) [or Eq. (4.19)] was derived by Schrödinger [146] for pure states (see also Refs. [145, 149]). Here it is proved for arbitrary (pure or mixed) states.

Combining Eqs. (4.3) and (C.4) results in the relation

$$|\,\overline{F_c^l\, R_c}\,| \;=\; |\,\overline{R_c\, F_c^l}\,| \;\lesssim\; \Delta R\,(\Delta F)^l \qquad (l \ge 1). \tag{C.6}$$

Using the relation

$$|\,\overline{F^n R_c}\,| \;=\; |\,\overline{(F_c + \bar{F})^n R_c}\,| \;\le\; \sum_{l=0}^{n} \binom{n}{l} |\bar{F}^{n-l}\, \overline{F_c^l R_c}\,| \tag{C.7}$$

and Eq. (C.6), we obtain

$$|\,\overline{F^n\, R_c}\,| \;=\; |\,\overline{R_c\, F^n}\,| \;\lesssim\; \Delta R\, \Delta F\, (\Delta F + |\bar{F}|)^{n-1} \qquad (n \ge 1). \tag{C.8}$$

C.2 Estimating the moments

Let us now estimate the magnitude of the moments $\overline{F^k R_c F^{n-k}}$ $(0 \le k \le n)$.

We begin with the important case of canonically conjugate variables F and R, where the calculation is simple. Indeed, using the commutation relation $\hat{R}_c \hat{F} = \hat{F}\hat{R}_c \pm i$, we can move $\hat{R}_c$ to the last place in the product $\hat{F}^k \hat{R}_c \hat{F}^{n-k}$, so that

$$|\overline{F^k R_c F^{n-k}}| \lesssim |\overline{F^{n-1}}| + |\overline{F^n R_c}| \lesssim \Delta R\, \Delta F\, (|\bar{F}| + \Delta F)^{n-1}. \tag{C.9}$$

Here in the last inequality we used Eqs. (C.8), (4.4), and the Heisenberg uncertainty relation $\Delta R\, \Delta F \ge 1/2$.

In the case when F and R are not canonically conjugate, we use the equality $F = \bar{F} + F_c$ to write that

$$\overline{F^k R_c F^{n-k}} = \sum_{l=0}^{k} \sum_{m=0}^{n-k} \binom{k}{l} \binom{n-k}{m} \bar{F}^{n-l-m}\, \overline{F_c^l R_c F_c^m}. \tag{C.10}$$

This reduces the problem to the estimation of the moments $\overline{F_c^k R_c F_c^{n-k}}$ where $0 \le k \le n$.

When $\Delta R = 0$ (i.e., when ρ_{M} is an eigenstate of $\hat{R}$ or a mixture of eigenstates of $\hat{R}$ with the same eigenvalue), the moments $\overline{F_c^l R_c}$ and $\overline{R_c F_c^l}$ vanish, at least, when $\hat{R}$ has a discrete spectrum.[6] In contrast, the moments $\overline{F_c^l R_c F_c^m}$ with $l, m \ge 1$ generally do not vanish in the limit $\Delta R \to 0$. To proceed further, we make the simplifying assumption

$$\max_{1 \le l \le m-1} |\overline{F_c^l R_c F_c^{m-l}}| \sim \tilde{R}\, (\Delta F)^m, \tag{C.11}$$

where $\tilde{R}$ does not depend very significantly on m and generally does not vanish in the limit $\Delta R \to 0$. With the help of Eqs. (C.6) and (C.11), the quantity (C.10) can be estimated by the relation

$$|\overline{F^k R_c F^{n-k}}| \lesssim \Delta R\, \Delta F\, \bar{F}^{k'} (|\bar{F}| + \Delta F)^{n-k'-1} + \tilde{R}\, (\Delta F)^2 (|\bar{F}| + \Delta F)^{n-2} \qquad (1 \le k \le n-1), \tag{C.12}$$

where $k' = \min\{k, n-k\}$.

Equation (C.12) is equivalent to two simpler inequalities, which are obtained in two possible cases. First, in a typical situation, when ΔR is not too small, Eqs. (C.12) and (C.8) yield for $0 \le k \le n$

$$|\overline{F^k R_c F^{n-k}}| \lesssim \Delta R\, \Delta F\, (|\bar{F}| + \Delta F)^{n-1} \quad (\Delta R \gtrsim \tilde{R}), \tag{C.13}$$

which coincides with the estimate (C.9) for canonically conjugate F and R. Second, when ΔR vanishes or is very small, the first term on the rhs of Eq. (C.12) can be neglected, yielding

$$|\overline{F^k R_c F^{n-k}}| \lesssim \tilde{R}\, (\Delta F)^2\, (|\bar{F}| + \Delta F)^{n-2} \quad (\Delta R \ll \tilde{R}) \tag{C.14}$$

for $1 \le k \le n-1$, whereas $|\overline{F^n R_c}| = |\overline{R_c F^n}|$ are zero or negligibly small [cf. Eq. (C.8)].

In either case (C.13) or (C.14), the terms of orders higher than two in Eq. (3.16a) can be neglected under the condition (4.5), when, at least, one of the two following cases takes place:

(a) The quadratic term in Eq. (3.16a) is not anomalously small, i.e., $\overline{F R_c F}$ is of the order of the rhs of Eq. (C.13) or (C.14) with $n = 2$.

(b) The first-order term in Eq. (3.16a) is not anomalously small, i.e., it is of order $|\gamma A_{\phi\psi}|\, \Delta R\, \Delta F$. Then, even when the quadratic term is vanishing or small, it can be shown that under the condition (4.5) the contribution of the third- and higher-order terms into the pointer deflection (3.9) is negligibly small, except for the unimportant case when the quadratic term in $\langle \Pi_\phi \rangle_f$ becomes very large, making the pointer deflection (3.9) negligibly small.

(Moreover, it is assumed above in this paragraph that the first- and second-order terms do not cancel each other.)

When the first- and second-order terms in Eq. (3.16a) vanish or are anomalously small or cancel each other, the validity condition (4.5) may be inapplicable. However, generally such cases are of little interest, since then the pointer deflection is very small.

Appendix D Calculation of moments for canonically conjugate variables

Here we derive formulas for moments of canonically conjugate variables used in the main text. Let $G(p)$ be an arbitrary function, such that the integrals below in Eq. (D.2) converge and that

$$\lim_{p\to\pm\infty} G(p)\,\psi_{\mathrm{M}}(p) = 0. \tag{D.1}$$

Using the expression $q = i\partial/\partial p$ and Eq. (7.11), we obtain that

$$\begin{aligned}\overline{G(p)\,q\,G(p)} &= (2\pi)^{-1}\int_{-\infty}^{\infty} dp\,\psi^*_{\mathrm{M}}(p)\,G(p)i[G(p)\,\psi_{\mathrm{M}}(p)]' \\ &= (2\pi)^{-1}\int_{-\infty}^{\infty} dp\; f_p(p)\,G(p)\,\{i[G(p)\;f_p(p)]' + \zeta'(p)\,G(p)\;f_p(p)\} \\ &= i(4\pi)^{-1}[G(p)\;f_p(p)]^2|_{-\infty}^{\infty} + (2\pi)^{-1}\int_{-\infty}^{\infty} dp\; f_p^2(p)\,G^2(p)\,\zeta'(p),\end{aligned} \tag{D.2}$$

where the prime denotes differentiation over p. The first term in the last expression in Eq. (D.2) vanishes in view of Eq. (D.1), and we obtain that

$$\overline{G(p)\,q\,G(p)} \;=\; \overline{\zeta'(p)G^2(p)}. \tag{D.3}$$

In particular, Eq. (D.3) implies the formulas (7.22) and (7.15), whereas Eqs. (D.3) and (7.15) imply the first two lines in Eq. (10.15).

In a similar fashion, it is not difficult to obtain that

$$K(\chi_1,\chi_2) \;\equiv\; \overline{\exp(i\chi_1 p)\,q\,\exp(i\chi_2 p)} \;=\; \overline{[(\chi_1-\chi_2)/2 + \zeta'(p)]\,\exp[i(\chi_1+\chi_2)p]}. \tag{D.4}$$

The characteristic function $K(\chi_1,\chi_2)$ provides linear in q mixed moments of p and q by

$$\overline{p^n\,q\,p^m} \;=\; (-i)^{n+m}\,\frac{\partial^{n+m}K(\chi_1,\chi_2)}{\partial\chi_1^n\,\partial\chi_2^m}\bigg|_{\chi_1=\chi_2=0}. \tag{D.5}$$

Equation (D.4) implies that

$$\overline{\cos(\gamma p)\,q\,\sin(\gamma p)} \;=\; \frac{K(\gamma,\gamma) - K(\gamma,-\gamma) + K(-\gamma,\gamma) - K(-\gamma,-\gamma)}{4i}. \tag{D.6}$$

Equations (D.6) and (D.4) yield the third line of Eq. (10.15).

It is easy to check that the expressions for averages of functions of p and q derived above hold also under the simultaneous replacements

$$q \;\leftrightarrow\; p, \qquad \zeta(p) \;\to\; \xi(q). \tag{D.7}$$

In particular, Eqs. (D.3)-(D.5) yield respectively

$$\overline{G(q)\,p\,G(q)} \;=\; \overline{\xi'(q)G^2(q)}, \tag{D.8}$$

$$\tilde{K}(\chi_1,\chi_2) \;\equiv\; \overline{\exp(i\chi_1 q)\,p\,\exp(i\chi_2 q)} \;=\; \overline{[(\chi_1-\chi_2)/2 + \xi'(q)]\,\exp[i(\chi_1+\chi_2)q]}, \tag{D.9}$$

$$\overline{q^n\,p\,q^m} \;=\; (-i)^{n+m}\,\frac{\partial^{n+m}\tilde{K}(\chi_1,\chi_2)}{\partial\chi_1^n\,\partial\chi_2^m}\bigg|_{\chi_1=\chi_2=0}. \tag{D.10}$$

Equation (D.8) implies Eq. (7.16). Taking into account that $\overline{\{q,p\}} = 2\mathrm{Re}\,\overline{qp}$, Eq. (D.5) calculated for $n=0, m=1$ and Eq. (D.10) with $n=1, m=0$ yield Eq. (7.12).

References

[1] J. von Neumann, Mathematical Foundations of Quantum Mechanics, Princeton University, Princeton, NJ, 1955.
[2] J. A. Wheeler, W. H. Zurek (Eds.), Quantum Theory and Measurement, Princeton University, Princeton, NJ, 1983.
[3] V. B. Braginsky, F. Y. Khalili, Quantum Measurement, Cambridge University Press, 1992.
[4] H. M. Wiseman, G. J. Milburn, Quantum Measurements and Control, Cambridge University Press, 2010.
[5] M. Schlosshauer, Decoherence, the measurement problem, and interpretations of quantum mechanics, Rev. Mod. Phys. 76 (2004) 1267–1305.
[6] V. Giovannetti, S. Lloyd, L. Maccone, Quantum-enhanced measurements: Beating the standard quantum limit, Science 5700 (2004) 1330–1336.
[7] J. A. Dunningham, Using quantum theory to improve measurement precision, Contemp. Phys. 47 (2006) 257–267.
[8] M. A. Nielsen, I. L. Chuang, Quantum Computation and Quantum Information, Cambridge University Press, 2000.
[9] J. Q. You, F. Nori, Superconducting circuits and quantum information, Physics Today 58 (11) (November, 2005) 42–47.
[10] I. Buluta, F. Nori, Quantum simulators, Science 326 (2009) 108.
[11] K. Maruyama, F. Nori, V. Vedral, Physics of Maxwell's demon and information, Rev. Mod. Phys. 81 (2009) 1.
[12] S. N. Shevchenko, S. Ashhab, F. Nori, Landau-Zener-Stuckelberg interferometry, Phys. Rep. 492 (2010) 1.
[13] J. Q. You, F. Nori, Atomic physics and quantum optics using superconducting circuits, Nature 474 (2011) 589.
[14] I. Buluta, S. Ashhab, F. Nori, Natural and artificial atoms for quantum computation, Rep. Progr. Phys., in press (September 2011); arXiv:1002.1871v2.
[15] J. Ma, X. Wang, C. P. Sun, F. Nori, Quantum spin squeezing, Phys. Rep., in press (2011); arXiv:1011.2978v2.
[16] I. Georgescu, F. Nori, Quantum simulations, preprint (2011).
[17] P. D. Nation, J. R. Johansson, M. P. Blencowe, F. Nori, Stimulating uncertainty: Amplifying the quantum vacuum with superconducting circuits, Rev. Mod. Phys., in press (2011); arXiv:1103.0835.
[18] J. S. Bell, On the Einstein Podolsky Rosen paradox, Physics 1 (1964) 195–200.
[19] A. Aspect, Bell's theorem : The naive view of an experimentalist, in: R. A. Bertlmann, A. Zeilinger (Eds.), Quantum [Un]speakables – From Bell to Quantum Information, Springer, 2002, pp. 119–153.
[20] M. Ansmann, H. Wang, R. C. Bialczak, M. Hofheinz, E. Lucero, M. Neeley, A. D. O'Connell, D. Sank, M. Weides, J. Wenner, A. N. Cleland, J. M. Martinis, Violation of Bell's inequality in Josephson phase qubits, Nature 461 (2009) 504–506.
[21] L. F. Wei, Y. X. Liu, F. Nori, Testing Bell's inequality in constantly coupled Josephson circuits by effective single-qubit operations, Phys. Rev. B 72 (2005) 104516.
[22] L. F. Wei, Y. X. Liu, M. J. Storcz, F. Nori, Macroscopic Einstein-Podolsky-Rosen pairs in superconducting circuits, Phys. Rev. A 73 (2006) 052307.
[23] A. G. Kofman, A. N. Korotkov, Analysis of Bell inequality violation in superconducting phase qubits, Phys. Rev. B 77 (2008) 104502.
[24] Y. Aharonov, D. Z. Albert, L. Vaidman, How the result of a measurement of a component of the spin of a spin-1/2 particle can turn out to be 100, Phys. Rev. Lett. 60 (1988) 1351–1354.
[25] B. Misra, E. C. G. Sudarshan, Zeno's paradox in quantum theory, J. Math. Phys. 18 (1977) 756–763.
[26] W. M. Itano, D. J. Heinzen, J. J. Bollinger, D. J. Wineland, Quantum Zeno effect, Phys. Rev. A 41 (1990) 2295–2300.
[27] A. G. Kofman, G. Kurizki, Quantum Zeno effect on atomic excitation decay in resonators, Phys. Rev. A 54 (1996) R3750–R3753.
[28] S. A. Gurvitz, Measurements with a noninvasive detector and dephasing mechanism, Phys. Rev. B 56 (1997) 15215–15223.
[29] A. G. Kofman, G. Kurizki, Acceleration of quantum decay processes by frequent observations, Nature 405 (2000) 546–550.
[30] M. C. Fischer, B. Gutierrez-Medina, M. G. Raizen, Observation of the quantum Zeno and anti-Zeno effects in an unstable system, Phys. Rev. Lett. 87 (2001) 040402.
[31] P. Facchi, H. Nakazato, S. Pascazio, From the quantum Zeno to the inverse quantum Zeno effect, Phys. Rev. Lett. 86 (2001) 2699–2703.
[32] K. Koshino, A. Shimizu, Quantum Zeno effect by general measurements, Phys. Rep. 412 (2005) 191–275.
[33] X.-B. Wang, J. Q. You, F. Nori, Quantum entanglement via two-qubit quantum Zeno dynamics, Phys. Rev. A 77 (2008) 062339.
[34] L. Zhou, S. Yang, Y. X. Liu, C. P. Sun, F. Nori, Quantum Zeno switch for single-photon coherent transport, Phys. Rev. A 80 (2009) 062109.
[35] X. Cao, J. Q. You, H. Zheng, A. G. Kofman, F. Nori, Dynamics and quantum Zeno effect for a qubit in either a low- or high-frequency bath beyond the rotating-wave approximation, Phys. Rev. A 82 (2010) 022119.
[36] Q. Ai, D. Xu, S. Yi, A. G. Kofman, F. N. C. P. Sun, Quantum anti-Zeno effect without wave function reduction, arXiv:1007.4859 (2010).
[37] X. Cao, Q. Ai, C. P. Sun, F. Nori, The transition from quantum Zeno to anti-Zeno effects of a qubit in a cavity by modulating the cavity frequency, arXiv:1011.3862 (2010).
[38] E. Knill, R. Laflamme, G. J. Milburn, A scheme for efficient quantum computation with linear optics, Nature 409 (2001) 46–52.
[39] R. Raussendorf, H. J. Briegel, A one-way quantum computer, Phys. Rev. Lett. 86 (2001) 5188–5191.
[40] R. Raussendorf, D. E. Browne, H. J. Briegel, Measurement-based quantum computation on cluster states, Phys. Rev. A 68 (2003) 022312.
[41] M. A. Nielsen, Cluster-state quantum computation, Rep. Math. Phys. 57 (2006) 147–161.
[42] T. Tanamoto, Y. Liu, S. Fujita, X. Hu, F. Nori, Producing cluster states in charge qubits and flux qubits, Phys. Rev. Lett. 97 (2006) 230501.
[43] J. Q. You, X.-B. Wang, T. Tanamoto, F. Nori, Efficient one-step generation of large cluster states with solid-state circuits, Phys. Rev. A 75 (2007) 052319.
[44] T. Tanamoto, Y. X. Liu, X. Hu, F. Nori, Efficient quantum circuits for one-way quantum computing, Phys. Rev. Lett. 102 (2009) 100501.
[45] H. J. Briegel, D. E. Browne, W. Dür, R. Raussendorf, M. V. den Nest, Measurement-based quantum computation, Nature Phys. 9 (2009) 19–26.
[46] S. Ashhab, F. Nori, Control-free control: Manipulating a quantum system using only a limited set of measurements, Phys. Rev. A 82 (2010) 062103.
[47] H. M. Wiseman, Quantum control: Squinting at quantum systems, Nature 470 (2011) 178–179.
[48] E. B. Davies, Quantum Theory of Open Systems, Academic, 1976.

[49] K. Kraus, States, Effects, and Operations, Springer, 1983.
[50] M. A. Naimark, Spectral functions of a symmetric operator, Izv. Akad. Nauk SSSR Ser. Mat. 4 (1940) 277–318.
[51] K. Banaszek, Fidelity balance in quantum operations, Phys. Rev. Lett. 86 (2001) 1366–1369.
[52] V. P. Belavkin, P. Staszevski, Nondemolition observation of a free quantum particle, Phys. Rev. A 45 (1992) 1347–1356.
[53] A. Barchielli, Stochastic differential-equations and a posteriori states in quantum-mechanics, Int. J. Theor. Phys. 32 (1993) 2221–2233.
[54] J. Dalibard, Y. Castin, K. Mølmer, Wave-function approach to dissipative processes in quantum optics, Phys. Rev. Lett. 68 (1992) 580–583.
[55] C. W. Gardiner, A. S. Parkins, P. Zoller, Wave-function quantum stochastic differential-equations and quantum-jump simulation methods, Phys. Rev. A 46 (1992) 4363–4381.
[56] H. J. Carmichael, An Open Systems Approach to Quantum Optics, Springer, Berlin, 1993.
[57] A. N. Korotkov, Continuous quantum measurement of a double dot, Phys. Rev. B 60 (1999) 5737–5742.
[58] D. V. Averin, E. V. Sukhorukov, Counting statistics and detector properties of quantum point contacts, Phys. Rev. Lett. 95 (2005) 126803.
[59] N. Katz, M. Ansmann, R. C. Bialczak, E. Lucero, R. McDermott, M. Neeley, M. Steffen, E. M. Weig, A. N. Cleland, J. M. Martinis, A. N. Korotkov, Coherent state evolution in a superconducting qubit from partial-collapse measurement, Science 312 (2006) 1498–1500.
[60] K. Jacobs, D. A. Steck, A straightforward introduction to continuous quantum measurement, Contemp. Phys. 47 (2006) 279–303.
[61] S. Ashhab, J. Q. You, F. Nori, Weak and strong measurement of a qubit using a switching-based detector, Phys. Rev. A 79 (2009) 032317.
[62] S. Ashhab, J. Q. You, F. Nori, Information about the state of a charge qubit gained by a weakly coupled quantum point contact, Phys. Scr. T137 (2009) 014005.
[63] S. Ashhab, J. Q. You, F. Nori, The information about the state of a qubit gained by a weakly coupled detector, New J. Phys. 11 (2009) 083017.
[64] A. A. Clerk, M. H. Devoret, S. M. Girvin, F. Marquardt, R. J. Schoelkopf, Introduction to quantum noise, measurement, and amplification, Rev. Mod. Phys. 82 (2010) 1155–1208.
[65] A. Palacios-Laloy, F. Mallet, F. Nguyen, P. Bertet, D. Vion, D. Esteve, A. N. Korotkov, Experimental violation of a bell's inequality in time with weak measurement, Nature Phys. 6 (2010) 442–447.
[66] Y. Aharonov, P. G. Bergmann, J. L. Lebowitz, Time symmetry in the quantum process of measurement, Phys. Rev. 134 (1964) B1410–B1416.
[67] V. Aharonov, L. Vaidman, The two-state vector formalism, in: J. Muga, R. S. Mayato, I. L. Egusquiza (Eds.), Time in Quantum Mechanics, Springer, 2002‘, pp. 399–447.
[68] Y. Aharonov, D. Rohrlich, Quantum Paradoxes, Wiley-VCH, Weinheim, 2005.
[69] Y. Aharonov, S. Popescu, J. Tollaksen, A time-symmetric formulation of quantum mechanics, Physics Today 63 (11) (November, 2010) 27–32.
[70] N. W. M. Ritchie, J. G. Story, R. G. Hulet, Realization of a measurement of a weak value, Phys. Rev. Lett. 66 (1991) 1107–1110.
[71] D. Suter, M. Ernst, R. R. Ernst, Quantum time-translation machine - an experimental realization, Mol. Phys. 78 (1993) 95–102.
[72] D. Suter, Weak measurements and the quantum time-translation machine in a classical system, Phys. Rev. A 51 (1995) 45–49.
[73] A. D. Parks, D. W. Cullin, D. C. Stoudt, Observation and measurement of an optical Aharonov-Albert-Vaidman effect, Proc. R. Soc. Lond. 454 (1998) 2997–3008.
[74] D. R. Solli, C. F. McCormik, R. Y. Chiao, S. Popescu, J. M. Hickmann, Fast light, slow light, and phase singularities: A connection to generalized weak values, Phys. Rev. Lett. 92 (2004) 043601.
[75] N. Brunner, V. Scarani, M. Wegmüller, M. Legré, N. Gisin, Direct measurement of superluminal group velocity and signal velocity in an optical fiber, Phys. Rev. Lett. 93 (2004) 203902.
[76] K. J. Resch, J. S. Lundeen, A. M. Steinberg, Experimental realization of the quantum box problem, Phys. Lett. A 324 (2004) 125–131.
[77] G. J. Pryde, J. L. O'Brien, A. G. White, T. C. Ralph, H. M. Wiseman, Measurement of quantum weak values of photon polarization, Phys. Rev. Lett. 94 (2005) 220405.
[78] Q. Wang, F.-W. Sun, Y.-S. Zhang, Jian-Li, Y.-F. Huang, G.-C. Guo, Experimental demonstration of a method to realize weak measurement of the arrival time of a single photon, Phys. Rev. A 73 (2006) 023814.
[79] R. Mir, J. S. Lundeen, M. W. Mitchell, A. M. Steinberg, J. L. Garretson, H. M. Wiseman, A double-slit 'which-way' experiment on the complementarity - uncertainty debate, New J. Phys. 9 (2007) 287.
[80] O. Hosten, P. Kwiat, Observation of the spin Hall effect of light via weak measurements, Science 319 (2008) 787–790.
[81] J. S. Lundeen, A. M. Steinberg, Experimental joint weak measurement on a photon pair as a probe of Hardy's paradox, Phys. Rev. Lett. 102 (2009) 020404.
[82] K. Yokota, T. Yamamoto, M. Koashi, N. Imoto, Direct observation of Hardy's paradox by joint weak measurement with an entangled photon pair, New J. Phys. 11 (2009) 033011.
[83] P. B. Dixon, D. J. Starling, A. N. Jordan, J. C. Howell, Ultrasensitive beam deflection measurement via interferometric weak value amplification, Phys. Rev. Lett. 102 (2009) 173601.
[84] J. C. Howell, D. J. Starling, P. B. Dixon, P. K. Vudyasetu, A. N. Jordan, Interferometric weak value deflections: Quantum and classical treatments, Phys. Rev. A 81 (2010) 033813.
[85] D. J. Starling, P. B. Dixon, A. N. Jordan, J. C. Howell, Optimizing the signal-to-noise ratio of a beam-deflection measurement with interferometric weak values, Phys. Rev. A 80 (2009) 041803(R).
[86] D. J. Starling, P. B. Dixon, A. N. Jordan, J. C. Howell, Precision frequency measurements with interferometric weak values, Phys. Rev. A 82 (2010) 063822.
[87] Y.-W. Cho, H.-T. Lim, Y.-S. Ra, Y.-H. Kim, Weak value measurement with an incoherent measuring device, New J. Phys. 12 (2010) 023036.
[88] M. E. Goggin, M. P. Almeida, M. Barbieri, B. P. Lanyon, J. L. O'Bryen, A. G. White, G. J. Pryde, Violation of the Leggett-Garg inequality with weak measurements of photons, Proc. Nat. Acad. Sci. 108 (2011) 1256–1261.
[89] M. D. Turner, C. A. Hagedorn, S. Schlamminger, J. H. Gundlach, Picoradian deflection measurement with an interferometric quasi-autocollimator using weak value amplification, Opt. Lett. 36 (2011) 1479–1481.
[90] S. Kocsis, B. Braverman, S. Ravets, M. J. Stevens, R. P. Mirin, L. K. Shalm, A. M. Steinberg, Observing the average trajectories of single photons in a two-slit interferometer, Science 332 (2011) 1170–1173.

[91] J. S. Lundeen, B. Sutherland, A. Patel, C. Stewart, C. Bamber, Direct measurement of the quantum wavefunction, Nature 474 (2011) 188–191.
[92] L. M. Johansen, A. Luis, Nonclassicality in weak measurements, Phys. Rev. A 70 (2004) 052115.
[93] N. S. Williams, A. N. Jordan, Weak values and the leggett-garg inequality in solid-state qubits, Phys. Rev. Lett. 100 (2008) 026804.
[94] A. J. Leggett, A. Garg, Quantum-mechanics versus macroscopic realism - is the flux there when nobody looks, Phys. Rev. Lett. 54 (1985) 857–860.
[95] A. J. Leggett, Testing the limits of quantum mechanics: motivation, state of play, prospects, J. Phys. Condens. Matter 14 (2002) R415–R451.
[96] N. Lambert, C. Emary, Y. N. Chen, F. Nori, Distinguishing quantum and classical transport through nanostructures, Phys. Rev. Lett. 105 (2010) 176801.
[97] N. Lambert, Y.-N.Chen, F. Nori, Unified single-photon and single-electron counting statistics: from cavity-QED to electron transport, Phys. Rev. A 82 (2010) 063840.
[98] G.-Y. Chen, N. Lambert, C.-M. Li, Y.-N. Chen, F. Nori, Quantum signatures in a macroscopic dipole moment, preprint (2011).
[99] A. J. Leggett, Comment on "How the result of a measurement of a component of the spin of a spin-1/2 particle can turn out to be 100", Phys. Rev. Lett. 62 (1989) 2325.
[100] A. Peres, Quantum measurements with postselection, Phys. Rev. Lett. 62 (1989) 2326.
[101] H. M. Wiseman, Grounding Bohmian mechanics in weak values and bayesianism, New J. Phys. 9 (2007) 165.
[102] J. Dressel, S. Agarwal, A. N. Jordan, Contextual values of observables in quantum measurements, Phys. Rev. Lett. 104 (2010) 240401.
[103] I. M. Duck, P. M. Stevenson, E. C. G. Sudarshan, The sense in which a weak measurement of a spin-1/2 particles spin component yields a value 100, Phys. Rev. D 40 (1989) 2112–2117.
[104] Y. Aharonov, L. Vaidman, Properties of a quantum system during the time interval between 2 measurements, Phys. Rev. A 41 (1990) 11–20.
[105] J. M. Knight, L. Vaidman, Weak measurement of photon polarization, Phys. Lett. A 143 (1990) 357–361.
[106] H. M. Wiseman, Weak values, quantum trajectories, and the cavity-qed experiment on wave-particle correlation, Phys. Rev. A 65 (2002) 032111.
[107] N. Brunner, A. Acín, D. Collins, N. Gisin, V. Scarani, Optical telecom networks as weak quantum measurements with postselection, Phys. Rev. Lett. 91 (2003) 180402.
[108] L. M. Johansen, Weak measurements with arbitrary probe states, Phys. Rev. Lett. 93 (2004) 120402.
[109] T. C. Ralph, S. D. Bartlett, J. L. O'Brien, G. J. Pryde, H. M. Wiseman, Quantum nondemolition measurements for quantum information, Phys. Rev. A 73 (2006) 012113.
[110] R. Jozsa, Complex weak values in quantum measurement, Phys. Rev. A 76 (2007) 044103.
[111] A. D. Lorenzo, J. C. Egues, Weak measurement: Effect of the detector dynamics, Phys. Rev. A 77 (2008) 042108.
[112] T. A. Brun, L. Diósi, W. T. Strunz, Test of weak measurement on a two- or three-qubit computer, Phys. Rev. A 77 (2008) 032101.
[113] A. C. Lobo, C. A. Ribeiro, Weak values and the quantum phase space, Phys. Rev. A 80 (2009) 012112.
[114] S. Wu, K. Mølmer, Weak measurements with a qubit meter, Phys. Lett. A 374 (2009) 34–39.
[115] S. Ashhab, F. Nori, How the results of a measurement of a component of the spin of a spin-1/2 particle can turn out to be 100 without using weak measurements, arXiv:0907.4823 (2009).
[116] T. Geszti, Postselected weak measurement beyond the weak value, Phys. Rev. A 81 (2010) 044102.
[117] N. Brunner, C. Simon, Measuring small longitudinal phase shifts: Weak measurements or standard interferometry?, Phys. Rev. Lett. 105 (2010) 010405.
[118] A. M. Steinberg, Quantum measurement a light touch, Nature 463 (2010) 890–891.
[119] A. Hosoya, Y. Shikano, Strange weak values, J. Phys. A 43 (2010) 385307.
[120] Y. Kedem, L. Vaidman, Modular values and weak values of quantum observables, Phys. Rev. Lett. 105 (2010) 230401.
[121] C. Simon, E. S. Polzik, Fock-state view of weak-value measurements and implementation with photons and atomic ensembles, Phys. Rev. A 83 (2011) 040101(R).
[122] S. Wu, Y. Li, Weak measurements beyond the Aharonov-Albert-Vaidman formalism, Phys. Rev. A 83 (2011) 052106.
[123] A. Romito, Y. Gefen, Y. M. Blanter, Weak values of electron spin in a double quantum dot, Phys. Rev. Lett. 100 (2008) 056801.
[124] V. Shpitalnik, Y. Gefen, A. Romito, Tomography of many-body weak values: Mach-Zehnder interferometry, Phys. Rev. Lett. 101 (2008) 226802.
[125] O. Cohen, Pre- and postselected quantum systems, counterfactual measurements, and consistent histories, Phys. Rev. A 51 (1995) 4373–4380.
[126] Y. Aharonov, L. Vaidman, Complete description of a quantum system at a given time, J. Phys. A 24 (1991) 2315–2328.
[127] M. S. Leifer, R. W. Spekkens, Logical pre- and post-selection paradoxes, measurement-disturbance and contextuality, Int. J. Theor. Phys. 44 (2005) 1977–1987.
[128] A. M. Steinberg, How much time does a tunneling particle spend in the barrier region, Phys. Rev. Lett. 74 (1995) 2405–2409.
[129] M. Onoda, S. Murakami, N. Nagaosa, Hall effect of light, Phys. Rev. Lett. 93 (2004) 083901.
[130] K. Y. Bliokh, A. Niv, V. Kleiner, E. Hasman, Geometrodynamics of spinning light, Nature Photonics 2 (2008) 748–753.
[131] F. Nori, The dynamics of spinning light, Nature Photonics 2 (2008) 716–717.
[132] R. J. Glauber, Optical coherence and photon statistics, in: C. DeWitt, A. Blandin, C. Cohen-Tannoudji (Eds.), Quantum Optics and Electronics, Gordon and Breach, New York, 1965, pp. 65–185.
[133] D. J. Starling, P. B. Dixon, N. S. Williams, A. N. Jordan, J. C. Howell, Continuous phase amplification with a Sagnac interferometer, Phys. Rev. A 82 (2010) 011802(R).
[134] C. K. Hong, Z. Y. Ou, L. Mandel, Measurement of subpicosecond time intervals between 2 photons by interference, Phys. Rev. Lett. 59 (1987) 2044–2046.
[135] D. Sokolovski, Weak values, "negative probability", and the uncertainty principle, Phys. Rev. A 76 (2007) 042125.
[136] G. T. Foster, L. A. Orozco, H. M. Castro-Beltran, H. J. Carmichael, Quantum state reduction and conditional time evolution of wave-particle correlations in cavity QED, Phys. Rev. Lett. 85 (2000) 3149–3152.

[137] L. Hardy, Quantum-mechanics, local realistic theories, and lorentz-invariant realistic theories, Phys. Rev. Lett. 68 (1992) 2981–2984.
[138] M. Brooks, Curiouser and curiouser, New Scientist 178 (10 May 2003) 28.
[139] A. C. Elitzur, L. Vaidman, Quantum-mechanical interaction-free measurements, Found. Phys. 23 (1993) 987–997.
[140] Y. Aharonov, A. Botero, S. Popescu, B. Reznik, J. Tollaksen, Revisiting Hardy's paradox: counterfactual statements, real measurements, entanglement and weak values, Phys. Lett. A 301 (2002) 130–138.
[141] M. O. Scully, B.-G. Englert, H. Walther, Quantum optical tests of complementarity, Nature 351 (1991) 111–116.
[142] E. P. Storey, S. M. Tan, M. J. Collett, D. F. Walls, Path detection and the uncertainty principle, Nature 367 (1994) 626–628.
[143] H. G. Winful, Tunneling time, the Hartman effect, and superluminality: A proposed resolution of an old paradox, Phys. Rep. 436 (2006) 1–69.
[144] H. P. Robertson, The uncertainty principle, Phys. Rev. 31 (1929) 163–164.
[145] C. W. Gardiner, P. Zoller, Quantum Noise, Springer, Berlin, 2000.
[146] E. Schrödinger, To the Heisenberg uncertainty principle, Sitsungsber. Preuss. Akad. Wiss. 19 (1930) 296–303.
[147] C. W. Helstrom, Quantum Detection and Estimation Theory, Academic Press, New York, 1976.
[148] G. A. Korn, T. M. Korn, Mathematical Handbook, McGraw-Hill, New York, 1968.
[149] E. D. Chisolm, Generalizing the Heisenberg uncertainty relation, Am. J. Phys. 69 (2001) 368–371.